

Copyright  
by  
Junyuan Ding  
2016

**The Thesis Committee for Junyuan Ding**  
**Certifies that this is the approved version of the following thesis:**

**Modeling the Advanced Flash Stripper for CO<sub>2</sub> capture using 5 m  
Piperazine**

**APPROVED BY**  
**SUPERVISING COMMITTEE:**

---

Gary T. Rochelle, Supervisor

---

Eric Chen

**Modeling the Advanced Flash Stripper for CO<sub>2</sub> capture using 5 m  
Piperazine**

**by**

**Junyuan Ding, B.E.**

**Thesis**

Presented to the Faculty of the Graduate School of

The University of Texas at Austin

in Partial Fulfillment

of the Requirements

for the Degree of

**Master of Science in Engineering**

**The University of Texas at Austin**

**December 2016**

## **Dedication**

To my parents

## **Acknowledgements**

I would like to firstly thank my graduate supervisor Dr. Gary T. Rochelle for his unswerving support throughout my graduate study at the University of Texas at Austin. He is always positive, energetic, insightful, patient, and supportive. Being mentored by him is the coolest thing in the world. I could not do so much work without his encouragement and dedication. The research experience with him is the most precious treasure in my life. While spending tremendous time supervising his students, he is superb intellectual in balancing between work and family. He knew me and remembered my schedule even more clearly than I did. Every time he gave me mental and life guidance, I saw how he loves his family, which made me think of my parents in the distance.

I am also deeply grateful to my parents and friends. My parents set a good example of keeping positive and happy in the down times. With their firm support, I find the solution to problems much more quickly. Because of Yanran Wang, Yawen He, Wen Liao, Qiang Liu, and Siyun Wang, I laugh a little harder, cry a little less, and smile a lot more.

I would also like to thank all my colleagues in Rochelle group for their contributions in my knowledge: Maeve Cooney, Yu-Jeng Lin, Brent Sherman, Eric Chen, Nathan Fine, Peter Frailie, Darshan Sachde, Yang Du, Yue Zhang, and Kent Fischer. I would thank Kate Baird in the Department of Chemical Engineering for her excellent work and helpful advice.

Financial support for this work was provided by the Texas Carbon Management Program and Membrane Technology and Research, Inc., and by the U.S. Department of Energy under DE-FE0013118.

## **Abstract**

# **Modeling the Advanced Flash Stripper for CO<sub>2</sub> capture using 5 m Piperazine**

Junyuan Ding, M.S.E.

The University of Texas at Austin, 2016

Supervisor: Gary T. Rochelle

Amine scrubbing is the most mature technology for post-combustion CO<sub>2</sub> capture. Several studies have demonstrated that the advanced flash stripper (AFS) consumes less energy among stripper alternatives.

This thesis seeks to demonstrate the AFS energy performance and cost over a wide range of CO<sub>2</sub> loading. Solvent models based on experimental results have been created by previous researchers and are available for simulation and process modeling in Aspen Plus<sup>®</sup>. In collaboration with Membrane Technology and Research Inc., various hybrid amine/membrane configurations were studied to minimize the total CO<sub>2</sub> capture cost. CO<sub>2</sub> in the flue gas is enriched by membranes from 12% to 18 and 23% for coal-fired power plant, and from 6% to 12~18% for natural gas combined cycle power plant (NGCC). The CO<sub>2</sub> loading covers the range of flue gas CO<sub>2</sub> from coal-fired power plants and NGCC. For each configuration, the cold and warm rich bypasses are optimized to minimize the energy cost. The cost optimization is also demonstrated on 5 m PZ, 5 m MDEA/5 m PZ, and 2 m PZ/3 m HMPD. The most cost-effective solvent varies with the flue gas CO<sub>2</sub>.

When applied to a coal-fired power plant, hybrid parallel amine/membrane designs with 99% and 95% CO<sub>2</sub> removal cost less than hybrid series with 60% CO<sub>2</sub> removal. The equivalent work of the parallel configuration with 99% CO<sub>2</sub> removal using 5 m MDEA/5 m PZ (32.3 kJ/mol CO<sub>2</sub>) is less than using 5 m PZ (34.0 kJ/mol CO<sub>2</sub>). The equivalent work with 95% CO<sub>2</sub> removal (Case 19) using 5 m MDEA/5 m PZ (32.5 kJ/mol CO<sub>2</sub>) is less than using 5 m PZ (33.3 kJ/mol CO<sub>2</sub>). The capital cost with 99% CO<sub>2</sub> removal using 5 m MDEA/5 m PZ (\$70.5MM) is more than using 5 m PZ (\$67.5MM). The capital cost with 95% CO<sub>2</sub> removal using 5 m MDEA/5 m PZ (\$73.5MM) is less than using 5 m PZ (\$79.5MM). The total annual cost with 95% CO<sub>2</sub> removal using 2 m PZ/3 m HMPD (\$38.7/tonne CO<sub>2</sub>) is less than using 5 m PZ (\$41.5/tonne CO<sub>2</sub>).

When applied to NGCC, the cost of amine scrubbing is reduced by increasing absorber inlet CO<sub>2</sub> by membranes. However, this is offset by the membrane cost. As absorber inlet CO<sub>2</sub> increases from 6% to 18%, the operating cost decreases from \$18.8 to \$15.4/tonne CO<sub>2</sub>, while total regeneration cost decreases from \$35.6 to \$33.1/tonne CO<sub>2</sub>.

## Table of Contents

List of Tables .....	x
List of Figures .....	xiii
Chapter 1: Introduction .....	1
Chapter 2: Optimization of the Advanced Flash Stripper using 5 m PZ .....	4
2.1 Methods.....	5
2.1.1 Equivalent Work Calculation.....	6
2.1.2 Minimum Work .....	6
2.2 Regression analysis over a wider range of rich loading .....	7
2.3 Regression analysis at optimum lean loading .....	12
2.4 The Second Law Efficiency.....	14
2.5 Conclusions.....	18
Chapter 3: Regenerator Design for CO <sub>2</sub> Capture from Coal with Hybrid Amine/Membrane .....	19
3.1 Hybrid Amine/Membrane Configuration .....	23
3.2 Stripper Performance of Series and Parallel using 5 m PZ.....	24
3.3 Stripper Performance of Parallel using 5 m MDEA/5 m PZ .....	28
3.4 Stripper Performance of Parallel using 2 m PZ/3 m HMPD .....	31
3.5 Conclusions.....	36
Chapter 4: Regeneration Design for NGCC CO <sub>2</sub> Capture with Amine-only and Hybrid Amine/Membrane.....	37
4.1 amine-only, hybrid amine/membrane and reference cases .....	40
4.2 CAPEX and OPEX .....	44
4.2.1 Capital Cost.....	44
4.2.2 Operating Cost .....	45
4.3 Optimization Specifications.....	46
4.4 Stripping Temperature Optimization .....	47
4.5 Cost of Hybrid Amine/Membrane Designs with and without DCC .....	52
4.6 Cost of Amine-Only and Hybrid Amine/Membrane Designs .....	54



4.7 Cost of Stripping using 5 m PZ with or without CRBP.....	58
4.8 Conclusions.....	59
Appendix A: Managing NH <sub>3</sub> Emissions from Amine Scrubbing.....	64
Appendix B: Air Stripping and AFS with Compressor Intercooled by parallel cold rich bypasses .....	84
References.....	97
Vita.....	99

## List of Tables

Table 2-1:	Prediction of results from CO <sub>2</sub> rich and lean loading. Using 5 m PZ stripping at 150 °C with 2 m Mellapak 250 X packing at the optimum cold and warm rich bypasses, main exchanger LMTD = 5 °C, top exchanger LMTD = 20 °C. ....	7
Table 2-2:	Prediction of optimum conditions from CO <sub>2</sub> rich loading using 5 m PZ stripping at 150 °C with 2 m Mellapak 250 X packing at the optimum cold and warm rich bypasses, main exchanger LMTD = 5 °C, hot exchanger LMTD = 20 °C. ....	13
Table 3-1:	Stripper energy performance of series and parallel designs using 5 m PZ. ....	26
Table 3-2:	Equipment purchase cost of series and parallel designs using 5 m PZ at 593 MWe in Million dollars. ....	27
Table 3-3:	Comparison of stripper performance of parallel designs using 5 m PZ and 5 m MDEA/5 m PZ. ....	29
Table 3-4:	Equipment purchase cost of parallel designs using 5 m PZ and 5 m PZ and 5 m MDEA/5 m PZ at 593 MWe in Million dollars. ....	30
Table 3-5:	Parallel designs with 95% CO <sub>2</sub> removal using 5 m PZ/5 m MDEA and 2 m PZ/3 m HMPD. ....	33
Table 3-6:	Equipment purchase cost for Cases 19-4 and 19-5 (million \$).....	33
Table 3-7:	Annual capital and operating cost using 5 m PZ/5 m MDEA and 2 m PZ/3 m HMPD (\$/tonne CO <sub>2</sub> ). ....	34
Table 3-8:	Equipment purchase cost for all Cases (million \$). ....	35
Table 4-1:	Flue gas parameters.....	41

Table 4-2:	Annual Cost of amine-only designs with 6.3% absorber inlet CO <sub>2</sub> (\$/tonne CO <sub>2</sub> ) at different stripping temperatures, with and without DCC.	49
Table 4-3:	Summary of cases.	50
Table 4-4:	Cost of hybrid designs with 14.1% absorber inlet CO <sub>2</sub> (\$/tonne CO <sub>2</sub> ).	52
Table 4-5:	Cost of amine-only design and hybrid amine/membrane designs using 5 m PZ (\$/tonne CO <sub>2</sub> ) at varied absorber inlet CO <sub>2</sub> .	55
Table 4-6:	Annual cost with and without CRBP (\$/tonne CO <sub>2</sub> ) at CO <sub>2</sub> 18.2%.	58
Table 4-7:	Equipment Cost (million \$).	60
Table 4-8:	Operating Energy Consumption (MWe).	61
Table 4-9:	Annual Capital and Operating Cost (\$/tonne CO <sub>2</sub> ).	62
Table A-1:	Total mass flow rate and CO <sub>2</sub> , PZ, and NH <sub>3</sub> mole flows in purge of with and without split ammonia purging configuration (5 m PZ, NH <sub>3</sub> /H <sub>2</sub> O=1 ppm; CO <sub>2</sub> rich loading: 0.4 mol/N; CO <sub>2</sub> lean loading: 0.157 mol/N; cold rich bypass: 10%; warm rich bypass: 20%; stripping temperature: 150 °C; stripping pressure: 5 bar; reflux ratio: 2.1).	71
Table A-2:	Stream table of ammonia purging by one part of condensate and side stripper (5 m PZ, NH <sub>3</sub> /H <sub>2</sub> O=1 ppm; CO <sub>2</sub> rich loading: 0.4 mol/N; CO <sub>2</sub> lean loading: 0.24 mol/N; cold rich bypass: 6.8%; warm rich bypass: 23%; stripping temperature: 150 °C; stripping pressure: 6.4 bar; the mass flow rate of the side split is the same as that of the purge at reflux ratio of 9; condensing temperature of the side stripper: 155 °C; total distillate rate of the side stripper: 1000 kg/hr; mole reflux ratio of the side stripper: 10).	82

Table B-1: Energy performance of air stripper changing with delta lean loading (at rich loading of 0.4 mol CO <sub>2</sub> /mol N and high lean loading of 0.2 mol CO <sub>2</sub> /mol N). .....	90
Table B-2: Energy performance of air stripper changing with high lean loading (at rich loading of 0.4 mol CO <sub>2</sub> /mol N and delta lean loading of 0.01 mol CO <sub>2</sub> /mol N). .....	91
Table B-3: Energy performance of AFS before recovering the compressor intercooling heat (at rich loading of 0.4 mol CO <sub>2</sub> /mol N). .....	92
Table B-4: Energy performance of AFS recovering the compressor intercooling heat (at rich loading of 0.4 mol CO <sub>2</sub> /mol N). .....	93

## List of Figures

Figure 2-1: Stripping configuration using 5 m PZ.....	5
Figure 2-2: Performance of the advanced flash stripper. Using 5 m PZ stripping at 150 °C with 2 m Mellapak 250 X packing at the optimum cold and warm rich bypasses, main exchanger LMTD = 5 °C, top exchanger LMTD = 20 °C. Lines predicted by Equation 4. ....	8
Figure 2-3: Heat duty of the advanced flash stripper and its predicted value at different rich and lean loadings. Using 5 m PZ stripping at 150 °C with 2 m Mellapak 250 X packing at the optimum cold and warm rich bypasses, main exchanger LMTD = 5 °C, top exchanger LMTD = 20 °C. Lines predicted by Equation 5. ....	9
Figure 2-4: Stripping pressure and its predicted value at 0.37 to 0.43 rich loading. Using 5 m PZ stripping at 150 °C with 2 m Mellapak 250 X packing at the optimum cold and warm rich bypasses, main exchanger LMTD = 5 °C, top exchanger LMTD = 20 °C. Lines predicted by Equation 6..	10
Figure 2-5: Cold rich bypass and its optimum value at 0.37 to 0.43 rich loading. Using 5 m PZ stripping at 150 °C with 2 m Mellapak 250 X packing, main exchanger LMTD = 5 °C, top exchanger LMTD = 20 °C. Lines predicted by Equation 7. ....	11
Figure 2-6: Optimum warm rich bypass in the advanced flash stripper with 5 m PZ. Using 5 m PZ stripping at 150 °C with 2 m Mellapak 250 X packing, main exchanger LMTD = 5 °C, top exchanger LMTD = 20 °C. Lines predicted by Equation 8. ....	12

Figure 2-7: Second law efficiency of the advanced flash stripper with 5 m PZ. Marks calculated by $W_{\min} / W_{\text{total,ideal}}$ . Lines predicted by Equation 15. .....	15
Figure 2-8: Pump work at variable CO <sub>2</sub> rich loading. Using 5 m PZ stripping at 150 °C with 2 m Mellapak 250 X packing at the optimum cold and warm rich bypasses, main exchanger LMTD = 5 °C, hot exchanger LMTD = 20 °C. ....	16
Figure 2-9: Cold and warm rich bypass for different CO <sub>2</sub> rich loading with CO <sub>2</sub> loading difference. Using 5 m PZ stripping at 150 °C with 2 m Mellapak 250 X packing at the optimum cold and warm rich bypasses, main exchanger LMTD = 5 °C, hot exchanger LMTD = 20 °C. The upper three lines are warm rich bypass presented on the right Y axis in %. The lower three lines are cold rich bypass presented on the left Y axis in %. ....	17
Figure 3-1: Series and Parallel configurations of hybrid amine/membrane CO <sub>2</sub> capture model (MTR, 2014). ....	20
Figure 3-2: Stripper configuration for hybrid amine/membrane using 5 m PZ and 5 m MDEA/5 m PZ.....	21
Figure 3-3: Total equivalent work of 5 m PZ (at 0.38 mol CO <sub>2</sub> /mol N rich loading), 8 m PZ (at 0.39 mol CO <sub>2</sub> /mol N rich loading), and 2 m PZ/3m HMPD (at 0.40 mol CO <sub>2</sub> /mol N rich loading). CO <sub>2</sub> equilibrium partial pressures of all rich loadings are 5.6 kPa.....	32
Figure 4-1: Configuration of advanced flash stripper with cold and warm bypass.	39
Figure 4-2: The complete configuration of a NGCC with CO <sub>2</sub> capture for Case 1C1. .....	42

Figure 4-3: The complete configuration of a NGCC with CO <sub>2</sub> capture for Case 1C2.	42
Figure 4-4: The complete configuration of a NGCC with CO <sub>2</sub> capture for Cases 1D4 1D1, and 1D3.	43
Figure 4-5: The complete configuration of a NGCC with CO <sub>2</sub> capture for Case 1D2.	43
Figure 4-6: Total equivalent work at varied stripping temperature, 0.4 rich loading, 4 m stripper packing.	47
Figure 4-7: Annual cost of hybrid amine/membrane at varied absorber inlet CO <sub>2</sub> 6.3%, 12.1%, 15.2%, and 18.2%.	56
Figure A-1: Stripping configuration using 5 m PZ.	66
Figure A-2: Stripping configuration of ammonia purging from the condensate with split.	67
Figure A-3: Stripping configuration of ammonia purging from the condensate.	67
Figure A-4: Stripping configuration of ammonia purging from the condensate with a side stripper.	68
Figure A-5: Total NH <sub>3</sub> and PZ in purge changing with reflux ratio (5 m PZ, NH <sub>3</sub> /H <sub>2</sub> O=1 ppm; CO <sub>2</sub> rich loading: 0.4 mol/N; CO <sub>2</sub> lean loading: 0.157 mol/N; cold rich bypass: 18%; warm rich bypass: 52%; stripping temperature: 150 °C; stripping pressure: 5 bar; R: Reflux ratio).	72
Figure A-6: Total NH <sub>3</sub> and PZ in purge changing with NH <sub>3</sub> /H <sub>2</sub> O (5 m PZ; CO <sub>2</sub> rich loading: 0.4 mol/N; CO <sub>2</sub> lean loading: 0.155 mol/N; cold rich bypass: 18%; warm rich bypass: 52%; stripping temperature: 150 °C; stripping pressure: 5 bar; reflux ratio: 9).	73

Figure A-7: Total NH <sub>3</sub> and PZ in purge changing with NH <sub>3</sub> /H <sub>2</sub> O stripping at 4.6 bar, 5 bar, and 6 bar (corresponding respectively to 0.1, 0.15, and 0.22 mol/mol N CO <sub>2</sub> lean loading)(5 m PZ; CO <sub>2</sub> rich loading: 0.4 mol/N; cold rich bypass: 19%; warm rich bypass: 54%; stripping temperature: 150 °C; reflux ratio: 9).	75
Figure A-8: Total NH <sub>3</sub> and PZ in purge changing with CO <sub>2</sub> lean loading target (5 m PZ, NH <sub>3</sub> /H <sub>2</sub> O=1 ppm; CO <sub>2</sub> rich loading: 0.4 mol/N; cold rich bypass and warm rich bypass are optimized at each lean loading; stripping temperature: 150 °C; reflux ratio: 9).	76
Figure A-9: Total NH <sub>3</sub> and PZ in purge changing with CO <sub>2</sub> lean loading compared with initial advanced flash stripper (5 m PZ, NH <sub>3</sub> /H <sub>2</sub> O=1 ppm; CO <sub>2</sub> rich loading: 0.4 mol/N; cold rich bypass and warm rich bypass are optimized at each lean loading; stripping temperature: 150 °C; reflux ratio: 9).	78
Figure A-10: Total equivalent work changing with CO <sub>2</sub> lean loading (5 m PZ, NH <sub>3</sub> /H <sub>2</sub> O=1 ppm; CO <sub>2</sub> rich loading: 0.4 mol/N; cold rich bypass and warm rich bypass are optimized at each lean loading; stripping temperature: 150 °C; reflux ratio: 9).	79
Figure A-11: NH <sub>3</sub> /PZ mole ratio in the liquid side at each stage of the stripper (5 m PZ, NH <sub>3</sub> /H <sub>2</sub> O=1 ppm; CO <sub>2</sub> rich loading: 0.4 mol/N; CO <sub>2</sub> lean loading: 0.24 mol/N; cold rich bypass: 6.8%; warm rich bypass: 23%; stripping temperature: 150 °C; stripping pressure: 6.4 bar).	81
Figure B-1: Complete configuration of air stripping and brine cooling in Kentucky.	86



Figure B-2: Advanced Flash Stripper with compressor intercooling heat recovered.	88
Figure B-3: Advanced Flash Stripper with compressor intercooling heat recovered.	89
Figure B-4: Total equivalent work of air stripper and AFS at rich loading of 0.4 mol CO <sub>2</sub> /mol N.	91
Figure B-5: Total equivalent work of AFS with and without Q <sub>compintc</sub> recovered.	93
Figure B-6: Energy performance of AFS with and without Q <sub>compintc</sub> recovered.	95

## Chapter 1: Introduction

CO<sub>2</sub> emissions from coal-fired power plants account for about 40% of the total emissions from the United States. Currently, the use of Natural Gas Combined Cycle (NGCC) power plants has been increasing since it emits fewer pollutants than coal-fired power plants. The expectation for an increase in NGCC and coal-fired power plants in the future and the heightening concern of global warming as a political issue brings attention to developing carbon capture and sequestration at these sites in the near future. The most favorable technology is to capture the CO<sub>2</sub> from the exhaust gas with an amine solvent through the use of an absorber and a stripper. The CO<sub>2</sub> would then be compressed and stored in a deep geological formation or sent for use in another industrial application.

To reduce the energy requirement, alternative stripper configurations have been proposed to improve the capture efficiency. Previous studies improved the energy performance by configuration modification and operating parameter optimization. Alternative stripper configurations include split flow, lean vapor compression, and other modifications using MEA (Tobiesen and Svendsen, 2006; Cousins et al., 2011; Le Moullec and Kanniche, 2011; Sanchez Fernandez et al., 2012).

More alternative stripper configurations have been proposed in work at the University of Texas. Advanced solvents such as MDEA and PZ were also evaluated. Rochelle and coworkers evaluated a multi-pressure configuration that operates the stripper at different pressure levels (Jassim and Rochelle, 2006; Oyenekan and Rochelle, 2006, 2007). The improvement comes from the recovery of stripping steam heat at higher pressure. Van Wagener and Rochelle (Van Wagener, 2011; Van Wagener and Rochelle, 2011) emphasized the importance of increasing process reversibility by introducing more complex configurations including the multi-stage flash, multi-pressure, double matrix, and

the interheated stripper. Van Wagener showed that the interheated stripper with 8 m PZ offers the best energy savings. Madan (Madan, 2013) proposed that the multi-feed flash stripper can effectively reduce the energy requirement by bypassing a portion of rich solvent into the stripper at different temperature levels. Lin (Lin, 2015) demonstrated that the advanced flash stripper provides the best energy performance among other alternatives using 8 m PZ. It reduces the reboiler duty by 16% and the total equivalent work by 11% compared to the simple stripper using aqueous piperazine.

Most of the previous work focused on CO<sub>2</sub> capture applied on coal-fired power plants, where CO<sub>2</sub> is 10~15%. Lower loadings matching operation with NGCC at 5~8% CO<sub>2</sub> were not considered. Also, 8 m PZ may precipitate at lean loading if the temperature drops to ambient with a process upset. This work with Membrane Technology Research Inc. (MTR) proposed hybrid amine/membrane configurations for CO<sub>2</sub> Capture from both Coal and NGCC. The stripper energy performance and cost using 5 m PZ are evaluated over a wide range of rich and lean loading (mol CO<sub>2</sub>/mol amine alkalinity). The precipitation problem of 8 m PZ is minimized by using this diluted amine.

MTR is a company provides a full range of membranes for gas separation. They can enrich CO<sub>2</sub> in the flue gas from 12% to 18 and 23% for coal-fired power plant, and from 6% to 12~18% for NGCC by membranes. The higher CO<sub>2</sub> enhances the CO<sub>2</sub> absorbing driving force and reduces the amine scrubbing capital costs.

Desulfurized flue gas from coal combustion with 6~20% CO<sub>2</sub> is contacted with the aqueous amine in the absorber where 60~99% of the CO<sub>2</sub> is removed. The rich solvent from the bottom of the absorber is sent to the stripper and heated for CO<sub>2</sub> regeneration. The cold rich solvent is preheated by the hot lean solvent in the cross exchanger. The

lean solvent is recycled back to the absorber. The stripped CO<sub>2</sub> is then compressed to 150 bar for further storage and sequestration.

The Independence model for PZ in Aspen Plus<sup>®</sup> (Frailie, 2014) is used to simulate the absorber and stripper performance. In order to reduce the solvent recirculation rate and minimize plant investment and operating cost, stripper energy performance and cost using 5 m MDEA/5 m PZ and 2 m PZ/3 m HMPD are compared to using 5 m PZ.

## **Chapter 2: Optimization of the Advanced Flash Stripper using 5 m PZ**

Aqueous piperazine (PZ) is a superior solvent for CO<sub>2</sub> capture by amine scrubbing because of its outstanding energy properties, including high CO<sub>2</sub> capacity (mol CO<sub>2</sub> removed/kg solvent), high thermal stability, moderately high viscosity, resistance to oxidative degradation, and low volatility in CO<sub>2</sub>-loaded solution. 8 m PZ consumes significantly less regeneration energy than monoethanolamine (MEA). However, 8 m PZ may precipitate at lean loadings if the temperature drops below ambient with a process upset. 5 m PZ minimizes the precipitation problem that the more viscous 8 m PZ causes in the solvent loop. Lin (2016) optimized stripping with 8 m piperazine (PZ). The advanced flash with warm rich bypass and cold rich exchanger bypass is used for stripping. The Independence model for PZ in Aspen Plus® was used to simulate the stripping performance. The energy performance using 5 m PZ with rich loading from 0.34 to 0.43 mol CO<sub>2</sub>/mol N was optimized in this chapter. Output CO<sub>2</sub> pressure, heat duty, compression work, pump work, and cold/warm rich bypass are recorded and calculated. An optimum lean loading requires the minimum equivalent work at each CO<sub>2</sub> rich loading.

Stripping data for 21 cases, including heat duty, equivalent work, CO<sub>2</sub> output pressure, and optimum cold and warm rich bypass, were used to build a correlation with CO<sub>2</sub> rich and lean loading. The Second Law efficiency based on the ratio of stripping minimum work and total ideal work was introduced to explain the stripping work. The Second Law efficiency has a maximum value at a specific CO<sub>2</sub> loading.

## 2.1 METHODS

The amine regeneration system was simulated using the Independence model in Aspen Plus®. Figure 2-1 shows the advanced flash stripper configuration. All of these cases are simulated using 5 m PZ stripping at 150 °C, main exchanger LMTD = 5 °C, top exchanger LMTD = 20 °C, lean solvent output at 40 °C, and 150 bar CO<sub>2</sub> product.

When CO<sub>2</sub> rich loading and lean loading of the advanced flash stripper are given, the overall equivalent work will vary with the cold rich bypass and warm rich bypass. There is a lean loading where the equivalent work is minimized. The corresponding cold rich bypass and warm rich bypass is the optimum bypass for this specific CO<sub>2</sub> rich and lean loading. In order to distinguish this from the bypass at the optimum lean loading for each CO<sub>2</sub> rich loading, the former is described as “bypass” and the latter “optimum bypass”.

Regression analysis in Excel is used to build the correlations of heat duty, equivalent work, CO<sub>2</sub> output pressure, optimum cold and warm rich bypass, and CO<sub>2</sub> rich and lean loading.

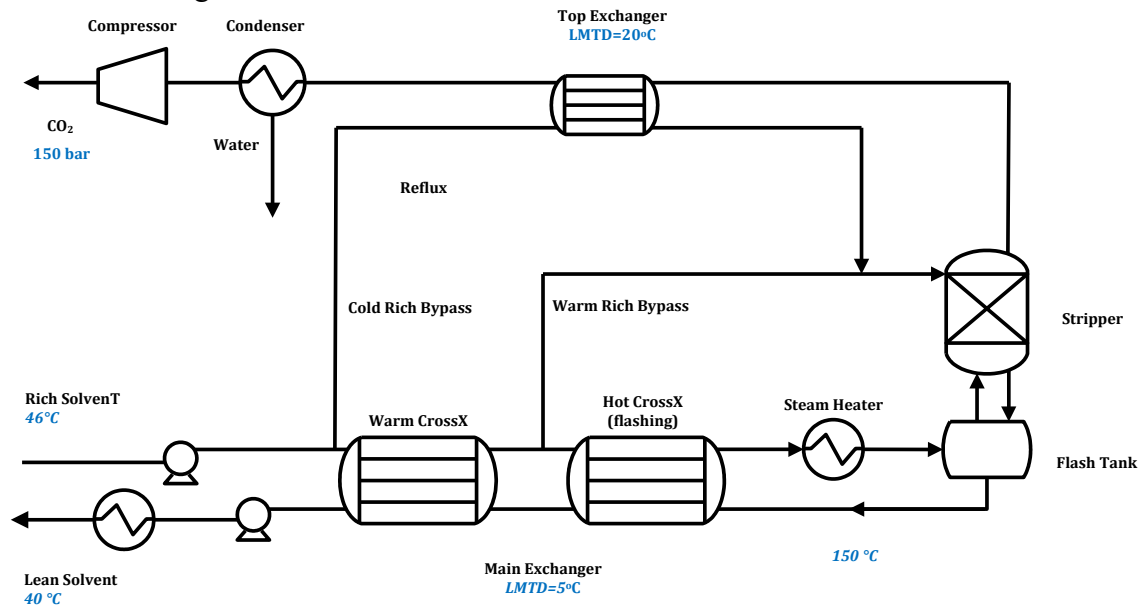


Figure 2-1: Stripping configuration using 5 m PZ.

### 2.1.1 Equivalent Work Calculation

Equivalent work replaces heat duty as a more general metric of energy use than heat duty alone. It is defined as the sum of pump work, compression work, and heat work, as Equation 1 shows.

$$W_{eq} \text{ (kJ/mol CO}_2\text{)} = W_{heat} + W_{pump} + W_{comp} \quad (1)$$

Heat work can be generated from the heat duty of the reboiler using Equation 2. A typical value of 90% is used for the turbine efficiency ( $\eta$ ) and  $T_{sink}$  is taken as 313K.

$$W_{heat} \text{ (kJ/mol CO}_2\text{)} = \eta \left( \frac{T_{source} + \Delta T - T_{sink}}{T_{source} + \Delta T} \right) Q_{reb} \quad (2)$$

Compression work can be approximated by Equation 3, which is typically assumed to be at a discharge pressure of 150 bar.

$$W_{comp} \text{ (kJ/mol CO}_2\text{)} = \begin{cases} 4.572 \ln\left(\frac{150}{P_{in}}\right) - 4.096 \cdots P_{in} \leq 4.56bar \\ 4.023 \ln\left(\frac{150}{P_{in}}\right) - 2.181 \cdots P_{in} \geq 4.56bar \end{cases} \quad (3)$$

### 2.1.2 Minimum Work

Minimum work is the total reversible work required considering the stripping process as a Carnot cycle. Minimum work can be estimated as  $W_{min} \text{ (kJ/mol CO}_2\text{)} = \Delta G = \Delta H - T\Delta S$ .

In a real process, part of the work produced is consumed by irreversible operations, such as heat transfer in the cross exchanger, condenser, reboiler, etc. The Second Law efficiency, which is the ratio of minimum work to total ideal work, is chosen to reflect the utilization of energy. To estimate total ideal work the heat work,  $W_{heat}$ , is replaced by ideal heat work,  $W_{heat,ideal}$ , setting the turbine efficiency in Equation 2 to 1.0.

## 2.2 REGRESSION ANALYSIS OVER A WIDER RANGE OF RICH LOADING

Total equivalent work, heat duty, stripping pressure, warm rich bypass, and cold rich bypass for each case were regressed in Excel as a function of CO<sub>2</sub> rich loading and lean loading. Comparisons between simulation results and predicted values by regression are shown in Table 2-1 and Figures 2-2–2-6.

Table 2-1: Prediction of results from CO<sub>2</sub> rich and lean loading. Using 5 m PZ stripping at 150 °C with 2 m Mellapak 250 X packing at the optimum cold and warm rich bypasses, main exchanger LMTD = 5 °C, top exchanger LMTD = 20 °C.

Case	RLDG (mol CO <sub>2</sub> /mol N)	LLDG (mol CO <sub>2</sub> /mol N)	Q (kJ/mol CO <sub>2</sub> )	Q pre (kJ/mol CO <sub>2</sub> )	W <sub>EQ</sub> (kJ/mol CO <sub>2</sub> )	W <sub>EQ</sub> pre (kJ/mol CO <sub>2</sub> )	P (bar)	P pre (bar)	ln P	(ln P) pre
1	0.34	0.20	115.3	114.3	40.2	40.5	5.5	5.6	1.7	1.7
2	0.34	0.22	115.3	115.4	40.0	39.7	5.9	5.9	1.8	1.8
3	0.34	0.24	116.9	118.4	40.2	39.8	6.4	6.4	1.9	1.9
4	0.34	0.28	131.1	130.6	43.8	42.6	7.8	7.8	2.1	2.1
5	0.37	0.23	103.7	102.8	36.9	36.9	6.1	6.1	1.8	1.8
6	0.37	0.24	103.8	103.5	36.7	36.8	6.4	6.4	1.9	1.9
7	0.37	0.25	104.5	104.7	36.8	36.9	6.7	6.7	1.9	1.9
8	0.37	0.27	106.9	108.4	37.3	37.8	7.4	7.4	2.0	2.0
9	0.37	0.31	121.8	121.3	41.4	42.0	9.6	9.7	2.3	2.3
10	0.4	0.2	96.0	97.1	35.2	36.3	5.6	5.6	1.7	1.7
11	0.4	0.24	93.7	93.0	34.1	33.6	6.4	6.4	1.9	1.9
12	0.4	0.26	93.9	93.3	33.9	33.5	7.0	7.0	2.0	1.9
13	0.4	0.27	94.1	94.1	33.9	33.7	7.4	7.4	2.0	2.0
14	0.4	0.28	94.9	95.3	34.0	34.2	7.8	7.8	2.1	2.1
15	0.4	0.3	97.4	98.9	34.5	35.6	8.9	9.0	2.2	2.2
16	0.4	0.34	112.8	110.9	39.0	41.0	12.4	12.4	2.5	2.5
17	0.43	0.27	83.6	83.9	31.2	29.4	7.4	7.4	2.0	2.0
18	0.43	0.29	83.9	83.7	31.0	29.8	8.4	8.4	2.1	2.1
19	0.43	0.31	85.2	84.9	31.1	30.9	9.6	9.7	2.3	2.3
20	0.43	0.33	88.1	87.5	31.7	32.8	11.4	11.4	2.4	2.4
21	0.43	0.37	102.6	107.2	36.8	38.9	16.7	16.8	2.8	2.8



Figure 2-2 compares the total equivalent work for variable CO<sub>2</sub> rich loading. As CO<sub>2</sub> rich loading increases, the equivalent work requirement decreases for the same loading difference between rich and lean. Since CO<sub>2</sub> capacity becomes dominant at high lean loading, total equivalent work for all these rich loadings changes rapidly at high lean loading values and becomes flat at the low lean loading end. At all three minimum points, the loading difference between rich and lean is 0.14.

The expression of total equivalent work by regression is:

$$W_{eq} = 39.4 + 101.0LLDG + 583.2LLDG^2 + 177.8RLDG^2 - 961.9RLDG * LLDG \quad (4)$$

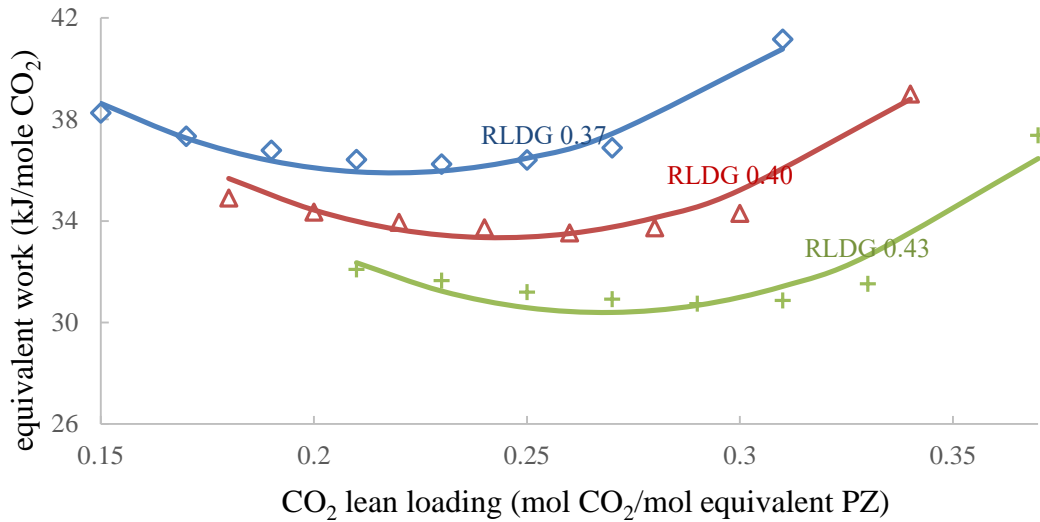


Figure 2-2: Performance of the advanced flash stripper. Using 5 m PZ stripping at 150 °C with 2 m Mellapak 250 X packing at the optimum cold and warm rich bypasses, main exchanger LMTD = 5 °C, top exchanger LMTD = 20 °C. Lines predicted by Equation 4.

Heat duty of the reboiler is composed of sensible heat, latent heat, and stripping steam heat. Heat work accounts for about 70% of the total equivalent work. Figure 2-3 shows the comparison of heat duty for variable CO<sub>2</sub> rich loading. Heat duty also has its minimum value at a CO<sub>2</sub> loading difference of 0.14 mol CO<sub>2</sub>/mol PZ. The sensible heat requirement dominates at high lean loading (low capacity). The stripping steam requirement dominates at low lean loading.

The expression of heat duty (Figure 2-3) by regression is:

$$Q = 119.1 + 342.2LLDG + 1891.5LLDG^2 + 497.7RLDG^2 - 3098.8RLDG * LLDG \quad (5)$$

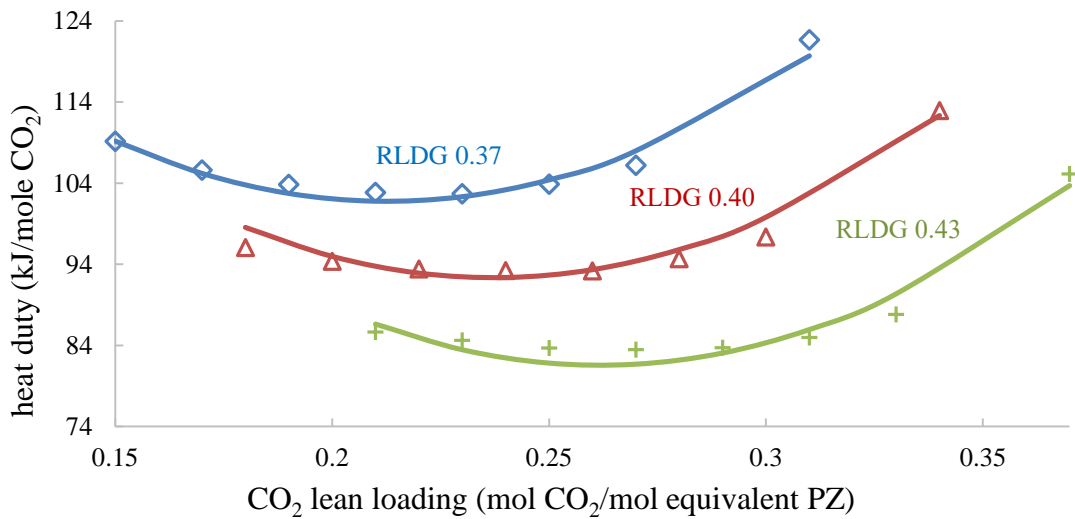


Figure 2-3: Heat duty of the advanced flash stripper and its predicted value at different rich and lean loadings. Using 5 m PZ stripping at 150 °C with 2 m Mellapak 250 X packing at the optimum cold and warm rich bypasses, main exchanger LMTD = 5 °C, top exchanger LMTD = 20 °C. Lines predicted by Equation 5.

Thermodynamically, the stripping pressure at 150 °C (Figure 2-4) depends only on the lean loading and is given empirically by:

$$\ln P = 6.6 - 5.9LLDG + 21.7LLDG^2 \quad (6)$$

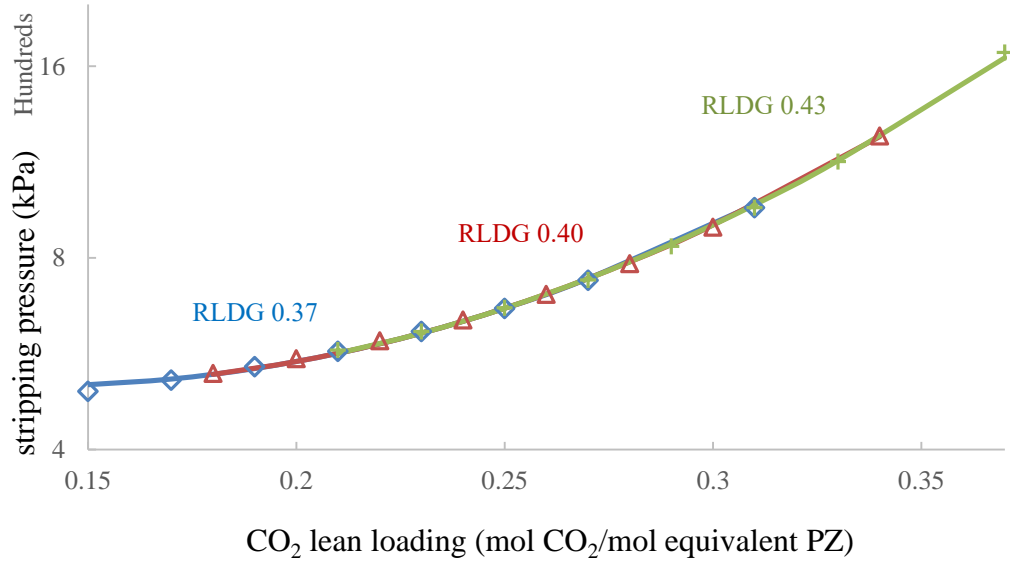


Figure 2-4: Stripping pressure and its predicted value at 0.37 to 0.43 rich loading. Using 5 m PZ stripping at 150 °C with 2 m Mellapak 250 X packing at the optimum cold and warm rich bypasses, main exchanger LMTD = 5 °C, top exchanger LMTD = 20 °C. Lines predicted by Equation 6.

The optimum cold rich bypass (Figure 2-5) is not a function of rich loading and is given by:

$$CRBP = 0.38 - 1.91LLDG + 2.44LLDG^2 \quad (7)$$

As CO<sub>2</sub> lean loading increases, cold rich bypass plays a less important role in the advanced flash stripper, because for high CO<sub>2</sub> lean loading, less water is heated to the vapor phase, and so less steam stripping heat needs to be recovered by cold rich bypass. The cold rich bypass can be removed from the advanced flash stripper design when stripping very high CO<sub>2</sub> lean loading.

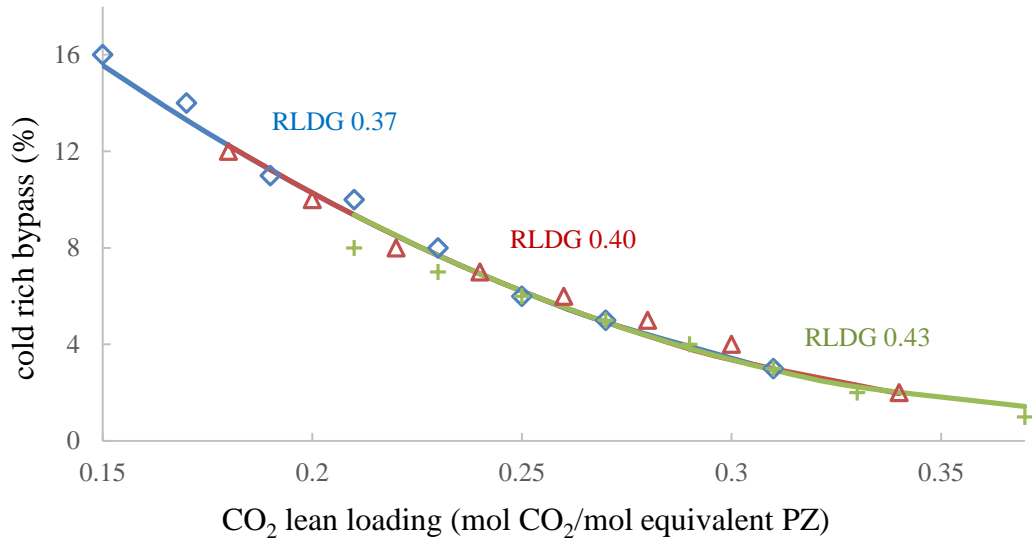


Figure 2-5: Cold rich bypass and its optimum value at 0.37 to 0.43 rich loading. Using 5 m PZ stripping at 150 °C with 2 m Mellapak 250 X packing, main exchanger LMTD = 5 °C, top exchanger LMTD = 20 °C. Lines predicted by Equation 7.

As Figure 2-6 shows, the expression of the optimum rich bypass is:

$$WRBP = 2.43 - 9.56LLDG + 4.98LLDG^2 - 3.00RLDG^2 + 1.09RLDG * LLDG \quad (8)$$

Warm rich bypass depends in large part on CO<sub>2</sub> lean loading, and changes in the same way that cold rich bypass does. It also depends on CO<sub>2</sub> rich loading. Warm rich bypass at low CO<sub>2</sub> rich loading decreases more rapidly with CO<sub>2</sub> lean loading than at high CO<sub>2</sub> rich loading. At low CO<sub>2</sub> lean loading, low CO<sub>2</sub> rich loading has a greater warm rich bypass. All the lines decrease and cross at the same point, CO<sub>2</sub> lean loading 0.27 mol/equivalent PZ. At high CO<sub>2</sub> lean loading, warm rich bypass with high CO<sub>2</sub> rich loading becomes higher than low CO<sub>2</sub> rich loading, but they all tend to zero. Combined with the profile of cold rich bypass, both warm rich bypass and cold rich bypass play less important roles in recovering energy at high CO<sub>2</sub> lean loading. In other words, at high

CO<sub>2</sub> lean loading, the simple stripper is more economical than the advanced stripper because of the cross exchanger capital cost.

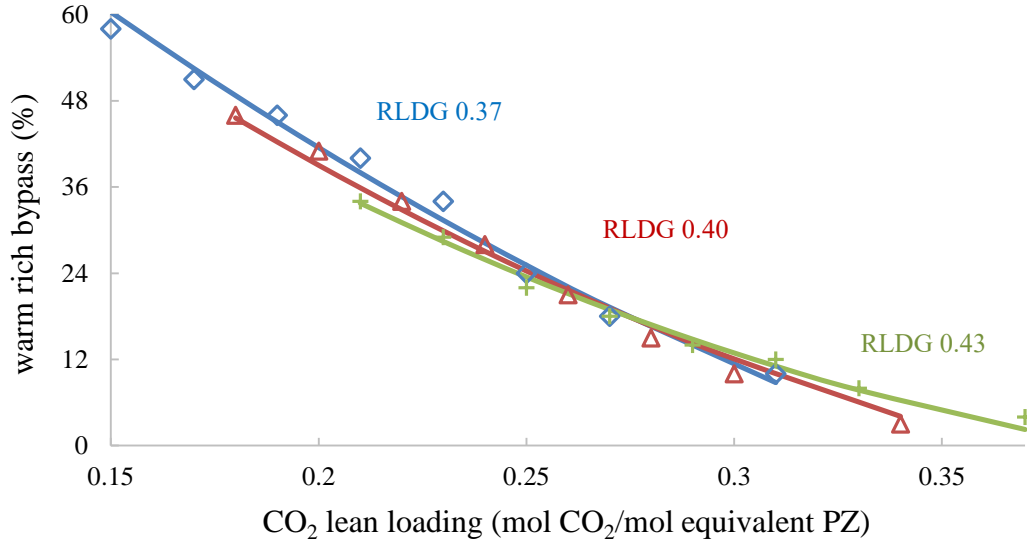


Figure 2-6: Optimum warm rich bypass in the advanced flash stripper with 5 m PZ. Using 5 m PZ stripping at 150 °C with 2 m Mellapak 250 X packing, main exchanger LMTD = 5 °C, top exchanger LMTD = 20 °C. Lines predicted by Equation 8.

### 2.3 REGRESSION ANALYSIS AT OPTIMUM LEAN LOADING

Similarly, optimum lean loading at each CO<sub>2</sub> rich loading and its corresponding stripping pressure, heat duty, total equivalent work, optimum cold rich bypass, and warm rich bypass are regressed as functions of rich loading.

Table 2-2 shows optimum CO<sub>2</sub> lean loading, cold rich bypass, warm rich bypass, ln P, and equivalent work for each of the CO<sub>2</sub> rich loading cases that were analyzed. Approximate expressions of the relationship between them were derived and predicted values of them are calculated from these expressions. Comparisons between original values and predicted values are shown in Table 2-2.

Table 2-2: Prediction of optimum conditions from CO<sub>2</sub> rich loading using 5 m PZ stripping at 150 °C with 2 m Mellapak 250 X packing at the optimum cold and warm rich bypasses, main exchanger LMTD = 5 °C, hot exchanger LMTD = 20 °C.

Optimum Case Number	RLDG (mol CO <sub>2</sub> /mol N)	RLDG <sup>2</sup>	Opt. LLDG (mol CO <sub>2</sub> /mol N)	LLDG Pre (mol CO <sub>2</sub> /mol N)	CRBP	CRBP pre	WRBP	WRBP pre	ln P	(ln P) pre	W <sub>EQ</sub> (kJ/mol CO <sub>2</sub> )	W <sub>EQ</sub> pre (kJ/mol CO <sub>2</sub> )
1	0.34	0.12	0.22	0.22	9%	9%	35%	35%	1.8	1.8	40.0	40.0
2	0.37	0.14	0.24	0.24	8%	8%	24%	24%	1.9	1.9	36.7	36.8
3	0.40	0.16	0.26	0.26	7%	7%	16%	16%	2.0	1.9	33.9	33.5
4	0.43	0.18	0.29	0.29	3%	3%	10%	10%	2.1	2.1	31.0	29.8

$$OPTLLDG = RLDG - 0.14 \quad (9)$$

$$OPTQ = 223.95 - 337.07RLDG + 25.30RLDG^2 \quad (10)$$

$$OPTW_{eq} = 62.88 - 54.93RLDG - 46.13RLDG^2 \quad (11)$$

$$OPT \ln P = 8.03 - 12.51RLDG + 22.04RLDG^2 \quad (12)$$

$$OPTCRBP = 0.33 - 0.67RLDG \quad (13)$$

$$OPTWRBP = 6.88 - 30.00RLDG + 33.33RLDG^2 \quad (14)$$

## 2.4 THE SECOND LAW EFFICIENCY

Figure 2-7 shows the effective utilization of stripping energy represented by the Second Law efficiency. CO<sub>2</sub> loading difference ( $\Delta LDG$ ) is calculated by subtracting CO<sub>2</sub> lean loading from CO<sub>2</sub> rich loading. The regressed expression for the Second Law efficiency is:

$$EFF = 0.76 - 1.27LLDG - 9.58LLDG^2 - 2.84RLDG^2 + 12.74RLDG * LLDG \quad (15)$$

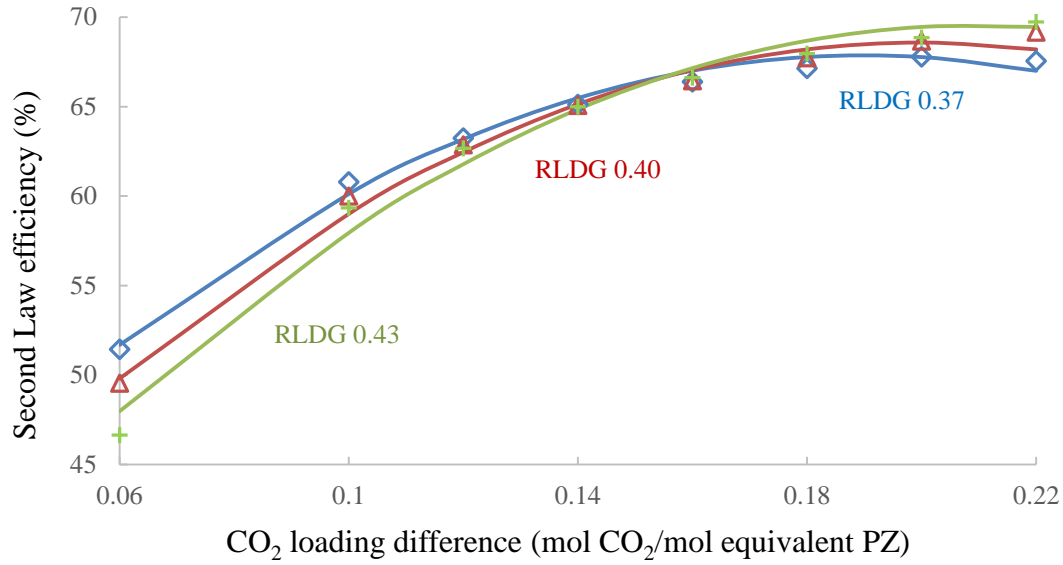


Figure 2-7: Second law efficiency of the advanced flash stripper with 5 m PZ. Marks calculated by  $W_{\min}/W_{\text{total,ideal}}$ . Lines predicted by Equation 15.

The curves on Figure 2-8 at different rich loading cross at a  $\Delta$ LDG of 0.14 mole CO<sub>2</sub>/mol equivalent PZ, which is the same as that giving the optimum equivalent work. The variation of efficiency with lean loading may result in part from the contribution of rich pump work as shown in Figure 2-8. The role of the bypass flows may also change with rich loading and delta loading as shown in Figure 2-9.

At low  $\Delta$ LDG (defined as CO<sub>2</sub> partial pressure irreversibility dominant part), the higher the CO<sub>2</sub> rich loading, the higher the CO<sub>2</sub> partial pressure. High CO<sub>2</sub> rich loading requires high pump work, as Figure 2-8 shows. The Second Law efficiency at high CO<sub>2</sub> rich loading is lower than that at low CO<sub>2</sub> rich loading at low  $\Delta$ LDG. As the pump work for different CO<sub>2</sub> rich loadings decreases and becomes closer to each other with increasing CO<sub>2</sub> loading difference, CO<sub>2</sub> partial pressure plays a less important role in the efficiency.



As CO<sub>2</sub> loading difference goes up, efficiency of different CO<sub>2</sub> rich loading increases and become close to each other.

The efficiency at different CO<sub>2</sub> rich loadings splits after 0.14 mole CO<sub>2</sub>/mol equivalent PZ loading difference. At high CO<sub>2</sub> loading difference (defined as sensible heat irreversibility dominant part), the Second Law efficiency of low CO<sub>2</sub> rich loading is lower than that of high CO<sub>2</sub> rich loading because lower CO<sub>2</sub> rich loading requires more bypasses, as Figure 2-9 shows. At high CO<sub>2</sub> loading difference, the steam stripping heat that must be recovered by rich solvent bypass is high. This leads to a corresponding higher irreversibility in cross exchanger and reboiler. The cross exchanger irreversibility has a stronger impact on low CO<sub>2</sub> rich loading. As a result, low CO<sub>2</sub> rich loading has lower Second Law efficiency at high CO<sub>2</sub> loading difference.

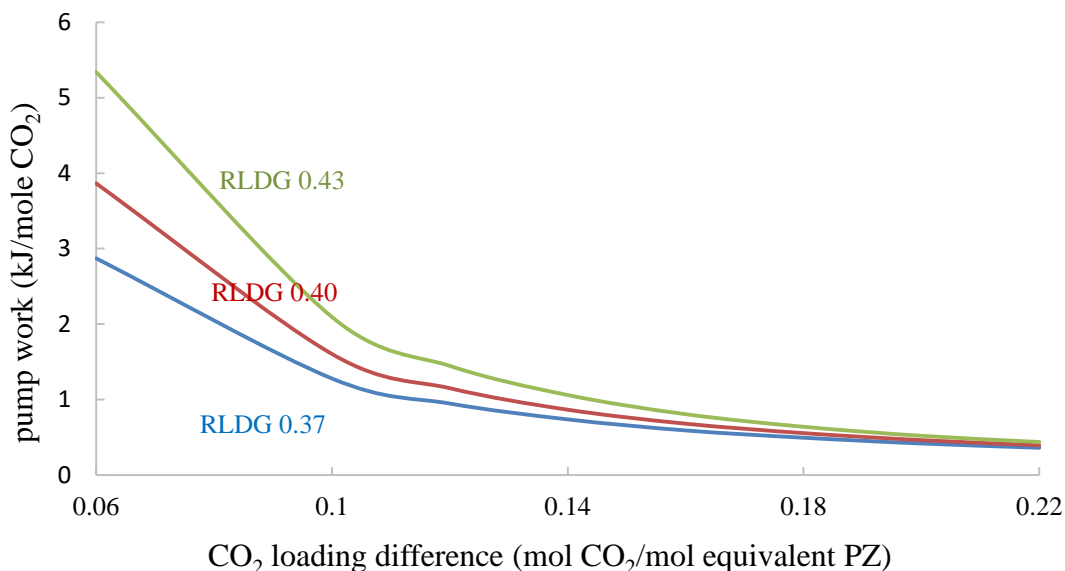


Figure 2-8: Pump work at variable CO<sub>2</sub> rich loading. Using 5 m PZ stripping at 150 °C with 2 m Mellapak 250 X packing at the optimum cold and warm rich bypasses, main exchanger LMTD = 5 °C, hot exchanger LMTD = 20 °C.

Due to the combined effect of pump irreversibility and cross exchanger irreversibility, there is a maximum efficiency with 0.37 mol/equivalent PZ CO<sub>2</sub> rich loading at 0.2 mol/equivalent PZ CO<sub>2</sub> loading difference (Figure 2-9). Since bypass has less impact at high CO<sub>2</sub> rich loading, the efficiencies of the other two CO<sub>2</sub> rich loadings are still increasing at 0.22 mol/equivalent PZ CO<sub>2</sub> loading difference, but tend to flatten out. They may reach maximum efficiency at higher CO<sub>2</sub> loading difference, where more energy recovery is required.

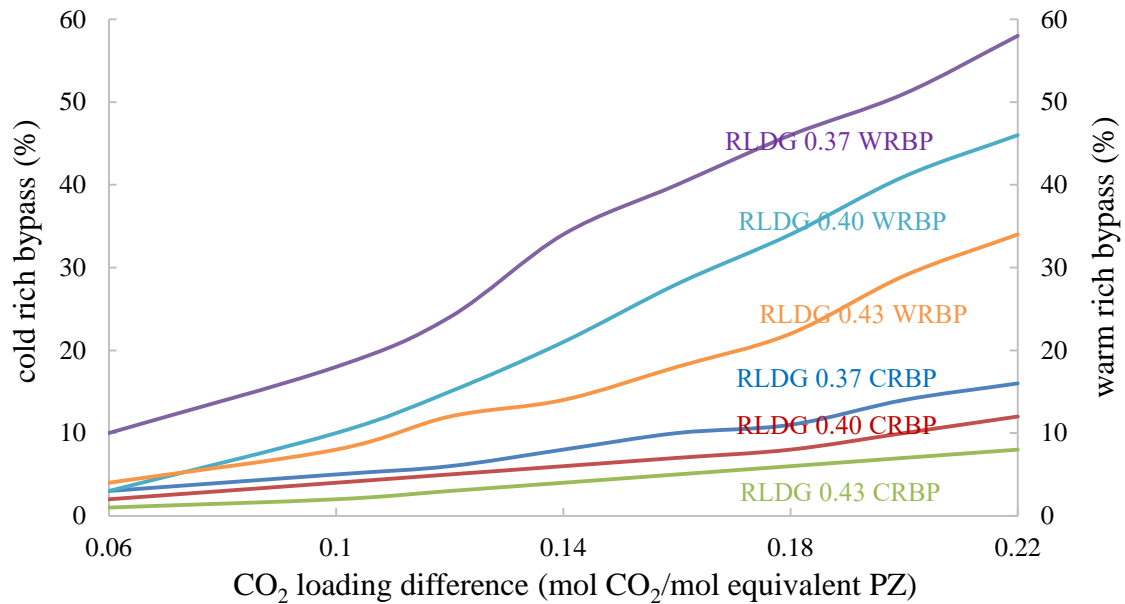


Figure 2-9: Cold and warm rich bypass for different CO<sub>2</sub> rich loading with CO<sub>2</sub> loading difference. Using 5 m PZ stripping at 150 °C with 2 m Mellapak 250 X packing at the optimum cold and warm rich bypasses, main exchanger LMTD = 5 °C, hot exchanger LMTD = 20 °C. The upper three lines are warm rich bypass presented on the right Y axis in %. The lower three lines are cold rich bypass presented on the left Y axis in %.

## 2.5 CONCLUSIONS

1. As the CO<sub>2</sub> rich loading varies from 0.37 to 0.43, the optimum lean loading occurs at a loading difference of 0.14 mol/equivalent PZ CO<sub>2</sub>.
2. The minimum total equivalent work decreases from 40.0 kJ/mol CO<sub>2</sub> to 31.0 kJ/mol CO<sub>2</sub> as the rich loading increases from 0.34 to 0.43 using 5 m PZ.
3. Heat duty, total equivalent work, stripping pressure, and bypasses are correlated as functions of CO<sub>2</sub> rich loading and lean loading.

$$Q = 119.1 + 342.2LLDG + 1891.5LLDG^2 + 497.7RLDG^2 - 3098.8RLDG * LLDG$$

$$W_{eq} = 39.4 + 101.0LLDG + 583.2LLDG^2 + 177.8RLDG^2 - 961.9RLDG * LLDG$$

$$\ln P = 6.6 - 5.9LLDG + 21.7LLDG^2$$

$$CRBP = 0.38 - 1.91LLDG + 2.44LLDG^2$$

$$WRBP = 2.43 - 9.56LLDG + 4.98LLDG^2 - 3.00RLDG^2 + 1.09RLDG * LLDG$$

$$OPTLLDG = RLDG - 0.14$$

$$OPTQ = 223.95 - 337.07RLDG + 25.30RLDG^2$$

$$OPTW_{eq} = 62.88 - 54.93RLDG - 46.13RLDG^2$$

$$OPT \ln P = 8.03 - 12.51RLDG + 22.04RLDG^2$$

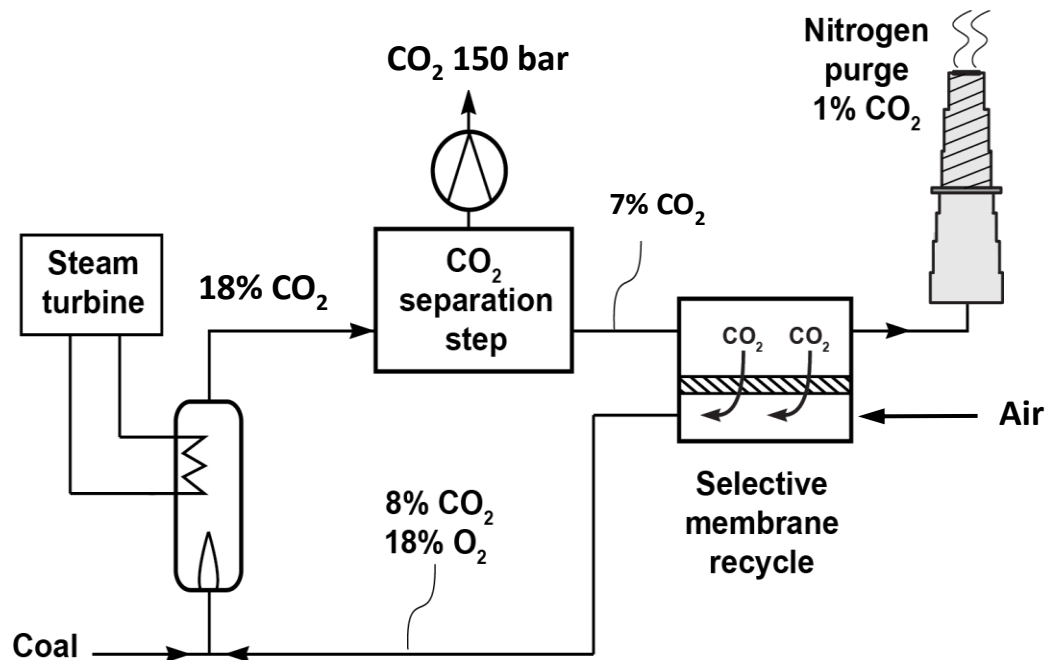
$$OPTCRBP = 0.33 - 0.67RLDG$$

$$OPTWRBP = 6.88 - 30.00RLDG + 33.33RLDG^2$$

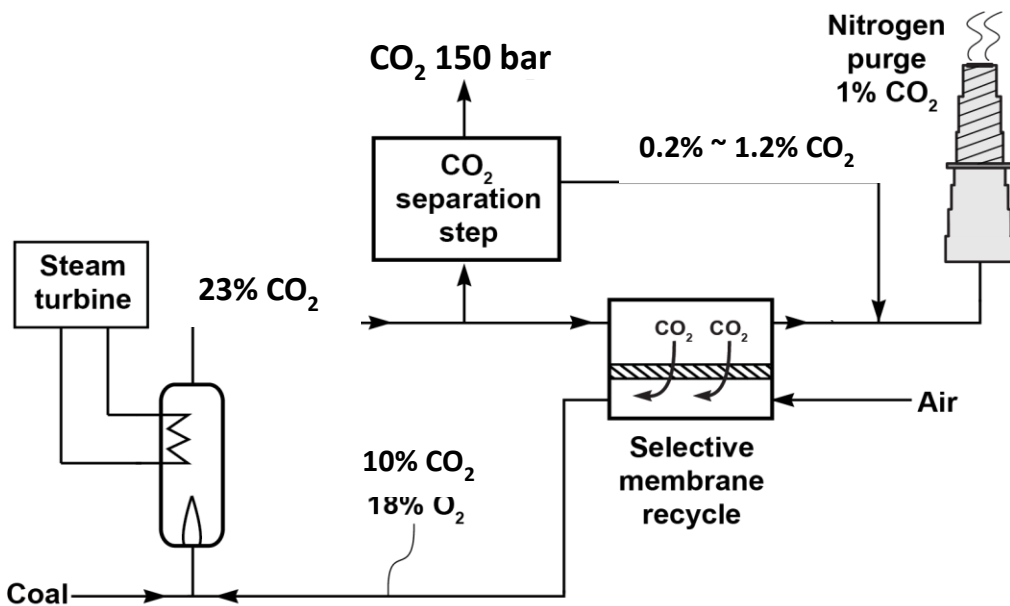
4. The Second Law efficiency of the advanced flash stripper varies from 45 to 70% as the delta loading varies from 0.06 to 0.22. At the optimum delta loading of 0.14 the efficiency is 65%.

### **Chapter 3: Regenerator Design for CO<sub>2</sub> Capture from Coal with Hybrid Amine/Membrane**

A hybrid amine/membrane system combining a CO<sub>2</sub> membrane separator with the absorber/stripper has been proposed for carbon capture from coal-fired power plants. The flue gas exits a coal-fired power plant with 12% CO<sub>2</sub>. Maintaining the same overall rate of CO<sub>2</sub> production, Membrane Technology and Research, Inc, (MTR) proposed enrich CO<sub>2</sub> in the flue gas from 12% to 18 and 23% by membranes via series and parallel hybrid amine/membrane CO<sub>2</sub> capture respectively. The configurations are shown in Figure 3-1. The membrane separator has been developed and modeled by MTR. The absorber and stripper performance is simulated using the Independence model for PZ in Aspen Plus<sup>®</sup>.



(a) A series hybrid amine/membrane configuration.



(b) A parallel hybrid amine/membrane configuration.

Figure 3-1: Series and Parallel configurations of hybrid amine/membrane CO<sub>2</sub> capture model (MTR, 2014).

Figure 3-2 shows the advanced flash stripper with cold rich exchanger bypass (CRBP) and warm rich bypass (WRBP), which offers better energy performance than a simple stripper. A cold rich bypass from the rich solvent recovers the steam stripping heat from the vapor in the heat recovery exchanger. A warm rich bypass is taken out from the rich solvent at boiling point between the cross exchangers and sent to the top of the stripper with cold rich bypass, serving as liquid feed. The flowrate of these two bypasses are optimized to have best stripper performance and recover most of the steam stripping heat. The vapor, which contains 90% CO<sub>2</sub>, is compressed to 150 bar and stored. The lean solvent generated at the bottom of the stripper is pumped back to the top of the absorber through the main cross exchangers.

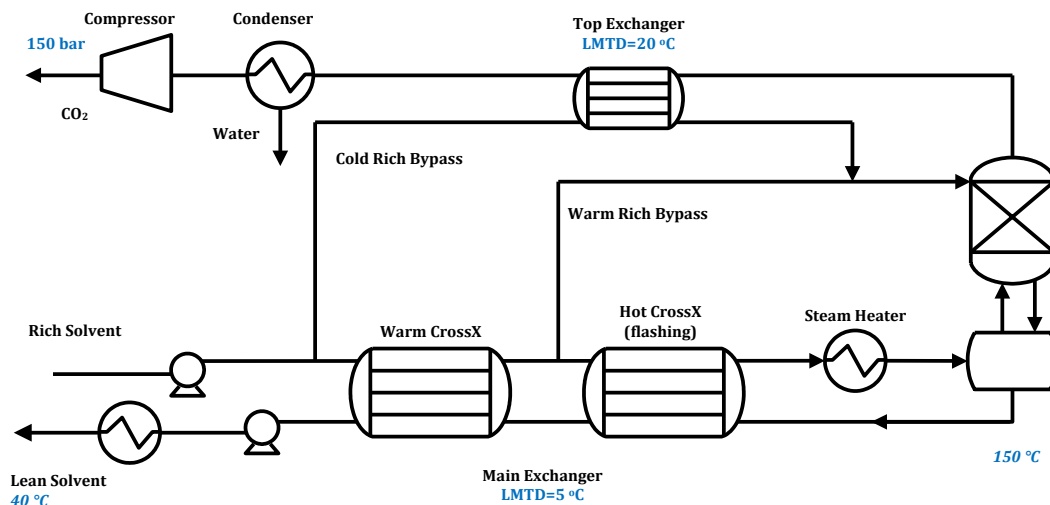


Figure 3-2: Stripper configuration for hybrid amine/membrane using 5 m PZ and 5 m MDEA/5 m PZ.

Due to the outstanding energy properties of aqueous piperazine (PZ), including high CO<sub>2</sub> capacity (mol CO<sub>2</sub> removed/kg solvent), high thermal stability, moderately high viscosity, oxidative degradation resistance, and low volatility in CO<sub>2</sub>-loaded solutions, it is a superior solvent for CO<sub>2</sub> capture by amine scrubbing. 8 m PZ consumes significantly

less regeneration energy than monoethanolamine (MEA). 5 m PZ solves the precipitation problem that the more viscous 8 m PZ causes in the solvent loop. 5 m PZ achieves a reduced approach temperature in the cross exchanger for its lower viscosity than 8 m PZ. The total energy performance for 5 m PZ is slightly higher than 8 m PZ.

Four base cases using 5 m PZ whose inlet CO<sub>2</sub> concentration and CO<sub>2</sub> removal rate were given by MTR (Cases 13, 14, 18-1, and 19-1) are simulated based on absorber performance. The total cost of CO<sub>2</sub> amine scrubbing is quantified to optimize process configuration and conditions. The capital cost and operating cost are used to evaluate the cost of amine regeneration. The capital cost is represented by the equipment purchase cost, which includes heat exchanger heat transfer area, compressor vapor flow rate, and reboiler steam flow rate. The operating cost is expressed by regeneration equivalent work.

Having higher CO<sub>2</sub> capacity than 5 m PZ, 5 m MDEA/5 m PZ and 2 m PZ/3 m 4-hydroxy-1-methylpiperidine (HMPD) are used to reduce the solvent recirculation rate, which has a major impact on both plant investment and operating cost. The Independence model for MDEA/PZ and PZ/HMPD in Aspen Plus<sup>®</sup> is used to simulate the stripper performance using 5 m MDEA/5 m PZ and 2 m PZ/3 m HMPD respectively. Equipment costs for Case 18 and 19 using 5 m PZ, 5 m MDEA/5 m PZ, and 2 m PZ/3 m HMPD are analyzed according to the economic part of the Frailie dissertation.

### 3.1 HYBRID AMINE/MEMBRANE CONFIGURATION

As input parameters of the stripper simulation, the lean and rich solvent conditions are simulated by a separate absorber model. For series design, which requires 60% CO<sub>2</sub> removal in amine scrubbing, a normal lean loading (LLDG) and an over-stripped lean loading are evaluated. The normal lean loading of 0.29 mol CO<sub>2</sub>/ mol N is established by setting the 0.037 ratio of the equilibrium partial pressure of CO<sub>2</sub> over the lean solvent and the partial pressure of the absorber outlet CO<sub>2</sub> (see Case 13). The over-stripped lean loading of 0.378 mol CO<sub>2</sub>/ mol N is established by 0.37 ratio of the equilibrium partial pressure of CO<sub>2</sub> over the lean solvent and the partial pressure of the absorber outlet CO<sub>2</sub> (see Case 14). Setting L/L<sub>min</sub> at 1.2 mol/mol in absorber, the rich solvent flowrate and rich (RLDG) and lean loadings of series design are calculated from the flue gas CO<sub>2</sub>, gas flowrate, and CO<sub>2</sub> removal rate.

Since the absorber outlet CO<sub>2</sub> is required to be 0.2~1.2% for parallel amine/membrane instead of 7% for series design, the amine CO<sub>2</sub> removal is set to be 99% and 95% for parallel design (see Cases 18 and 19 respectively). Only the over-stripped lean loading is evaluated. The over-stripped lean loading of 0.227 and 0.303 mol CO<sub>2</sub>/ mol N was established by setting the 0.37 ratio of the equilibrium partial pressure of CO<sub>2</sub> over the lean solvent and the partial pressure of the absorber outlet CO<sub>2</sub>. The rich solvent flowrate and rich and lean loadings of Cases 18 and 19 are calculated in the same way as the series design.



### 3.2 STRIPPER PERFORMANCE OF SERIES AND PARALLEL USING 5 M PZ

The amine regeneration system for the hybrid amine/membrane process was simulated by the Independence model in Aspen Plus®. As Figure 3-2 shows, the advanced flash stripper configuration was used. The equipment purchase cost incorporates two split cross-exchangers in series, a cold rich bypass exchanger, a convective steam heater, a low residence time flash tank, a smaller stripper column, a trim cooler, a compressor chain, pumps, and a condenser. The equipment cost of the whole process is the sum of the cost above and the cost of absorber, accumulator, reclainer, filter, and other safety equipment. The energy cost is evaluated by the total equipment cost, as discussed in Chapter 2.

The equipment cost of the heat exchanger depends on its heat transfer area, which can be calculated by Equation 1.

$$A = \frac{Q}{LMTD \times U} \quad (1)$$

Where,

$A$ : heat transfer area

$Q$ : heat duty transferred

$LMTD$ : log mean temperature difference

$U$ : overall heat transfer coefficient

$Q$  and  $LMTD$  are taken from the simulation result in Aspen Plus®. The overall heat transfer coefficient  $U$  can be calculated by Equation 2. The heat transfer resistance consists of the hot side fluid, cold side fluid and the exchanger wall between two fluids.

$$U = \left( \frac{1}{h_{hot}} + \frac{1}{h_{cold}} + \frac{\delta_w}{k_w} \right)^{-1} \quad (2)$$

Where,

$h_{hot}$ : heat transfer coefficient of hot side fluid

$h_{cold}$ : heat transfer coefficient of cold side fluid

$\delta_w$ : wall thickness

$k_w$ : thermal conductivity of wall

$h_{hot}$  and  $h_{cold}$  can be calculated by Equation 3. Thermal conductivity  $k$ , fluid density  $\rho$ , heat capacity  $C_p$ , fluid velocity  $v$ , and viscosity  $\mu$  are taken from the simulation result in Aspen Plus®.

$$h = 0.4 \times \left(\frac{k}{D}\right) \times \left(\frac{\rho v D}{\mu}\right)^{0.64} \times \left(\frac{C_p \mu}{k}\right)^{0.4} \quad (3)$$

The equipment cost of the pressure vessels depends on the its material weight, which is the product of its surface area, thickness, and material density. The surface area depends on the liquid flowrate and residence time. The wall thickness is calculated from the design pressure and the material used, which can be determined by Equation 4.

$$t = \frac{P_d D}{2SE - 1.2P_d} \quad (4)$$

Where,

$t$  (in): wall thickness

$P_d$  (psig): design pressure

$S$  (psi): maximum allowable stress

$E$ : weld efficiency

$D$  (in): diameter of vessel

Solvent flow rate, composition, and temperature of rich and lean solvent were put in the Independence model to match the inlet and outlet states with the absorber. Cases using 5 m PZ are stripped at 150 °C with a main exchanger LMTD of 5 °C, top exchanger LMTD of 20 °C, and CO<sub>2</sub> product compressed to 150 bar. The cold and warm rich bypasses are optimized to minimize the total equivalent work for each case.

Table 3-1 shows the stripper performance of Cases 13, 14, 18, and 19. Rich and lean loading values are from absorber results.

Table 3-1: Stripper energy performance of series and parallel designs using 5 m PZ.

<b>Hybrid Design</b>		<b>Series</b>		<b>Parallel</b>	
<b>Case Number</b>		<b>13</b>	<b>14</b>	<b>18</b>	<b>19</b>
<b>CO<sub>2</sub> Removal</b>	%	60	60	99	95
<b>L/G</b>		5	16	6	10
<b>LLDG</b>	mol CO <sub>2</sub> /mol N	0.290	0.378	0.227	0.303
<b>RLDG</b>	mol CO <sub>2</sub> /mol N	0.404	0.415	0.401	0.411
<b>Stripper Pressure</b>	bar	8.4	18.4	5.9	8.7
<b>Opt. CRB</b>	%	5	1	8	4
<b>Opt. WRB</b>	%	9	3	34	10
<b>W<sub>EQ</sub></b>	kJ/mol CO <sub>2</sub>	33.5	48.0	34.0	33.3
<b>heat duty</b>	kJ/mol CO <sub>2</sub>	94	134	94	93

Table 3-2 shows the equipment purchase cost of the Cases 13, 14, 18, and 19 at 593 MWe based on Frailie's spreadsheet (2014). The cost center of the stripper are the cross exchangers, compressors, steam heater, and reclaimer. Combining the energy performance and capital cost of the amine scrubbing system, parallel cases (Case 13&14) are better to be considered than series cases (Case 18&19).

Table 3-2: Equipment purchase cost of series and parallel designs using 5 m PZ at 593 MWe in Million dollars.

<b>MM\$</b>	<b>Hybrid-Series</b>		<b>Hybrid-Parallel</b>	
<b>Case Number</b>	<b>13</b>	<b>14</b>	<b>18</b>	<b>19</b>
<b>Absorber</b>	23.51	36.46	19.91	21.24
<b>Rich PZ Pump</b>	0.87	2.74	0.67	0.97
<b>Lean PZ Pump</b>	0.54	1.71	0.42	0.60
<b>Stripper</b>	1.67	2.45	1.87	1.72
<b>Steam Heater</b>	7.92	9.89	8.51	8.08
<b>Lean Solvent Trim Cooler</b>	1.17	3.39	0.91	1.31
<b>Cross Exchangers</b>	22.97	73.61	16.45	25.84
<b>Overhead Condenser &amp; CRBP Exchanger</b>	0.52	0.39	0.78	0.52
<b>Overhead Accumulator</b>	0.04	0.02	0.05	0.03
<b>Makeup Amine Tank</b>	0.36	0.36	0.36	0.36
<b>Water Tank</b>	0.11	0.11	0.11	0.11
<b>Surge Tank</b>	0.87	1.73	0.73	0.93
<b>Reclaimer</b>	4.43	13.86	3.28	4.92
<b>Rich Amine Carbon Filter</b>	0.18	0.28	0.16	0.17
<b>Particulate Filter</b>	0.14	0.14	0.14	0.14
<b>Compression</b>	12.2	12.0	13.1	12.5
<b>Total</b>	77.6	159.1	67.5	79.5
<b>Capture w/o compression</b>	65.3	147.2	54.3	66.9

### 3.3 STRIPPER PERFORMANCE OF PARALLEL USING 5 M MDEA/5 M PZ

Using PZ, hybrid parallel designs (Cases 18&19) are cheaper than series designs (Cases 13&14). Since 5 m MDEA/5 m PZ has a greater CO<sub>2</sub> capacity than 5 m PZ, Cases 18-2 and Case 19-2 using 5 m MDEA/5 m PZ stripped at 120 °C were studied to reduce the CO<sub>2</sub> recirculation rate compared with Case 18-1 (rich loading of 0.401 mol CO<sub>2</sub>/mol N and lean loading of 0.227 mol CO<sub>2</sub>/mol N) and Case 19-1 (rich loading of 0.411 mol CO<sub>2</sub>/mol N and lean loading of 0.303 mol CO<sub>2</sub>/mol N) using 5 m PZ. Chapter 2 optimized stripper using 5 m piperazine with rich loading from 0.37 to 0.43 mol CO<sub>2</sub>/mol N. 5 m PZ and 5m MDEA/5 m PZ are thermally stable up to 165 °C and 120 °C respectively. The stripper energy performance of 5 m PZ stripped at 150 °C and 5m MDEA/5 m PZ stripped at 120 °C are compared.

Table 3-3 compares the design information and energy consumption for parallel designs with 99% and 95% CO<sub>2</sub> removal using 5 m PZ (Cases 18-1 & 19-1) and 5 m PZ/5 m MDEA (Cases 18-2 & 19-2). For Cases 19-1 and 19-2, at the same CO<sub>2</sub> partial pressure, L/G and stripper pressure is much lower using 5 m MDEA/5 m PZ than using 5 m PZ. As a result, compression work is a little higher and pump work is much lower using 5 MDEA/5 m PZ. The total equivalent work of 5 m MDEA/5 m PZ is lower than that of 5 m PZ. L/G of Case 18-2 is not much lower than that of Case 18-1 since it is normal stripped (0.037 ratio of the equilibrium partial pressure of CO<sub>2</sub> over the lean solvent and the partial pressure of the absorber outlet CO<sub>2</sub> ) rather than over-stripped (0.37 ratio). Using 5 m MDEA/5 m PZ requires less total equivalent work than 5 m PZ. For Case 18, equivalent work using 5 m MDEA/5 m PZ (32.3 kJ/mol CO<sub>2</sub>) is less than using 5 m PZ (34.0 kJ/mol CO<sub>2</sub>). For Case 19, equivalent work using 5 m MDEA/5 m PZ (32.5 kJ/mol CO<sub>2</sub>) is less than using 5 m PZ (33.3 kJ/mol CO<sub>2</sub>).

Table 3-3: Comparison of stripper performance of parallel designs using 5 m PZ and 5 m MDEA/5 m PZ.

Case Number		18-1	18-2	19-1	19-2
CO <sub>2</sub> removal (%)		99		95	
Solvent		5 m PZ	5 m MDEA/ 5 m PZ	5 m PZ	5 m MDEA/ 5 m PZ
L/G		6	5	10	5
CO <sub>2</sub> rich loading	mol CO <sub>2</sub> /mol N	0.401	0.404	0.411	0.398
CO <sub>2</sub> lean loading	mol CO <sub>2</sub> /mol N	0.227	0.391	0.303	0.209
Pressure	bar	5.9	2.8	8.7	2.8
Stripper temperature	°C	150	120	150	120
Opt. CRBP	%	8	7	4	8
Opt. WRBP	%	34	29	10	30
Heat duty	kJ/mol CO <sub>2</sub>	93.6	93.7	93.3	94.6
Equivalent work	kJ/mol CO <sub>2</sub>	34.0	32.3	33.3	32.5

Table 3-4 compares the purchased equipment costs of parallel designs Cases 18 and 19 using 5 m PZ and 5 m MDEA/5 m PZ of 593 MWe based on Frailie (2014). Compared with 5 m PZ (5 cP), 5 m MDEA/5 m PZ has a higher viscosity (13 cP) and a lower absorption rate, which causes a higher required packing height. Compared with Case 18-1 using 5 m PZ, Case 18-2 using 5 m PZ/5 m MDEA costs \$3MM more in total mainly because of the higher absorber cost.

Table 3-4: Equipment purchase cost of parallel designs using 5 m PZ and 5 m PZ and 5 m MDEA/5 m PZ at 593 MWe in Million dollars.

<b>Case Number</b>	<b>18-1</b>	<b>18-2</b>	<b>19-1</b>	<b>19-2</b>
<b>Absorber</b>	19.91	31.09	21.24	33.70
<b>Rich PZ Pump</b>	0.67	0.50	0.97	0.54
<b>Lean PZ Pump</b>	0.42	0.31	0.60	0.33
<b>Stripper</b>	1.87	1.65	1.72	1.66
<b>Steam Heater</b>	8.51	8.27	8.08	8.15
<b>Lean Solvent Trim Cooler</b>	0.91	0.65	1.31	0.78
<b>Cross Exchangers</b>	16.45	8.61	25.84	8.88
<b>Overhead Condenser &amp; CRBP Exchanger</b>	0.78	0.78	0.52	0.78
<b>Overhead Accumulator</b>	0.05	0.03	0.03	0.03
<b>Makeup Amine Tank</b>	0.36	0.36	0.36	0.36
<b>Water Tank</b>	0.11	0.11	0.11	0.11
<b>Surge Tank</b>	0.73	0.62	0.93	0.63
<b>Reclaimer</b>	3.28	2.50	4.92	2.58
<b>Rich Amine Carbon Filter</b>	0.16	0.11	0.17	0.12
<b>Particulate Filter</b>	0.14	0.14	0.14	0.14
<b>Compression</b>	13.1	14.7	12.5	14.7
<b>Total</b>	67.5	70.5	79.5	73.5
<b>Capture w/o compression</b>	54.3	55.7	66.9	58.8

Due to the high CO<sub>2</sub> capacity of MDEA/PZ, less solvent recirculation rate is required for the same amount of CO<sub>2</sub> product. Case 19-2 using 5 m PZ/5 m MDEA costs \$6MM less in total than 19-1 using 5 m PZ mainly because of the lower cross exchanger cost, which is dominated by the less solvent recirculating rate. The costs using 5 m MDEA/5 m PZ associated with the rich amine pump, main heat exchanger, lean solvent cooler, and reclaimer are also lower due to the lower solvent rate.

Compared with 5 m PZ, compressors cost more using 5 m MDEA/5 m PZ because of their lower stripper pressures.

### 3.4 STRIPPER PERFORMANCE OF PARALLEL USING 2 m PZ/3 m HMPD

Similar with 5 m MDEA/5 m PZ, 2 m PZ/3 m HMPD requires less solvent recirculation rate because of its greater CO<sub>2</sub> capacity than 5 m PZ. Moreover, 2 m PZ/3 m HMPD has a viscosity as low as 5 m PZ (5 cP). Simulated in the Aspen Plus® model developed by Du, the energy performance using 2 m PZ 3 m HMPD changes less with varied lean solvent CO<sub>2</sub> partial pressure than PZ (see Figure 3-1). Compared with 5 m PZ, 2 m PZ/3 m HMPD is expected to reduce the regeneration capital cost due to its greater CO<sub>2</sub> capacity. Compared with 5 m MDEA/5 m PZ, 2 m PZ/3 m HMPD is expected to reduce the compression operating cost due to its greater stripper pressure at the same CO<sub>2</sub> partial pressure. Figure 3-3 suggests that using 2 m PZ/3 m HMPD costs more than 5 m PZ at low lean solvent CO<sub>2</sub> partial pressure (less than 0.12 kPa), but less at high lean solvent CO<sub>2</sub>.

Compared with 5 m PZ/5 m MDEA, Case 19 with 95% CO<sub>2</sub> removed by amine scrubbing system is simulated using 2 m PZ/3 m HMPD. In order to reduce the absorber cost, Case 19-2 using 5 m MDEA/5 m PZ has been developed into Case 19-4 with higher L/Lmin (1.3 instead of 1.2) and more coarse middle packing (2X instead of 250X). The capital cost of Case 19-4 (\$68.9MM) is less than Case 19-2 (\$73.5MM).



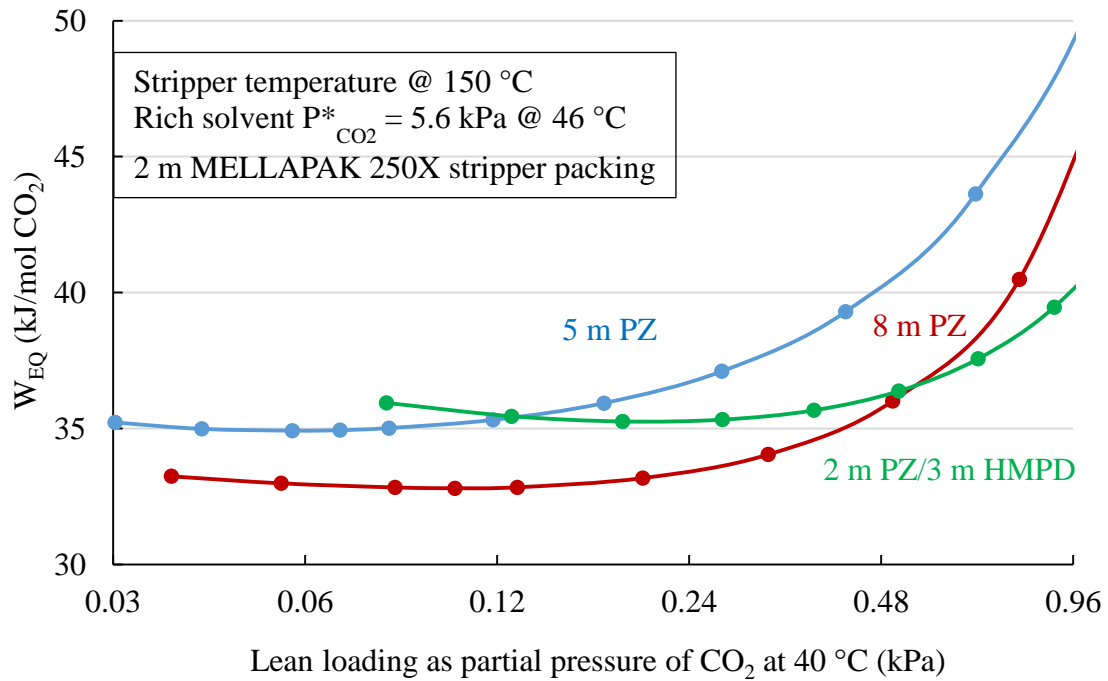


Figure 3-3: Total equivalent work of 5 m PZ (at 0.38 mol  $\text{CO}_2$ /mol N rich loading), 8 m PZ (at 0.39 mol  $\text{CO}_2$ /mol N rich loading), and 2 m PZ/3m HMPD (at 0.40 mol  $\text{CO}_2$ /mol N rich loading).  $\text{CO}_2$  equilibrium partial pressures of all rich loadings are 5.6 kPa.

Table 3-5 shows the design information and energy consumption for parallel designs with 95%  $\text{CO}_2$  removal using 5 m PZ/5 m MDEA (Case 19-4) and 2 m PZ/3 m HMPD (Case 19-5).

Table 3-5: Parallel designs with 95% CO<sub>2</sub> removal using 5 m PZ/5 m MDEA and 2 m PZ/3 m HMPD.

Case Number		19-4	19-5
Solvent		5 m PZ/5 m MDEA	2 m PZ/3 m HMPD
Solvent viscosity	cP	13	5
LLDG	mol CO <sub>2</sub> /mol N	0.21	0.26
RLDG	mol CO <sub>2</sub> /mol N	0.39	0.47
Lean Flow	kg/s	2159	2943
Stripper Temperature	(°C)	120	150
Pressure	bar	2.8	7.9
CRBP	%	11	8
WRBP	%	26	19
W <sub>EQ</sub>	kJ/mol CO <sub>2</sub>	31.4	32.1
Heat Duty	kJ/mol CO <sub>2</sub>	104	96

Table 3-6: Equipment purchase cost for Cases 19-4 and 19-5 (million \$).

Case Number	19-4	19-5
<b>Absorber</b>	28.67	25.42
<b>Rich PZ Pump</b>	0.54	0.73
<b>Lean PZ Pump</b>	0.33	0.45
<b>Stripper</b>	1.67	2.66
<b>Steam Heater</b>	8.21	7.97
<b>Lean Solvent Trim Cooler</b>	0.78	0.64
<b>Cross Exchangers</b>	9.14	10.02
<b>Overhead Condenser &amp; CRBP Exchanger</b>	0.78	1.32
<b>Overhead Accumulator</b>	0.03	0.03
<b>Makeup Amine Tank</b>	0.35	0.35
<b>Water Tank</b>	0.12	0.12
<b>Surge Tank</b>	0.65	0.89
<b>Reclaimer</b>	2.70	3.68
<b>Rich Amine Carbon Filter</b>	0.12	0.17
<b>Particulate Filter</b>	0.14	0.14
<b>Compression</b>	14.70	10.98
<b>Total</b>	68.93	65.57
<b>Capture w/o compression</b>	54.22	54.59

Table 3-7 shows the annual capital and operating cost of Cases 19-4 and 19-5 calculated by updated economic analysis. Compared with Case 19-4, the absorber of 19-5 costs less because of the lower viscosity of 2 m PZ/3 m HMPD. Case 19-5 has a lower cost for compression than 19-4 since higher stripper pressure is required. The duty of lean pump is cut down by operating at a high stripper pressure. More solvent required results in higher stripper cost and steam required for Case 19-5 than 19-4. All of this brings a lower total cost using 2 m PZ/3 m HMPD (\$38.7/tonne CO<sub>2</sub>) than 5 m PZ/5 m MDEA (\$41.5/tonne CO<sub>2</sub>) while the operating costs are almost the same.

Table 3-7: Annual capital and operating cost using 5 m PZ/5 m MDEA and 2 m PZ/3 m HMPD (\$/tonne CO<sub>2</sub>).

<b>Case Number</b>	<b>19-4</b>	<b>19-5</b>
<b>Absorber</b>	12.3	10.8
<b>Stripper</b>	6.6	7.7
<b>Compressor</b>	7.0	4.6
<b>Blower</b>	0.7	0.7
<b>TOTAL CAPEX</b>	26.6	23.8
<b>Rich Pump</b>	0.2	0.7
<b>Lean Pump</b>	0.4	0.0
<b>IC Pump &amp; Blower</b>	0.5	0.5
<b>Steam</b>	8.8	10.3
<b>Compression</b>	5.0	3.4
<b>TOTAL OPEX</b>	14.9	14.9
<b>TOTAL COST</b>	41.5	38.7

Table 3-8: Equipment purchase cost for all Cases (million \$).

MM\$	Hybrid-Series		Hybrid-Parallel					
Solvent	5 m PZ		5 m PZ	5 m MDEA/ 5 m PZ	5 m PZ	5 m MDEA/ 5 m PZ	2 m PZ/ 3 m HMPD	
Case Number	13	14	18-1	18-2	19-1	19-2	19-4	19-5
Absorber	23.51	36.46	19.91	31.09	21.24	33.7	28.67	25.42
Rich Pump	0.87	2.74	0.67	0.5	0.97	0.54	0.54	0.73
Lean Pump	0.54	1.71	0.42	0.31	0.6	0.33	0.33	0.45
Stripper	1.67	2.45	1.87	1.65	1.72	1.66	1.67	2.66
Steam Heater	7.92	9.89	8.51	8.27	8.08	8.15	8.21	7.97
Lean Solvent Trim Cooler	1.17	3.39	0.91	0.65	1.31	0.78	0.78	0.64
Cross Exchangers	22.97	73.61	16.45	8.61	25.84	8.88	9.14	10.02
Overhead Condenser & CRBP Exchanger	0.52	0.39	0.78	0.78	0.52	0.78	0.78	1.32
Overhead Accumulator	0.04	0.02	0.05	0.03	0.03	0.03	0.03	0.03
Makeup Amine Tank	0.36	0.36	0.36	0.36	0.36	0.36	0.35	0.35
Water Tank	0.11	0.11	0.11	0.11	0.11	0.11	0.12	0.12
Surge Tank	0.87	1.73	0.73	0.62	0.93	0.63	0.65	0.89
Reclaimer	4.43	13.86	3.28	2.5	4.92	2.58	2.7	3.68
Rich Amine Carbon Filter	0.18	0.28	0.16	0.11	0.17	0.12	0.12	0.17
Particulate Filter	0.14	0.14	0.14	0.14	0.14	0.14	0.14	0.14
Compression	12.2	12	13.1	14.7	12.5	14.7	14.7	10.98
Total	77.6	159.1	67.5	70.5	79.5	73.5	68.93	65.57
Capture w/o compression	65.3	147.2	54.3	55.7	66.9	58.8	54.22	54.59

### 3.5 CONCLUSIONS

1. Using PZ, hybrid parallel amine/membrane designs (Cases 18&19) are less expensive than series designs (Cases 13&14).
2. The energy cost of hybrid parallel using MDEA/PZ is lower than using 5 m PZ. The equivalent work of parallel with 99% CO<sub>2</sub> removal (Case 18) using 5 m MDEA/5 m PZ (32.3 kJ/mol CO<sub>2</sub>) is less than using 5 m PZ (34.0 kJ/mol CO<sub>2</sub>). The equivalent work of parallel with 95% CO<sub>2</sub> removal (Case 19) using 5 m MDEA/5 m PZ (32.5 kJ/mol CO<sub>2</sub>) is less than using 5 m PZ (33.3 kJ/mol CO<sub>2</sub>).
3. The capital cost of parallel with 99% CO<sub>2</sub> removal using 5 m MDEA/5 m PZ (\$70.5MM) is more than using 5 m PZ (\$67.5MM). The capital cost of parallel with 95% CO<sub>2</sub> removal using 5 m MDEA/5 m PZ (\$73.5MM) is less than using 5 m PZ (\$79.5MM).
4. The total annual cost of parallel with 95% CO<sub>2</sub> removal using 2 m PZ/3 m HMPD (\$38.7/tonne CO<sub>2</sub>) is less than using 5 m PZ (\$41.5/tonne CO<sub>2</sub>).

## **Chapter 4: Regeneration Design for NGCC CO<sub>2</sub> Capture with Amine-only and Hybrid Amine/Membrane**

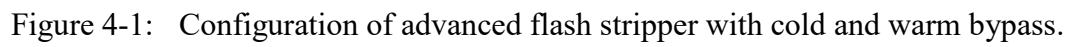
This chapter discusses the cost and performance of CO<sub>2</sub> capture from advanced natural gas combined-cycle (NGCC) plants by hybrid amine/membrane. The total cost of CO<sub>2</sub> amine scrubbing is quantified to optimize process configuration and conditions. The capital expense (CAPEX) and operating expense (OPEX) are annualized to show the effects of process conditions on the total cost. CAPEX is derived from the absorber packing volume, heat exchanger heat transfer area, compressor vapor flow rate, and reboiler steam flow rate. OPEX is derived from regeneration equivalent work.

Chapter 3 presents the hybrid amine/membrane for carbon capture from coal-fired power plants. The use of NGCC has been increasing since it emits fewer pollutants than coal-fired power plants. However, amine scrubbing cost for NGCC is higher than coal-fired power plants because of its much lower flue gas CO<sub>2</sub> concentration. Maintaining the same overall rate of CO<sub>2</sub> production, CO<sub>2</sub> selective membranes produced by MTR are combined with the amine scrubbing system to increase the CO<sub>2</sub> in the NGCC flue gas from 4% to over 12% by membranes, and reduce the flue gas volume entering the amine scrubbing system. 5 m PZ is used since it is cost effective and stable. The hybrid parallel design is applied to CO<sub>2</sub> capture for NGCC, which is more cost effective than series design based on the results for the Coal-fired power plant in Chapter 3. The flue gas parallel split ratio was calculated by ChemCAD®.

Three reference cases (without CO<sub>2</sub> capture, CO<sub>2</sub> capture using monoethanolamine, and CO<sub>2</sub> capture with 35% exhaust gas recycle (EGR) using advanced monoethanolamine) are compared to CO<sub>2</sub> capture with amine-only cases and hybrid amine/membrane cases.

In this chapter, the conditions and configurations of the amine scrubbing process are optimized at varied absorber inlet CO<sub>2</sub> concentration. As input parameters of the stripping simulation, the lean and rich solvent conditions are simulated by a separate absorber model at varied flue gas CO<sub>2</sub>. For each design, an intermediate lean loading and over-stripped lean loading are evaluated for CO<sub>2</sub> capture with amine-only and hybrid amine/membrane, respectively. The intermediate lean loading of 0.21 mol CO<sub>2</sub>/ mol N for amine-only is established by a 0.1 ratio of the equilibrium CO<sub>2</sub> partial pressure over the lean solvent to the partial pressure of the absorber outlet CO<sub>2</sub>. The over-stripped lean loading ranged from 0.25 to 0.27 mol CO<sub>2</sub>/ mol N for the hybrid amine/membrane and were determined as a 0.037 ratio of the equilibrium partial pressure of CO<sub>2</sub> over the lean solvent to the partial pressure of the varied absorber outlet CO<sub>2</sub>. The rich solvent flowrate and rich and lean loadings of the series design are set by  $L/L_{\min} = 1.2$  mol/mol in the absorber is determined by the flue gas CO<sub>2</sub>, gas flowrate, and CO<sub>2</sub> removal rate.

Based on the advanced flash stripper (AFS), stripper configurations and conditions are studied and optimized at each flue gas condition (see Figure 4-1) to minimize the total cost of the CO<sub>2</sub> capture system. Stripping temperature, cold rich bypass, and absorber inlet CO<sub>2</sub> are optimized to achieve the lowest cost-of-capture. The Independence model for piperazine (PZ) in Aspen Plus<sup>®</sup> with a rigorous e-NRTL thermodynamic framework is used to simulate the stripping performance. Equation Oriented Modeling in Aspen Plus<sup>®</sup> is used to find the optimum CRBP and warm rich bypass. CAPEX and OPEX in \$/tonne CO<sub>2</sub> removed was used to evaluate the CO<sub>2</sub> amine scrubbing system.





#### 4.1 AMINE-ONLY, HYBRID AMINE/MEMBRANE AND REFERENCE CASES

Nine configurations and sets of conditions were considered as described in Table 4-1. Flue gas parameters for different plant design configurations were analyzed and compared with three NGCC reference cases (DOE, 2010): without carbon capture (Case 13); with carbon capture (Case 14); and with carbon capture using 35% exhaust gas recycle EGR (Case 1c). Cases 1C1 and 1C2 are two post-combustion capture cases that combine 35% EGR with CO<sub>2</sub> amine scrubbing using 5 m PZ. Case 1C1 uses pump-around intercooling in the absorber instead of DCC, as Figure 4-2 shows. Flue gas enters the absorber at 135 °C. Case 1C2 uses DCC to cool the flue gas to 40 °C before it enters the absorber, as Figure 4-3 shows. The flue gas conditions for Ref 3 and 1C1 listed in Table 4-1 are before the DCC is employed. The absorber removes 90% of CO<sub>2</sub> from the flue gas.

A series of post-combustion cases (1D4, 1D2, 1D1, and 1D3) combine the CO<sub>2</sub> selective membrane with amine scrubbing. CO<sub>2</sub> in the absorber inlet is enriched by the membrane to 12.1% to 18.2% with varied membrane CO<sub>2</sub> removal capabilities, which is beneficial for absorber performance. Cases 1D4, 1D1, and 1D3 use 5 m PZ to remove 95% of CO<sub>2</sub> from the flue gas. Case 1D4 increases CO<sub>2</sub> to 12.1%, which is comparable to a coal-fired case. Figure 4-4 shows the complete configuration of a NGCC plant with CO<sub>2</sub> capture for Cases 1D4, 1D1, and 1D3. The flue gas conditions for these four cases in Table 4-1 are after the DCC. Case 1D2 uses pump-around intercooling in the absorber instead of DCC, as shown in Figure 4-5. Air cooling is used for the water wash. The optimum CRBP for CO<sub>2</sub> amine scrubbing at 18.2% absorber inlet CO<sub>2</sub> is only 5%, so a design without CRBP is simulated in order to cut down heat recovery exchanger cost.

Table 4-1: Flue gas parameters.

Case	Amine Scrubbing CO <sub>2</sub> removal	DCC	CO <sub>2</sub> Capture	Flow Rate (kmol/hr)	Flue Gas Temperature (°C)	Mole fraction		
						CO <sub>2</sub>	H <sub>2</sub> O	O <sub>2</sub>
13	0	-	N	113,831	106	0.04	0.09	0.12
14	90%	Y	MEA	111,116	135	0.06	0.10	0.09
1c	90%, combined w/ 35% EGR	Y						
1C1	90%, combined w/ 35% EGR	N	5 m PZ	35,830	29.7	0.12	0.03	0.09
1C2		Y						
1D4	95% <sup>1</sup> , hybrid amine/membrane	Y <sup>2</sup>						
1D2		N						
1D1		Y <sup>1</sup>						
Case 1D3		Y <sup>1</sup>						
				23,894	29.6	0.18	0.03	0.08

<sup>1</sup> When membranes are used in Case 1Dx, the total CO<sub>2</sub> removal rate of the entire hybrid system is 90%.

<sup>2</sup> The flue gas information is after DCC for Hybrid Amine/Membrane with DCC cases, and before DCC or without DCC for other cases.

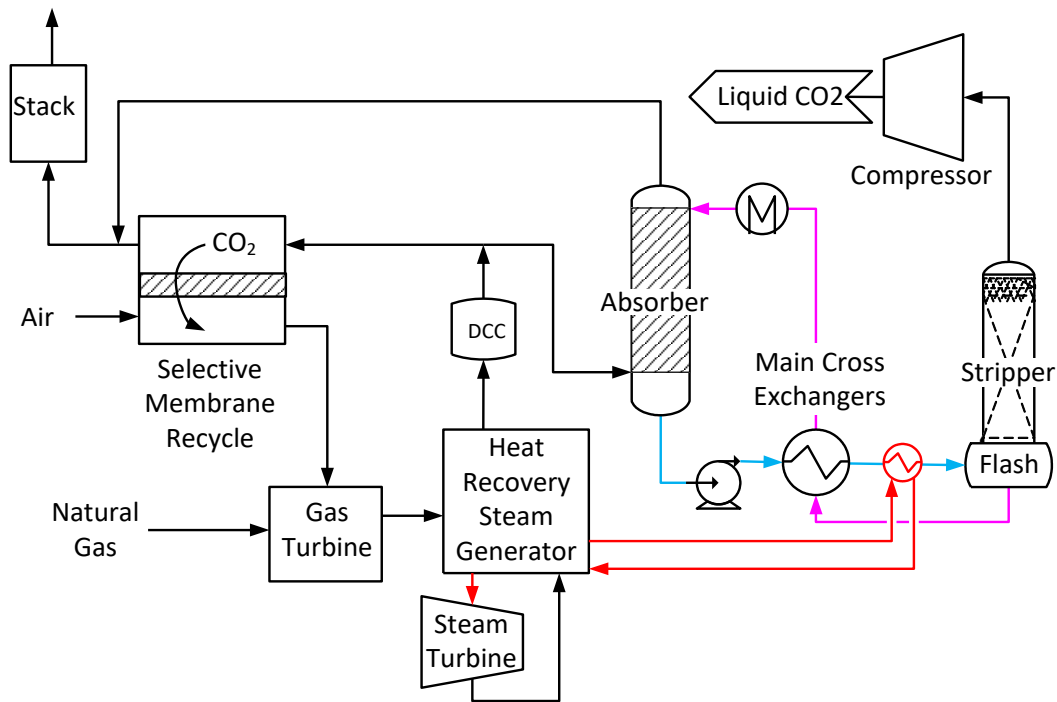


Figure 4-2: The complete configuration of a NGCC with CO<sub>2</sub> capture for Case 1C1.

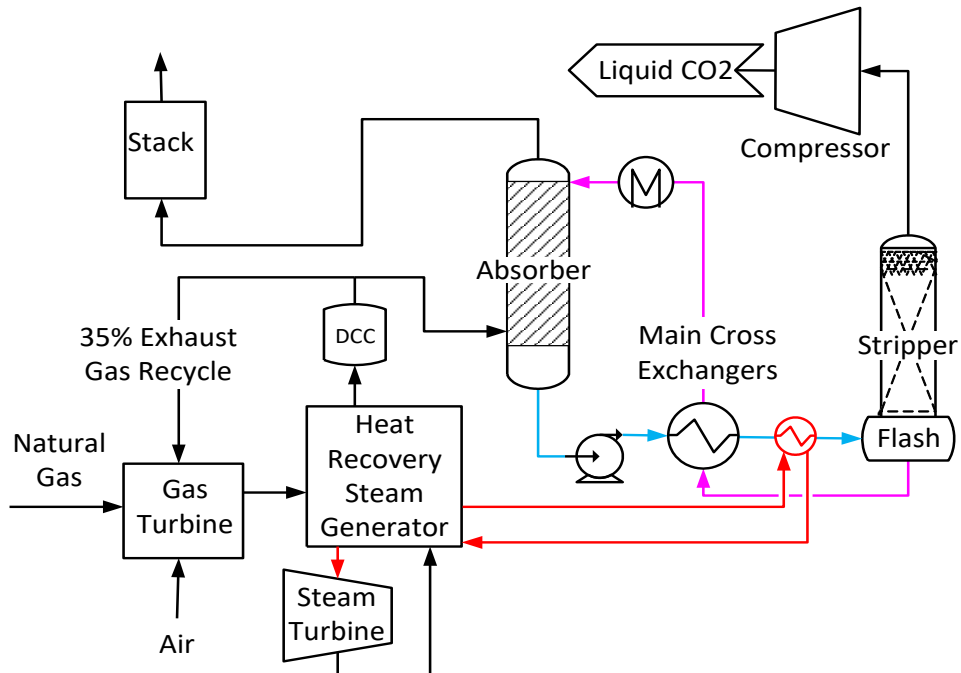


Figure 4-3: The complete configuration of a NGCC with CO<sub>2</sub> capture for Case 1C2.

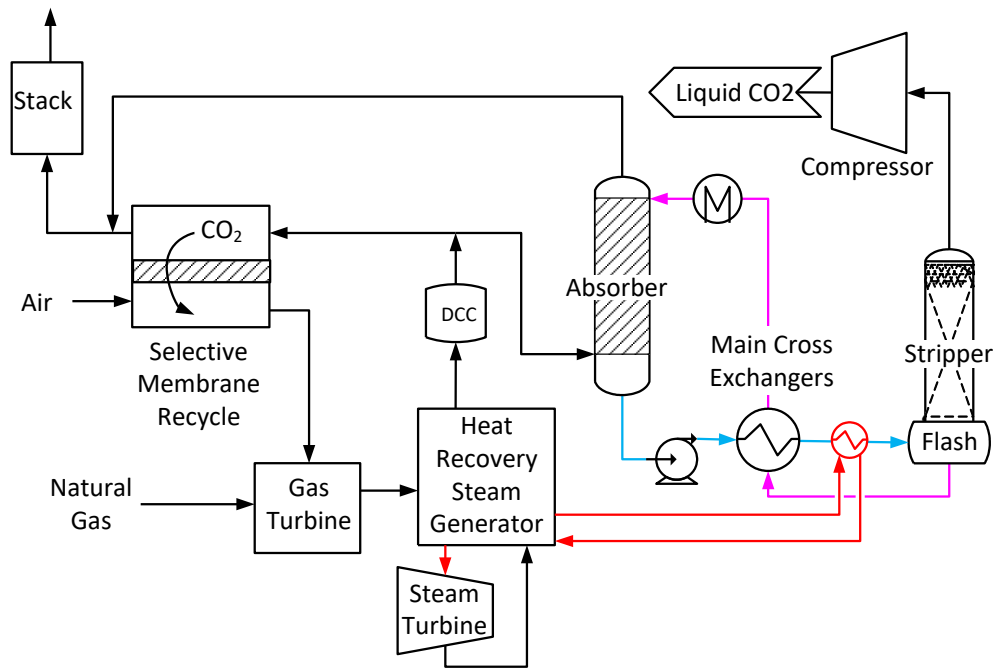


Figure 4-4: The complete configuration of a NGCC with CO<sub>2</sub> capture for Cases 1D4 1D1, and 1D3.

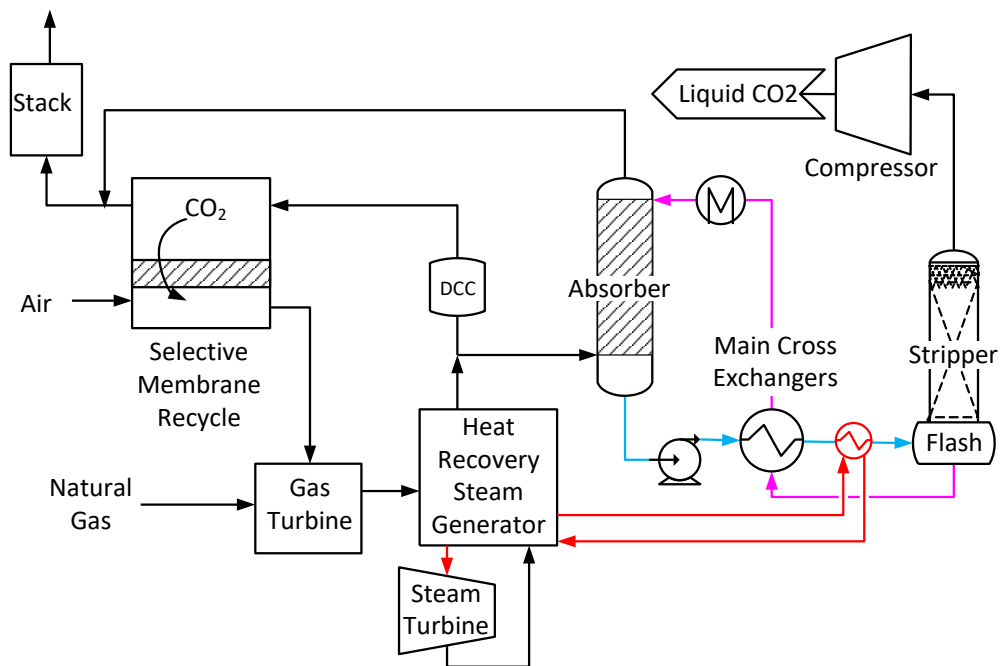


Figure 4-5: The complete configuration of a NGCC with CO<sub>2</sub> capture for Case 1D2.

## 4.2 CAPEX AND OPEX

Capital cost (CAPEX) and operating cost (OPEX) are used to evaluate the CO<sub>2</sub> amine scrubbing system.

### 4.2.1 Capital Cost

CAPEX includes equipment purchase cost, indirect cost, auxiliary facilities, installation, and labor. Equipment purchase cost for the regeneration system includes two cross exchangers, CRBP exchanger, steam heater, trim cooler, condenser, compressor, rich pump, lean pump, flash tank, and stripper column. Capital cost of pump-around pumps, intercooling pumps, and intercooling heat exchangers for the absorber system is calculated in the same way as lean pump and cross exchangers. In order to make CAPEX comparable to OPEX, CAPEX is in the form of annualized equipment purchase cost (PEC) (see Equation 1).

$$\text{CAPEX (\$/TONNE CO}_2\text{)} = \frac{PEC \times \alpha \times \beta}{MTCO_2 \text{ Captured}} \quad (1)$$

Where,

$\alpha$  is the total capital scaling factor, which is 5.

$\beta$  is the annualizing factor, which is 20%.

The annualizing factor is intended to represent return on investment, depreciation, income tax, and maintenance.

PEC in the regeneration process includes heat exchangers, columns, packings, compressor, and pumps. PEC of the heat exchangers is derived from heat transfer area, which is calculated from the heat duty, log mean temperature difference, and fluid heat transfer coefficient. PEC of the column and packing are determined by the vapor flow rate since the diameter of the stripper is varied to match 80% flooding. PEC of the

compressor depends on the gas flow rate while PEC of the pumps is calculated from its duty based on vendors' cost.

#### 4.2.2 Operating Cost

OPEX is calculated from total the equivalent work ( $W_{EQ}$ ) in units of kJ/mol  $CO_2$  (see Equation 2), which is the sum of pump work, compression work, and heat work (see Equation 3). It includes the electricity consumed by the rich pump, compressor, and steam heater.

$$OPEX (\$/TONNE CO_2) = W_{EQ} \times COE \quad (2)$$

Where,

$COE$  is the cost of electricity, which is \$70/MWhr.

$$W_{EQ} (kJ/mol CO_2) = W_{PUMP} + W_{COMP} + W_{HEAT} \quad (3)$$

Heat work is calculated from the thermal heat duty by applying Carnot cycle and an efficiency of 90% for a non-ideal expansion in the steam turbines (see Equation 4).

$$W_{HEAT} (kJ/mol CO_2) = 90\% \left( \frac{T_{STEAM} - 313.15}{T_{STEAM}} \right) Q_{steam\ heater} \quad (4)$$

Compression work can be approximated by Equation 5 from Lin (2014), which is assumes a discharge pressure of 150 bar.

$$W_{COMP} (kJ/mol CO_2) = -3.48 \ln(Pin) + 14.85 \quad (5)$$

### 4.3 OPTIMIZATION SPECIFICATIONS

Total annual cost for the whole CO<sub>2</sub> amine scrubbing system is the sum of CAPEX and OPEX. As operating cost accounts for 60% of the total regeneration cost, minimizing  $W_{EQ}$  is the objective for regeneration. The Independence model for PZ in Aspen Plus® was used as a base to simulate the regeneration performance.

The fixed variables for regeneration optimization are rich solvent inlet composition and temperature, lean solvent temperature, and CO<sub>2</sub> lean loading. In the regeneration model, the lean solvent outlet temperature of the trim cooler is set to match the lean solvent temperature. The stripping pressure is changed to match the CO<sub>2</sub> lean loading at stripping temperature.

Some other variables are fixed according to previous optimization. In the base case studies, 4 m stripper packing height is used. The log mean temperature difference (LMTD) of the CRBP exchanger (heat recovery exchanger) is 20 °C. The LMTD of the cross exchanger is 7 °C. The CO<sub>2</sub> product is condensed to 40 °C before it enters the compressor. The residence time in the flash tank is 5 minutes.

CRBP and WRBP flow rates are optimized to minimize the total equivalent work, where most steam stripping heat was recovered.

#### 4.4 STRIPPING TEMPERATURE OPTIMIZATION

Figure 4-6 shows the total equivalent work changing with CO<sub>2</sub> lean loading at varied stripping temperature with rich loading 0.4 mol CO<sub>2</sub>/mol alkalinity and 4 m stripper packing.

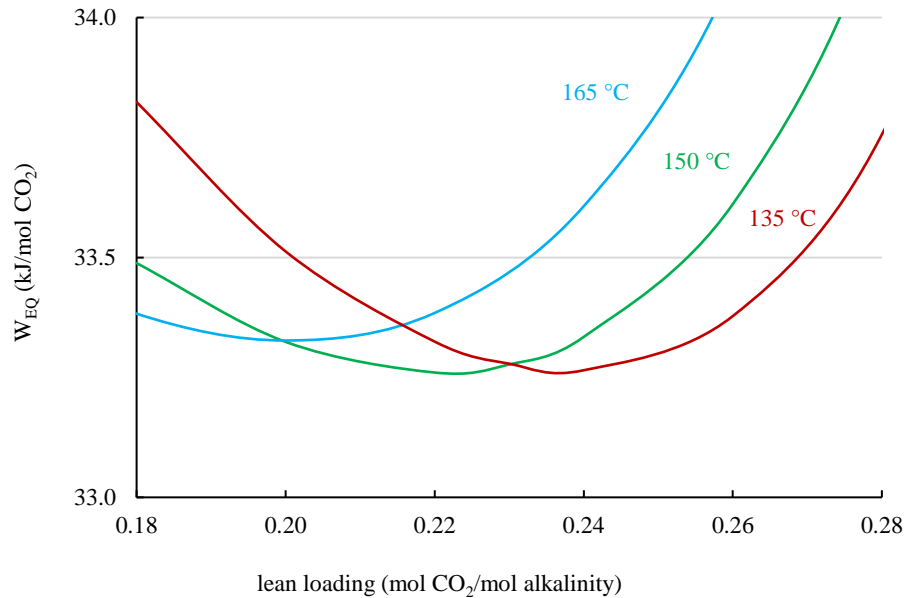


Figure 4-6: Total equivalent work at varied stripping temperature, 0.4 rich loading, 4 m stripper packing.

Higher stripping temperature requires less work at low lean loading and more work at high lean loading. At low lean loading more stripping steam is required to remove the CO<sub>2</sub>. At high lean loading the capacity of the solvent is reduced, so more sensible heat must be provided by the steam.

As stripping temperature increases, the optimum lean loading shifts towards a lower value. To optimize the regeneration cost, stripping at 145 °C and 150 °C using 5 m PZ



are compared, since the expected lean loading is in the range of 0.2 to 0.26 mol CO<sub>2</sub>/mol N for NGCC CO<sub>2</sub> capture using hybrid amine/membrane.

Table 4-2 shows the cost of amine-only designs with 35% EGR at different stripping temperatures, with and without DCC. The absorber inlet CO<sub>2</sub> is 6.3% enriched by EGR for all four cases. Stripping at 150 °C costs slightly less than at 145 °C. Capital cost for the first cross exchanger at 150 °C is higher than for 145 °C because less CRBP is separated from the rich solvent. Flash tank and rich pump capital costs are also higher, and compressor cost is lower, because of higher stripping pressure. All other capital costs for stripping at 150 °C are lower than for 145 °C.

Cases without DCC cost much less than those with DCC. While cases without DCC cost more for the absorber, capital cost of the DCC is eliminated. All other capital costs are lower for cases without DCC. The operating cost differences among the four cases are not as significant as the differences in capital cost.

The lowest capital cost of all amine scrubbing combined with EGR cases is achieved with stripping at 150 °C and no DCC. These four cases correspond to Cases 1C22, 1C21, 1C12, and 1C11 in sequence in Table 4-3.

Table 4-2: Annual Cost of amine-only designs with 6.3% absorber inlet CO<sub>2</sub> (\$/ tonne CO<sub>2</sub>) at different stripping temperatures, with and without DCC.

	145 °C With DCC	145 °C No DCC	150 °C With DCC	150 °C No DCC
Rich loading (mol CO <sub>2</sub> /mol N)	0.37	0.37	0.37	0.37
Lean loading (mol CO <sub>2</sub> /mol N)	0.21	0.21	0.21	0.21
CAPEX (\$/tonne CO <sub>2</sub> )				
Absorber	13.4	15.1	13.4	15.1
DCC	4.0	0	4.0	0
Cross EX1	3.7	3.3	4.1	3.7
Cross EX2	2.7	2.6	2.5	2.5
CRBP EX	2.0	2.0	1.9	1.9
Trim cooler	0.2	0.1	0.2	0.1
Steam heater	1.4	1.4	1.3	1.3
Flash tank	0.6	0.6	0.7	0.7
Stripper column	0.7	0.7	0.6	0.6
Condenser	0.2	0.3	0.2	0.2
Compressor	5.8	5.8	5.4	5.4
Rich pump	0.30	0.30	0.34	0.35
Lean pump	0.04	0.04	0.01	0.00
W <sub>EQ</sub> (kJ/mol CO <sub>2</sub> )	37.5	37.7	37.2	37.4
OPEX (\$/tonne CO <sub>2</sub> )	18.7	18.9	18.6	18.8
Total cost (\$/tonne CO <sub>2</sub> )	53.7	51.1	53.3	50.7

Table 4-3: Summary of cases.

	Amine-only				Hybrid amine/membrane						
Case	1C11	1C12	1C21	1C22	1D4	1D21A	1D22A	1D23A	1D1	1D31A	1D32A
Removal amine (%)		90						95			
Membrane		-				3rd Generation1				Nth of a kind <sup>1</sup>	
Flue gas temp. (°C)		135			29.7		146.0		29.6		29.6
Flue gas flow rate (knol/hr)		72,164			35,830		30,506		28,757		23,894
CO <sub>2</sub> (%)		6.3			12.1		14.1		15.2		18.2
Note	Parallel cooling		Wet cooling		Wet C.	Parallel cooling		Dry	Wet C.	Wet cooling	
DCC T (°C)	without		40		25	without			25	25	
Rich solvent T (°C)	49.2		43.3		30.9	57.0		64.3	28.8	27.7	
Trim cooler T (°C)	49		40		25	50		50	25	25	
Rich loading	0.368		0.369		0.396	0.369		0.321	0.403	0.408	
Lean loading	0.210		0.210		0.247	0.159		0.159	0.259	0.268	
Lean solvent flowrate (kg/s)	1082	1081	1073	1072	1169	780	777	1009	1224	1266	1267
Stripping temp (°C)	150	145	150	145	150	150	145	150	150	150	
CRBP & VEX	w/	w/	w/	w/	w/	w/	w/	w/	w/	w/	w/o
CRBP (%)	13	14	12	13	7	25	28	25	6	6	0
WRBP (%)	40	41	41	43	31	48	47	50	25	23	37
Stripping pressure (bar)	5.6	4.8	5.6	4.8	6.4	4.9	4.2	4.9	6.7	7.0	7.0
WHEAT (kJ/mol CO <sub>2</sub> )	27.9	27.7	27.7	27.5	25.1	30.4	30.8	35.4	24.6	24.3	26.1
WCOMP (kJ/mol CO <sub>2</sub> )	8.9	9.4	8.9	9.4	8.4	9.3	9.8	9.3	8.2	8.1	8.1

<sup>1</sup> These membranes are provided by Membrane Technology & Research, Inc.

Table 4-3 continued

WPUMP (kJ/mol CO <sub>2</sub> )	0.6	0.5	0.6	0.5	0.8	0.4	0.3	0.5	0.9	1.0	1.0
W <sub>EQ</sub> (kJ/mol CO <sub>2</sub> )	37.4	37.7	37.2	37.5	34.3	40.1	41.0	45.3	33.7	33.4	35.1
Stripper D (m)	5.3	5.5	5.2	5.5	4.6	5.7	5.9	6.1	4.4	4.3	4.5
CO <sub>2</sub> product (kmol/s)	1.14	1.14	1.14	1.14	1.14	1.14	1.14	1.14	1.15	1.14	1.14
CO <sub>2</sub> product (m <sup>3</sup> /s)	5.3	6.2	5.2	6.2	4.6	5.6	6.5	5.9	4.4	4.1	4.1
Amine total (\$/tonne CO <sub>2</sub> )	50.7	51.1	53.3	53.7	44.0	44.6	45.5	48.1	42.6	41.8	42.2
Total cost with membrane (\$/tonne CO <sub>2</sub> )	50.7	51.1	53.3	53.7	52.9	54.9	55.8	58.4	53.2	60.0	60.4

#### 4.5 COST OF HYBRID AMINE/MEMBRANE DESIGNS WITH AND WITHOUT DCC

Table 4-4 shows the cost comparison of hybrid amine/membrane designs with and without DCC. Two cases without DCC (absorber inlet CO<sub>2</sub> at 14.1%) are compared to cases with DCC (DCC inlet CO<sub>2</sub> at 14.1% and cooling at 25 °C). Parallel cooling means only water wash and trim cooler are cooled by air. Dry cooling means all the coolers are cooled by air. Wet cooling is all cooled by water. It is assumed that streams are cooled to 50 °C by air and to 25 °C by water.

Table 4-4: Cost of hybrid designs with 14.1% absorber inlet CO<sub>2</sub> (\$/tonne CO<sub>2</sub>).

	Parallel cooling	Dry cooling	Wet cooling <sup>1</sup>
Rich loading (mol CO <sub>2</sub> /mol N)	0.37	0.32	0.40
Lean loading (mol CO <sub>2</sub> /mol N)	0.16	0.16	0.26
CRBP (%)	25	25	6
Lean solvent flowrate (kg/sec)	780	1009	1224
CAPEX (\$/tonne CO <sub>2</sub> )			
Absorber	5.7	6.6	5.1
DCC	0	0	2.3
Cross EX1	1.9	2.2	5.8
Cross EX2	3.7	3.1	2.3
CRBP EX	2.7	3.4	1.2
Stripper	6.3	6.1	5.3
Compressor	5.7	5.7	5.0
W <sub>EQ</sub> (kJ/mol CO <sub>2</sub> )	40.1	45.3	33.7
OPEX (\$/tonne CO <sub>2</sub> )	18.6	21.0	15.7
Total cost (\$/tonne CO <sub>2</sub> )	44.6	48.1	42.6

<sup>1</sup> For Wet Cooling Case, DCC inlet CO<sub>2</sub> is 14.1%, while absorber inlet CO<sub>2</sub> is 15.2%.

Since the absorber gas inlet temperature is high without DCC, the lean loading chosen to match the absorber water balance is low. The low lean loading without DCC leads to more operating and capital cost for stripping and compressing. Without DCC requires more CRBP to recover the steam stripping heat and lower first cross exchanger capital cost.

Operating at the same lean loading, dry cooling requires more solvent than parallel cooling since the absorber is intercooled at a higher temperature. Both capital and operating cost are higher for dry cooling than parallel cooling.

These four cases correspond to Cases 1D21A, 1D23A, and 1D1 in sequence in Table 4-3.

#### **4.6 COST OF AMINE-ONLY AND HYBRID AMINE/MEMBRANE DESIGNS**

Table 4-5 shows a cost comparison of hybrid amine/membrane designs with varied inlet CO<sub>2</sub>. Amine-only designs with 35% EGR without DCC stripping at 150 °C is used as a reference. Figure 4-5 shows the capital cost, operating cost, and total cost at varied inlet CO<sub>2</sub>. The dashed lines represent the cost of the amine scrubbing element. Dots at 6.3% and higher than the without DCC represent the cost of amine-only with DCC (absorber intercooling at 40 °C). The solid lines represent the total cost including both amine and membrane. The difference between the dashed and solid lines shows the cost of the membrane.

6.3% is the absorber inlet CO<sub>2</sub> for the amine-only design with 35% EGR. The four cases in the table correspond to Cases 1C11, 1D4, 1D1 and 1D31A in sequence in Table 4-3. 12.1%, 15.2%, and 18.2% are the absorber inlet CO<sub>2</sub> concentrations for the hybrid amine/membrane designs. Stripping at 150 °C and absorber intercooling at 25 °C were used for all of these designs. The flue gas flow rates for hybrid amine/membrane designs are only one half of the amine-only designs.

Table 4-5: Cost of amine-only design and hybrid amine/membrane designs using 5 m PZ (\$/tonne CO<sub>2</sub>) at varied absorber inlet CO<sub>2</sub>.

Inlet CO <sub>2</sub> conc.	6.3%	12.1%	15.2%	18.2%
Rich loading (mol CO <sub>2</sub> /mol N)	0.37	0.40	0.40	0.41
Lean loading (mol CO <sub>2</sub> /mol N)	0.21	0.25	0.26	0.27
Solvent rate (kg/s)	1082	1169	1224	1267
Stripping Pressure (bar)	5.6	6.4	6.7	7.0
CRBP (%)	13	7	6	5
Absorber	15.1	10.4	9.4	8.6
Compressor	5.4	5.1	5.0	4.9
CRBP EX	1.9	1.3	1.2	1.1
Steam heater	1.3	1.1	1.0	1.0
Stripper column	0.6	0.5	0.5	0.5
Cross EX	6.2	7.9	8.1	8.4
Other regeneration	1.4	1.7	1.8	8.4
Amine CAPEX (\$/tonne CO <sub>2</sub> )	31.9	28.0	27.0	26.3
W <sub>EQ</sub> (kJ/mol CO <sub>2</sub> )	37.2	34.3	33.7	33.4
Amine OPEX (\$/tonne CO <sub>2</sub> )	18.8	16.1	15.7	15.4
Membrane cost (\$/tonne CO <sub>2</sub> )	0	8.8	10.6	18.3
Total cost (\$/tonne CO <sub>2</sub> )	50.7	52.9	53.2	60.0



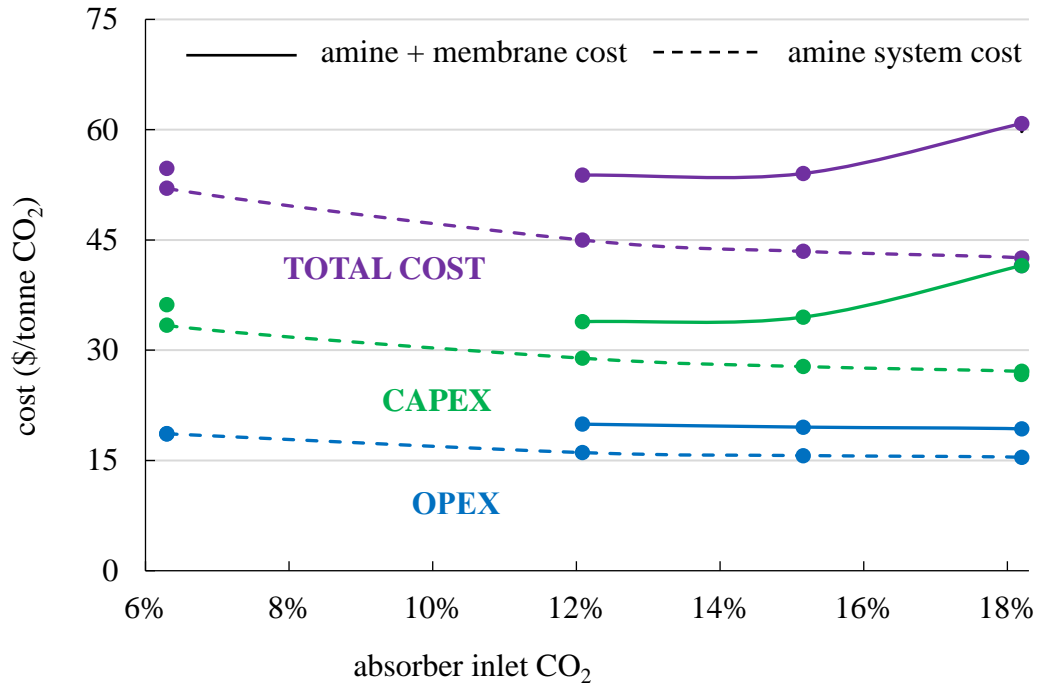


Figure 4-7: Annual cost of hybrid amine/membrane at varied absorber inlet CO<sub>2</sub> 6.3%, 12.1%, 15.2%, and 18.2%.

Compared with amine-only designs, as the inlet CO<sub>2</sub> is increased by the membrane, all of the capital costs for hybrid amine/membrane designs are reduced except the first cross exchanger. The reason for the high first cross exchanger cost is the low absorber outlet rich solvent temperature. For hybrid amine/membrane designs, the cost of the first cross exchanger increases with the inlet CO<sub>2</sub> because of decreasing required CRBP, and the flash tank and rich pump cost increases because of increasing stripping pressure. All of the other costs decrease with inlet CO<sub>2</sub>.

As absorber inlet CO<sub>2</sub> increases, total amine cost decreases. At the same time, the membrane cost increases rapidly, making the hybrid amine/membrane design cost lowest at 12.1%, the lowest absorber inlet CO<sub>2</sub> for hybrid designs.

So far, the total cost of a hybrid amine/membrane design is slightly higher than an optimum amine-only design.

#### 4.7 COST OF STRIPPING USING 5 M PZ WITH OR WITHOUT CRBP

Table 4-6 shows the comparison of total annual cost with (Case 1D31A) and without CRBP (Case 1D32A). This work is based on the hybrid amine/membrane design with 18.2% absorber inlet CO<sub>2</sub> mole fraction both stripping at 150 °C.

Table 4-6: Annual cost with and without CRBP (\$/tonne CO<sub>2</sub>) at CO<sub>2</sub> 18.2%.

CRBP	Y	N
CRBP EX (\$/tonne CO <sub>2</sub> )	1.1	0
Cross EX 1 (\$/tonne CO <sub>2</sub> )	6.1	6.6
Cross EX 2 (\$/tonne CO <sub>2</sub> )	2.3	2.1
Condenser (\$/tonne CO <sub>2</sub> )	0.1	0.4
Other CAPEX (\$/tonne CO <sub>2</sub> )	16.7	16.9
W <sub>EQ</sub> (kJ/mol CO <sub>2</sub> )	33.4	35.1
OPEX (\$/tonne CO <sub>2</sub> )	15.4	16.2
Total cost (\$/tonne CO <sub>2</sub> )	41.8	42.2

After the membrane enriches the absorber inlet CO<sub>2</sub> mole fraction to 18.2%, CO<sub>2</sub> loadings of both rich and lean solvents are high. The optimum CRBP is only 5% at this absorber inlet CO<sub>2</sub> mole fraction, leaving little steam stripping heat to be recovered. The capital cost can be reduced by removing CRBP and CRBP exchanger. If this is done, the optimum WRBP increases to 37.2% from 22.6% and the capital cost of the first cross exchanger increases while that of the second decreases. The saving on CRBP exchanger CAPEX at 18.2% absorber inlet CO<sub>2</sub> mole fraction is offset by the increasing OPEX and cross exchanger CAPEX.

## 4.8 CONCLUSIONS

1. In amine-only and hybrid cases, 150°C is the optimum stripping temperature.
2. The CAPEX saved by removing the cold rich bypass exchanger at high CO<sub>2</sub> lean loading is offset by the increased OPEX.
3. With the same CO<sub>2</sub> capture rate, membrane increases the absorber inlet CO<sub>2</sub> from 6% to 12~18%. As absorber inlet CO<sub>2</sub> increases from 6% to 18%, OPEX decreases from \$18.8 to \$15.4/tonne CO<sub>2</sub>, while total regeneration cost decreases from \$35.6 to \$33.1/tonne CO<sub>2</sub>.
4. The membrane can reduce the cost of amine scrubbing by increasing absorber inlet CO<sub>2</sub>. However, this is offset by the membrane cost.
5. Taken together, the total cost of the hybrid amine/membrane system is lowest at 12% absorber inlet CO<sub>2</sub>. It is competitive with the optimum CO<sub>2</sub> capture cost of the amine-only case.

Table 4-7: Equipment Cost (million \$).

PEC (MM\$)	1C11	1C12	1C21	1C22	1D4	1D21A	1D22A	1D23A	1D1	1D31A	1D32A
Trim cooler	0.15	0.16	0.23	0.24	0.58	0.21	0.21	0.27	0.56	0.56	0.52
Cross EX 1	5.3	4.7	5.8	5.2	7.8	2.7	2.2	3.2	8.4	8.8	9.4
Cross EX 2	3.5	3.7	3.6	3.8	3.4	5.2	5.3	4.4	3.3	3.3	3.0
CRBP Ex	2.7	2.8	2.7	2.9	1.8	3.8	4.2	4.8	1.7	1.6	0
Condenser	0.21	0.24	0.16	0.18	0	0.39	0.46	0.56	0	0	0
Steam heater	1.9	2.0	1.9	2.0	1.5	2.4	2.6	2.8	1.5	1.4	1.6
IC 1	0.38	0.38	0.40	0.40	0	0	0	0	0	0	0
IC2	0.64	0.64	0.32	0.32	0.73	1.31	1.31	0	0.78	0.80	0.79
Flash tank	1.0	0.9	1.0	0.9	1.1	0.8	0.7	0.9	1.2	1.3	1.3
Condenser separator	0.1	0.1	0.1	0.1	0.1	0.2	0.2	0.2	0.1	0.1	0.1
Stripper column	0.9	1.0	0.9	0.9	0.8	1.0	1.1	1.1	0.7	0.7	0.7
Absorber	10.0	10.0	8.7	8.7	4.8	4.4	4.4	5.2	4.3	4.0	4.0
DCC	0	0	5.69	5.69	3.65	0	0	0	3.25	2.93	2.93
Water wash	5.8	5.8	5.1	5.1	3.3	3.1	3.1	3.4	3.0	2.7	2.7
Water wash air cooler	0.07	0.07	0	0	0	0.56	0.56	0.78	0	0	0
Compressor	7.7	8.3	7.7	8.2	7.3	8.1	8.6	8.1	7.2	7.0	7.0
Rich pump	0.5	0.4	0.5	0.4	0.6	0.3	0.3	0.4	0.6	0.7	0.7
Lean pump	0	0.05	0.01	0.06	0	0.03	0.07	0.06	0	0	0
PA1	0.13	0.13	0.09	0.09	0	0	0	0	0	0	0
PA2	0.13	0.13	0.06	0.06	0.07	0.04	0.04	0.04	0.07	0.07	0.07
IC pump 1	0.37	0.37	0.37	0.37	0	0	0	0	0	0	0
IC pump 2	0.27	0.27	0.27	0.27	0.29	0.16	0.16	0.16	0.30	0.31	0.31
Blower	3.7	3.7	3.7	3.7	2.0	2.2	2.2	2.2	1.7	1.5	1.5
Amine total	45.6	45.9	49.4	49.8	39.9	36.9	37.6	38.5	38.8	37.7	37.1
Membrane	-	-	-	-	7.1	9.2	9.2	9.2	9.6	20.5	20.5
Total	45.6	45.9	49.4	49.8	47.0	46.0	46.8	47.7	48.3	58.2	57.6

Table 4-8: Operating Energy Consumption (MWe).

OPEX (MWe)	1C11	1C12	1C21	1C22	1D4	1D21A	1D22A	1D23A	1D1	1D31A	1D32A
Rich Pump	1.2	1.0	1.1	1.0	1.4	0.7	0.6	1.0	1.5	1.6	1.7
Lean Pump	0	0.12	0.02	0.15	0	0.08	0.16	0.14	0	0	0
PA1	0.3	0.3	0.2	0.2	0	0	0	0	0	0	0
PA2	0.3	0.3	0.1	0.1	0.2	0.1	0.1	0.1	0.2	0.2	0.2
Blower	4.7	4.7	4.7	4.7	1.7	2.0	2.0	2.0	1.3	1.1	1.1
Steam	31.8	31.6	31.5	31.3	28.7	34.6	35.1	40.4	28.3	27.8	29.8
Compressor	10.1	10.8	10.1	10.7	9.6	10.6	11.2	10.6	9.5	9.2	9.2
AMINE TOTAL	48.4	48.8	47.8	48.2	41.5	48.0	49.1	54.1	40.8	39.9	42.0
Blower Energy for membrane	-	-	-	-	0.07	0.07	0.07	0.07	0.07	0.07	0.07
((Mwe/tonne CO <sub>2</sub> /hr))											
TOTAL Consumption	48.4	48.8	47.8	48.2	54.2	60.6	61.7	66.7	53.6	52.6	54.7

Table 4-9: Annual Capital and Operating Cost (\$/tonne CO<sub>2</sub>).

PEC (MM\$)	1C11	1C12	1C21	1C22	1D4	1D21A	1D22A	1D23A	1D1	1D31A	1D32A
CAPEX (\$/tonne CO <sub>2</sub> )											
Trim cooler	0.1	0.1	0.2	0.2	0.4	0.1	0.2	0.2	0.4	0.4	0.4
Cross EX 1	3.7	3.3	4.1	3.7	5.5	1.9	1.6	2.2	5.8	6.1	6.6
Cross EX 2	2.5	2.6	2.5	2.7	2.4	3.7	3.7	3.1	2.3	2.3	2.1
CRBP Ex	1.9	2.0	1.9	2.0	1.3	2.7	2.9	3.4	1.2	1.1	0
Condenser	0.1	0.2	0.1	0.1	0.0	0.3	0.3	0.4	0	0	0.3
Steam heater	1.3	1.4	1.3	1.4	1.1	1.7	1.8	2.0	1.0	1.0	1.1
IC 1	0.3	0.3	0.3	0.3	0	0	0	0	0	0	0
IC2	0.4	0.4	0.2	0.2	0.5	0.9	0.9	0.0	0.5	0.6	0.6
Flash tank	0.7	0.6	0.7	0.6	0.8	0.5	0.5	0.6	0.8	0.9	0.9
Condenser separator	0.1	0.1	0.1	0.1	0.1	0.1	0.1	0.1	0.1	0.1	0.1
Stripper column	0.6	0.7	0.6	0.7	0.5	0.7	0.7	0.8	0.5	0.5	0.5
Absorber	7.0	7.0	6.1	6.1	3.3	3.1	3.1	3.6	3.0	2.8	2.8
DCC	0.0	0.0	4.0	4.0	2.6	0.0	0.0	0.0	2.3	2.0	2.0
Water wash	4.1	4.1	3.6	3.6	2.3	2.2	2.2	2.4	2.1	1.9	1.9
Water wash air cooler	0.0	0.0	0.0	0.0	0.0	0.4	0.4	0.5	0.0	0.0	0.0
Compressor	5.4	5.8	5.4	5.8	5.1	5.7	6.1	5.7	5.0	4.9	4.9
Rich pump	0.3	0.3	0.3	0.3	0.4	0.2	0.2	0.3	0.4	0.5	0.5
Lean pump	0	0.04	0.006	0.04	0	0.02	0.05	0.04	0	0	0
PA1	0.09	0.09	0.06	0.06	0	0	0	0	0	0	0
PA2	0.09	0.09	0.04	0.04	0.05	0.03	0.03	0.03	0.05	0.05	0.05
IC pump 1	0.26	0.26	0.26	0.26	0	0	0	0	0	0	0
IC pump 2	0.2	0.2	0.2	0.2	0.2	0.1	0.1	0.1	0.2	0.2	0.2

Table 4-9 continued

Blower	2.6	2.6	2.6	2.6	1.4	1.5	1.5	1.5	1.2	1.1	1.1
Amine total	32.0	32.2	34.8	35.0	28.0	25.9	26.5	27.1	27.0	26.4	25.9
Membrane	-	-	-	-	5.0	6.4	6.4	6.4	6.7	14.4	14.4
Total CAPEX	32.0	32.2	34.8	35.0	32.9	32.4	32.9	33.5	33.7	40.7	40.3
OPEX (\$/tonne CO <sub>2</sub> )											
Rich pump	0.4	0.4	0.4	0.4	0.5	0.3	0.3	0.4	0.6	0.6	0.6
Lean pump	0	0.05	0.01	0.06	0	0.03	0.06	0.05	0	0	0
PA1	0.12	0.12	0.08	0.08	0	0	0	0	0	0	0
PA2	0.12	0.12	0.05	0.05	0.07	0.04	0.04	0.04	0.07	0.06	0.06
Blower	1.8	1.8	1.8	1.8	0.6	0.8	0.8	0.8	0.5	0.4	0.4
Steam	12.3	12.3	12.3	12.2	11.1	13.4	13.6	15.7	10.9	10.8	11.5
Compressor	3.9	4.2	3.9	4.2	3.7	4.1	4.3	4.1	3.6	3.6	3.6
Amine total	18.8	18.9	18.6	18.7	16.1	18.6	19.1	21.0	15.7	15.4	16.2
Membrane	-	-	-	-	3.9	3.9	3.9	3.9	3.9	3.9	3.9
Total OPEX	18.8	18.9	18.6	18.7	19.9	22.5	22.9	24.9	19.5	19.3	20.1



## **Appendix A: Managing NH<sub>3</sub> Emissions from Amine Scrubbing**

Ammonia is a significant precursor of atmospheric fine particulate matter (PM<sub>2.5</sub>). Approximately half of PM<sub>2.5</sub> is composed of ammonium salts, which is developed from a series of reactions between ammonia (NH<sub>3</sub>), sulfur dioxide (SO<sub>2</sub>) and oxides of nitrogen (NO<sub>x</sub>) in the atmosphere, rather than directly emitted in to the ambient air. SO<sub>2</sub> and NO<sub>x</sub> ( $\equiv$  NO + NO<sub>2</sub>) are mostly from combustion sources. SO<sub>2</sub> and NO<sub>x</sub> in flue gases cannot be totally removed even though they are treated before CO<sub>2</sub> capture to decrease their amount in coal fired power plant or natural gas combined cycle power plant. Then they are oxidized to form sulfuric acid (H<sub>2</sub>SO<sub>4</sub>) and nitric acid (HNO<sub>3</sub>). NH<sub>3</sub> comes from the oxidative degradation of amine in the amine scrubbing system. Approximately 30~50% of the lost amine oxidizes to ammonia and a small part of it is taken into the air by treated flue gas. Although ammonia emitted itself is a very small fraction of the precursors, it is the only alkaline gas in the formation of PM<sub>2.5</sub>. Ammonia forms ammonium sulfate ((NH<sub>4</sub>)<sub>2</sub>SO<sub>4</sub>) or ammonium bisulfate (NH<sub>4</sub>HSO<sub>4</sub>) by neutralizing H<sub>2</sub>SO<sub>4</sub> and ammonium nitrate (NH<sub>4</sub>NO<sub>3</sub>) by neutralizing HNO<sub>3</sub> in gas phase. Ammonia emission reduction from post CO<sub>2</sub> combustion capture plays a crucial role in reducing PM<sub>2.5</sub>.

### **1 AMMONIA PURGING**

To mitigate this air quality problem, the scrubber must be designed to purge ammonia. The amine scrubbing system is at steady state and the amine is recycled. The amine oxidation products accumulate and volatile products leave in the treated flue gas. Therefore, ammonia can be purged in liquid from the stripper to reduce ammonia emission in the treated gas.

In this design, ammonia was concentrated with an additional section of packing on top of the stripper with condensate reflux. Different reflux ratios and configurations were chosen to vary the ammonium and flow rate in the purge. The base-case stripping configuration was the advanced flash with warm rich bypass (WRBP) and cold rich exchanger bypass (CRBP). The Independence model for piperazine (PZ) in Aspen Plus<sup>®</sup> was used to simulate the stripping performance. Ammonia purging was also studied with variable system ammonium concentration and CO<sub>2</sub> lean loading target. Lower solvent ammonia concentration and higher CO<sub>2</sub> lean loading increased the difficulty of separating ammonia from CO<sub>2</sub>-amine-water.

The ammonia distribution in the absorber was simulated by feeding ammonia with the lean solvent into a simple absorber. 5 m PZ solvent with 0.22 CO<sub>2</sub> lean loading and 0.0001 m NH<sub>3</sub> was fed into the top of a 9-meter high absorber while a 20% CO<sub>2</sub> flue gas was fed into the bottom of the absorber. Lean solvent flow rate was varied to reach 90% CO<sub>2</sub> removal.

## **2 STRIPPER CONFIGURATIONS**

The CO<sub>2</sub> amine scrubbing process with piperazine has been simulated by the Independence model in Aspen Plus<sup>®</sup>. The advanced flash stripper configuration is used. Ammonia emissions are controlled by adding reflux to the stripper and purging a water with a high concentration of ammonia. Figures A-1-A-4 show the initial advanced flash stripper configuration and the ammonia purging system.

The initial advanced flash stripper incorporates a cold and a warm rich bypass, two split cross-exchangers in series, a convective steam heater, a small stripper column, a low residence time flash tank, and a vapor/liquid heat exchanger to recover steam stripping heat. Vapor out from the top of the stripper goes through a vapor/liquid heat exchanger

to transfer its heat to the cold rich bypass and is condensed at 40 °C. The vapor from the condenser is compressed to 150 bar and stored.

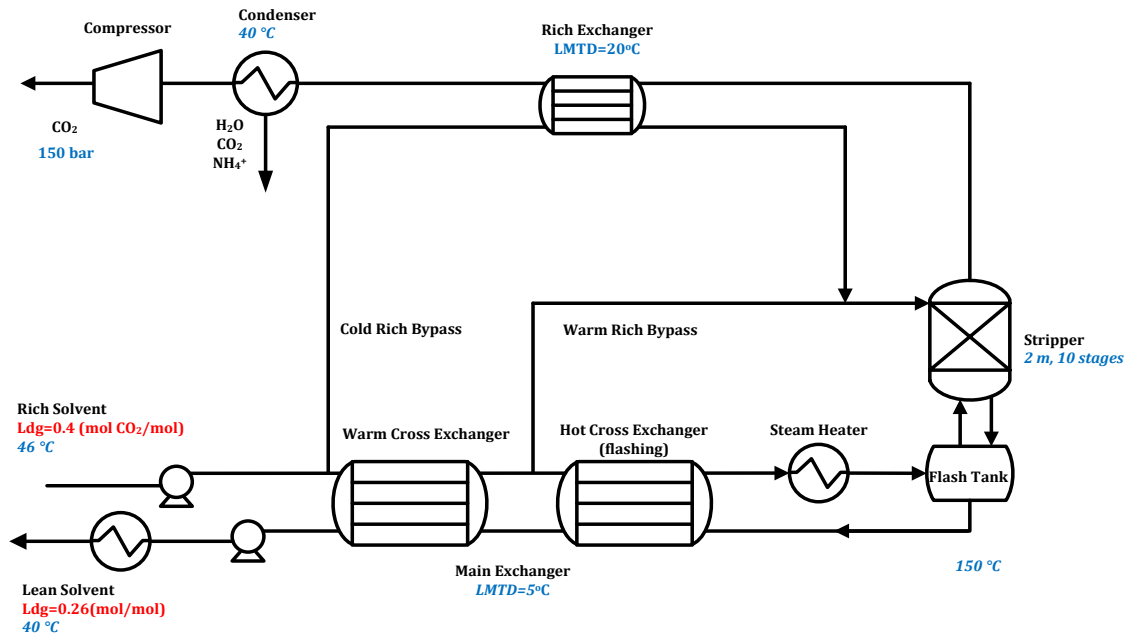


Figure A-1: Stripping configuration using 5 m PZ.

To concentrate and purge ammonia, the condensate is sent back to the top of the stripper. Ammonium is concentrated by this reflux. Since the condensate has the highest concentration of ammonium, a small part of the condensate is sent out to be purged while the remains reflow to the stripper.

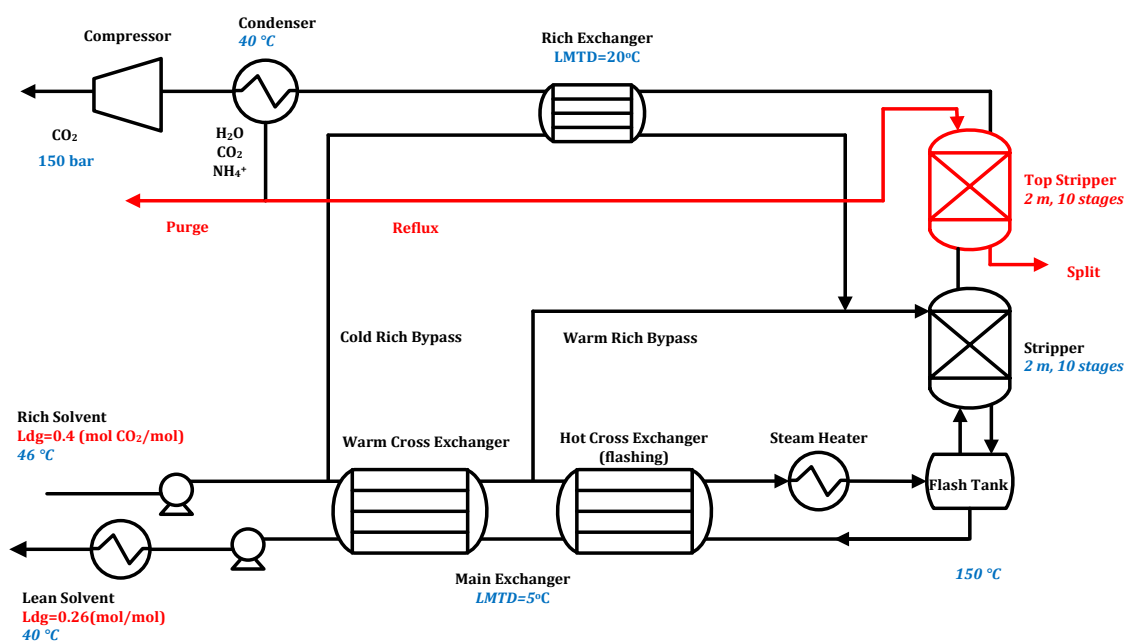


Figure A-2: Stripping configuration of ammonia purging from the condensate with split.

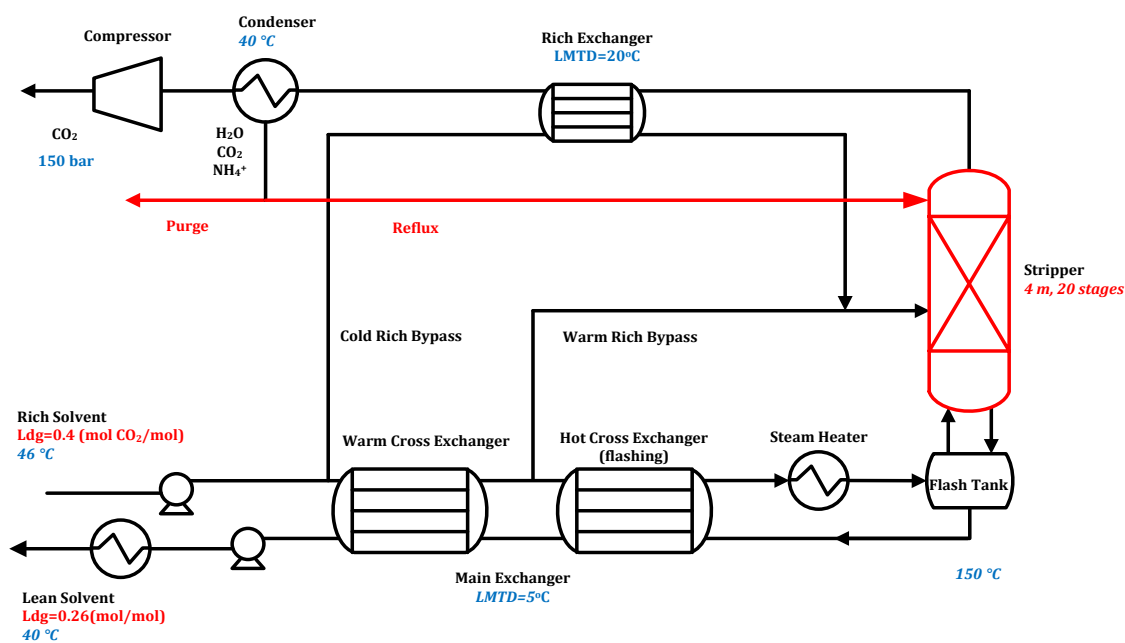


Figure A-3: Stripping configuration of ammonia purging from the condensate.

Figure A-4 shows another option. All of the condensate is back to the stripper. A high concentration  $\text{NH}_3$  is purged from the stripper. A side stripper is used to separate and recycle PZ from the purge. In this way, the ammonia accumulation from amine oxidative degradation is managed. The configurations in Figures A-3 and A-4 are developed from that in Figure A-2 to enhance the effectiveness of purging ammonia. Side stripper in Figure A-4 is used to separate  $\text{NH}_3$  and PZ in the purge at high  $\text{CO}_2$  lean loading target.

All cases are simulated using 5 m PZ stripping at 150 °C, main exchanger LMTD = 5 °C, top exchanger LMTD = 20 °C, rich solvent at 46 °C, lean solvent at 40 °C, and  $\text{CO}_2$  product compressed to 150 bar.

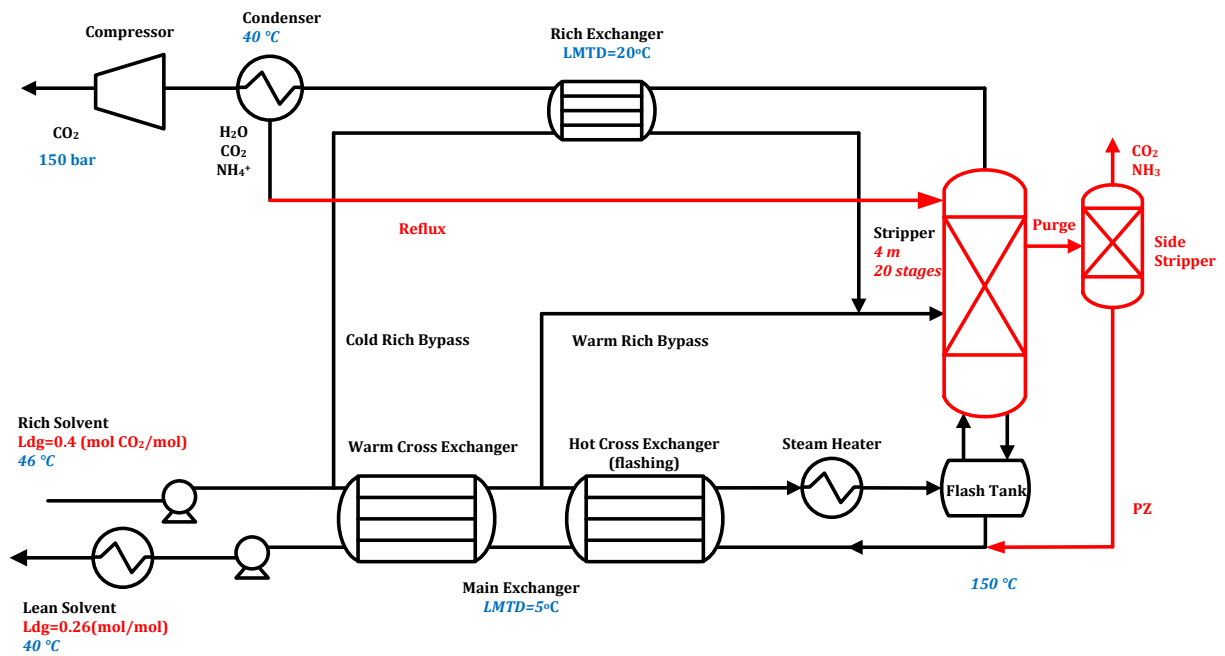


Figure A-4: Stripping configuration of ammonia purging from the condensate with a side stripper.

## 2.1 Reflux, Purge, and Split

The reflux ratio is the mass ratio of the reflux to the purge. For each reflux ratio, CRBP and WRBP are optimized to minimize the total equivalent work.

In Figure A-2, the liquid coming from the bottom of the top stripper at high temperature is discharged. Heat may be recovered from this hot split by exchange with cold rich solvent. The split can then be used as makeup to the absorber water wash. As the reflux ratio increases, ammonia in the reflux increase. As more condensate is used for reflux, the amount of the flow sent to be purged is reduced. Compared with the initial advanced flash stripper without reflux, ammonia purging can effectively concentrate ammonia in a small amount of purge and reduce PZ loss.

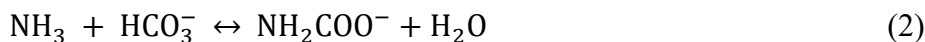
Configurations in Figure A-2 and Figure A-3 are compared. In Figure A-2, the split at high temperature is discharged. The flow rate of the split is set to be from 0% to 100% in mole of the reflux. Figure A-3 shows the stripping configuration of no split from the stripper.

## 2.2 NH<sub>3</sub> Concentration in the Solvent

Varied rich solvent ammonia concentrations from 1 ppm to 1 kg NH<sub>3</sub>/1000 kg H<sub>2</sub>O are studied to see the effectiveness of the ammonia purging system at different ammonia concentrations. 1 ppm NH<sub>3</sub>/H<sub>2</sub>O is based on the SRP pilot plant (March, 2015) minimum ammonia gas emission rate. In a real case, the ammonia concentration is between 1 ppm and 1 kg NH<sub>3</sub>/1000 kg H<sub>2</sub>O.

### 3 NH<sub>3</sub> CHEMISTRY

In addition to the chemical and physical reactions between PZ, CO<sub>2</sub>, and H<sub>2</sub>O, three reactions with ammonia occur in the amine scrubbing system.



The free energy and heat of formation of NH<sub>2</sub>COO<sup>-</sup> are given by Amine\_ELECNRTL in most updated Aspen Plus<sup>®</sup> Example.

### 4 NH<sub>3</sub> PURGING PERFORMANCE OVER DIFFERENT CONFIGURATIONS

#### 4.1 NH<sub>3</sub> Purging with and without Split (Figures A-2 and A-3)

Table A-1 shows the total mass flow rate and CO<sub>2</sub>, PZ, and NH<sub>3</sub> mole flows in purge with and without split ammonia purging configuration. In the with split configuration (Figure A-2), ammonia is taken from the amine scrubbing system by the streams Purge and Split. The total mass flow rate of the split is set to be 50%, 70%, 90% and 100% of the steam reflux. The purge is expected to have a high concentration of NH<sub>3</sub>, which is treated as wastewater. The split is at a high temperature. After cooled down, it is sent back to the system, probably at the top of the absorber. The split contains more CO<sub>2</sub> and PZ but less NH<sub>3</sub> than the reflux. As the split/reflux increases, PZ increases while NH<sub>3</sub> decreases in the purge. This indicates that a lower split/reflux is more efficient than a higher one.

Table A-1: Total mass flow rate and CO<sub>2</sub>, PZ, and NH<sub>3</sub> mole flows in purge of with and without split ammonia purging configuration (5 m PZ, NH<sub>3</sub>/H<sub>2</sub>O=1 ppm; CO<sub>2</sub> rich loading: 0.4 mol/N; CO<sub>2</sub> lean loading: 0.157 mol/N; cold rich bypass: 10%; warm rich bypass: 20%; stripping temperature: 150 °C; stripping pressure: 5 bar; reflux ratio: 2.1).

		Without Split	With Split			
Split/Reflux		0%	50%	70%	90%	100%
PURGE (kmol/s)	CO <sub>2</sub> <sup>1</sup>	5.6E-03	5.1E-03	5.0E-03	5.0E-03	5.0E-03
	PZ <sup>2</sup>	6.4E-04	9.1E-04	9.4E-04	9.7E-04	9.8E-04
	NH <sub>3</sub> <sup>3</sup>	4.4E-05	4.3E-05	4.2E-05	4.2E-05	4.1E-05
(kg/s)	Total	44	37	36	36	35
SPLIT (kmol/s)	CO <sub>2</sub>	-	7.6E-03	1.1E-02	1.4E-02	1.6E-02
	PZ	-	1.3E-02	1.8E-02	2.4E-02	2.7E-02
	NH <sub>3</sub>	-	1.7E-06	2.3E-06	3.0E-06	3.3E-06
(kg/s)	Total	-	40	55	70	77

When the split/reflux is zero, the configurations becomes without split as Figure A-3 shows. Compared to the with split configuration, the purge in the without split contains more NH<sub>3</sub> and less PZ. The advantage of without split is that it purges more NH<sub>3</sub>. At the same time, it saves the cost of recovering the heat in the split and pumping the split back to the absorber. The minor disadvantage is that while normalized the mole flow rate of NH<sub>3</sub> in the purge by its total mass flow, without split has a lower NH<sub>3</sub> normalized flow rate (1.0E-6 kmol/kg purge) than with split (1.2E-6).

<sup>1</sup>CO<sub>2</sub> in all graphs and tables stands for total carbon in a stream, including CO<sub>2</sub>, HCO<sub>3</sub><sup>-</sup>, PZ(COO<sup>-</sup>)<sub>2</sub>, PZCOO<sup>-</sup>, H<sup>+</sup>PZCOO<sup>-</sup>, and NH<sub>2</sub>COO<sup>-</sup>.

<sup>2</sup>NH<sub>3</sub> in all graphs and tables stands for total ammonia in a stream, including NH<sub>3</sub>, NH<sub>2</sub>COO<sup>-</sup>, and NH<sub>4</sub><sup>+</sup>.

<sup>3</sup>PZ in all graphs and tables stands for total piperazine in a stream, including PZ, PZ(COO<sup>-</sup>)<sub>2</sub>, PZCOO<sup>-</sup>, PZH<sup>+</sup> and H<sup>+</sup>PZCOO<sup>-</sup>.



Without a split, the reflux ratio, which is the mass ratio of the reflux to the purge, has a significant effect on the  $\text{NH}_3$  and PZ concentration in the purge. Figure A-5 shows the total  $\text{NH}_3$  and PZ in the purge changing with the reflux ratio from 99 to 1.5. The total mass flow rate of the purge normalized by  $\text{CO}_2$  removed decreases with the reflux ratio. As the purge mass flow rate increases, the normalized amount of  $\text{NH}_3$  and PZ increases, while the mole fraction of  $\text{NH}_3$  decreases, and mole fraction of PZ remains almost the same. In the reflux range of 99 to 4, a large amount of  $\text{NH}_3$  can be purged. At the same time, the mole fraction of  $\text{NH}_3$  in the purge is higher than that of PZ.

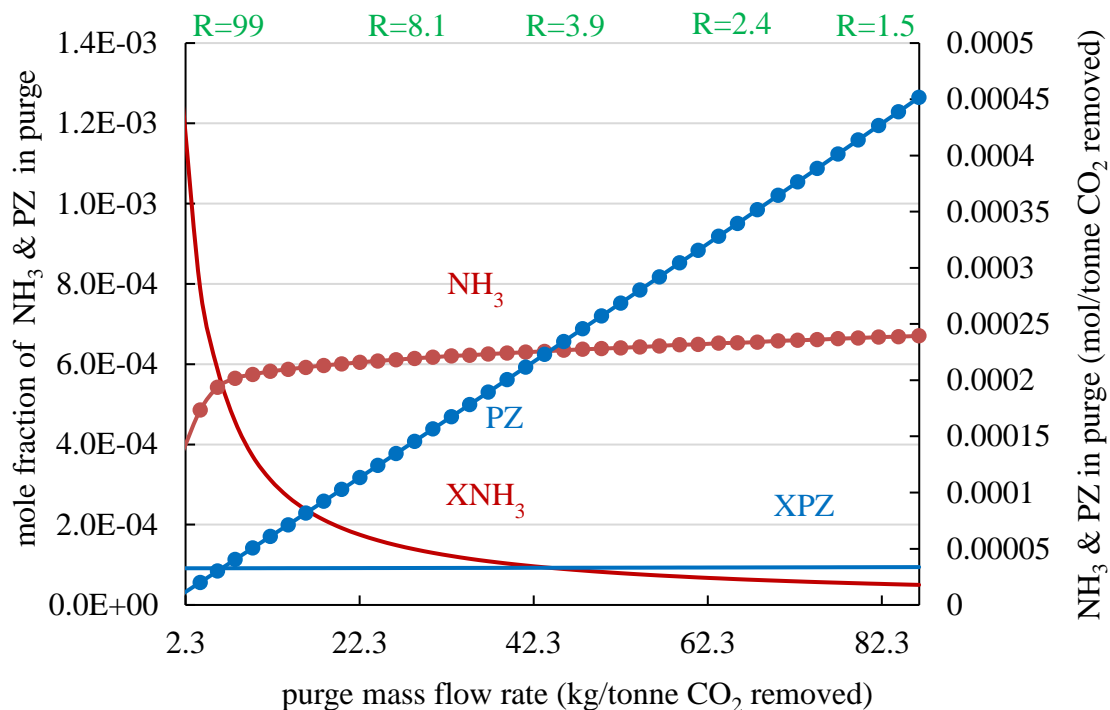


Figure A-5: Total  $\text{NH}_3$  and PZ in purge changing with reflux ratio (5 m PZ,  $\text{NH}_3/\text{H}_2\text{O}=1$  ppm;  $\text{CO}_2$  rich loading: 0.4 mol/N;  $\text{CO}_2$  lean loading: 0.157 mol/N; cold rich bypass: 18%; warm rich bypass: 52%; stripping temperature: 150 °C; stripping pressure: 5 bar; R: Reflux ratio).

## 4.2 NH<sub>3</sub> Purging at Varied Rich Solvent NH<sub>3</sub> Concentrations

Another factor that affects the mole fraction of NH<sub>3</sub> and PZ in the purge is the NH<sub>3</sub> feed concentration. In the Independence model, a certain amount of ammonia is fed into the regeneration system with the rich solvent. Figure A-6 shows the effectiveness of the ammonia purging system at varied rich solvent ammonia concentrations from 1 ppm to 1 kg NH<sub>3</sub>/1000 kg. 1 ppm NH<sub>3</sub>/H<sub>2</sub>O is based on the SRP pilot plant (March, 2015) minimum ammonia gas emission rate. In a real case, the ammonia concentration is higher than 1 ppm NH<sub>3</sub>/H<sub>2</sub>O but lower than 1 kg NH<sub>3</sub>/1000 kg H<sub>2</sub>O.

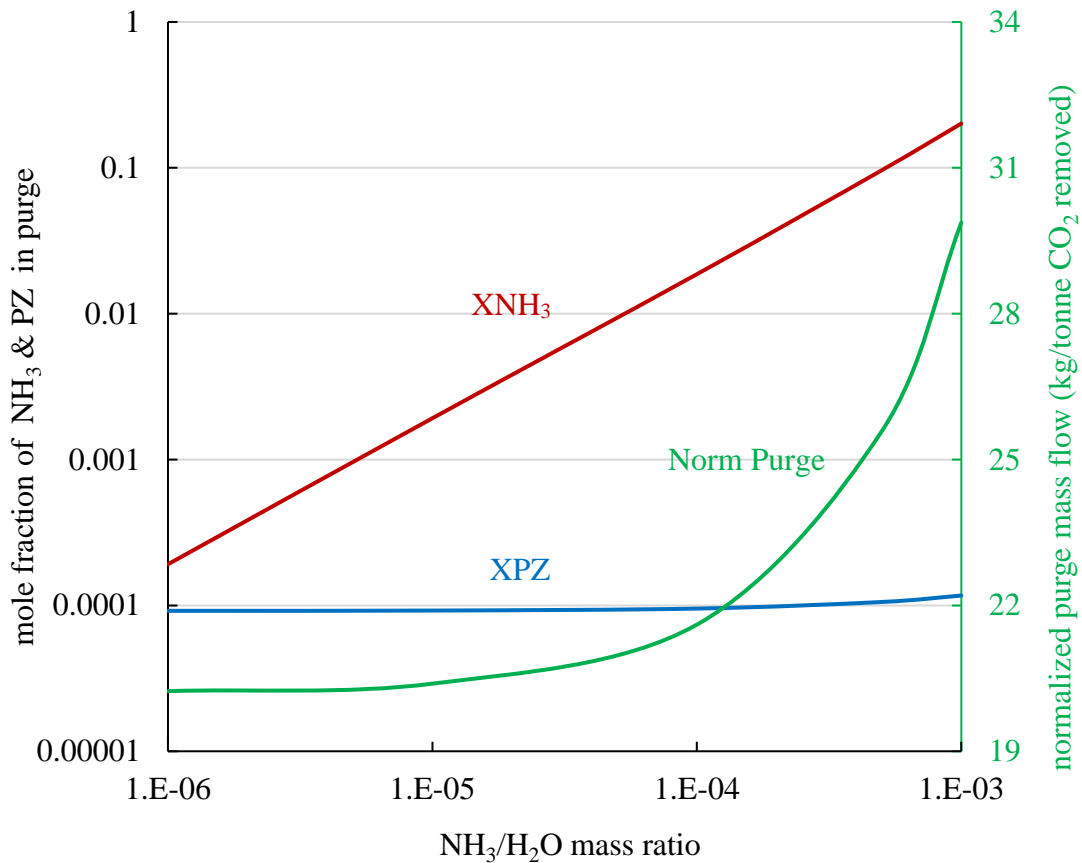


Figure A-6: Total NH<sub>3</sub> and PZ in purge changing with NH<sub>3</sub>/H<sub>2</sub>O (5 m PZ; CO<sub>2</sub> rich loading: 0.4 mol/N; CO<sub>2</sub> lean loading: 0.155 mol/N; cold rich bypass: 18%; warm rich bypass: 52%; stripping temperature: 150 °C; stripping pressure: 5 bar; reflux ratio: 9).

As the  $\text{NH}_3$  feed concentration increases, the mole fraction of ammonia increases proportionally, and is higher than PZ, while the mole fraction of PZ remains almost the same. The difference between the mole fraction of  $\text{NH}_3$  and PZ indicates the effectiveness of ammonia purging. The higher the concentration of  $\text{NH}_3$  in rich solvent, the easier  $\text{NH}_3$  would be purged by the reflux.

### 4.3 NH<sub>3</sub> Purging at Varied Stripping Pressures

Figure A-7 compares the effectiveness of the ammonia purging system changing with ammonia feed concentration at different stripping pressures. At all ammonia feed concentrations, the mole flow of NH<sub>3</sub> in the purge and the purge flow rate both decreases with the stripping pressure. The mole fraction of NH<sub>3</sub> stripping at 5 bar is higher than at either 4.6 bar or 6 bar. This is also demonstrated in Figure A-8.

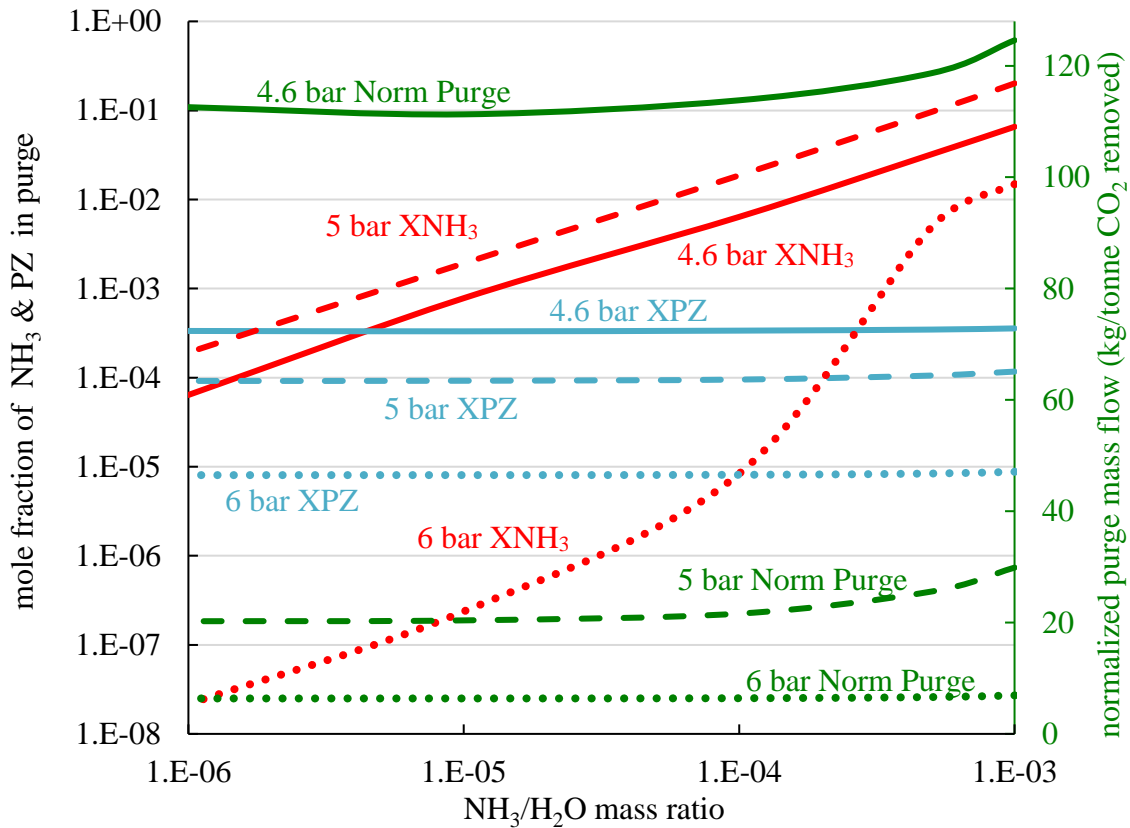


Figure A-7: Total NH<sub>3</sub> and PZ in purge changing with NH<sub>3</sub>/H<sub>2</sub>O stripping at 4.6 bar, 5 bar, and 6 bar (corresponding respectively to 0.1, 0.15, and 0.22 mol/mol N CO<sub>2</sub> lean loading)(5 m PZ; CO<sub>2</sub> rich loading: 0.4 mol/N; cold rich bypass: 19%; warm rich bypass: 54%; stripping temperature: 150 °C; reflux ratio: 9).

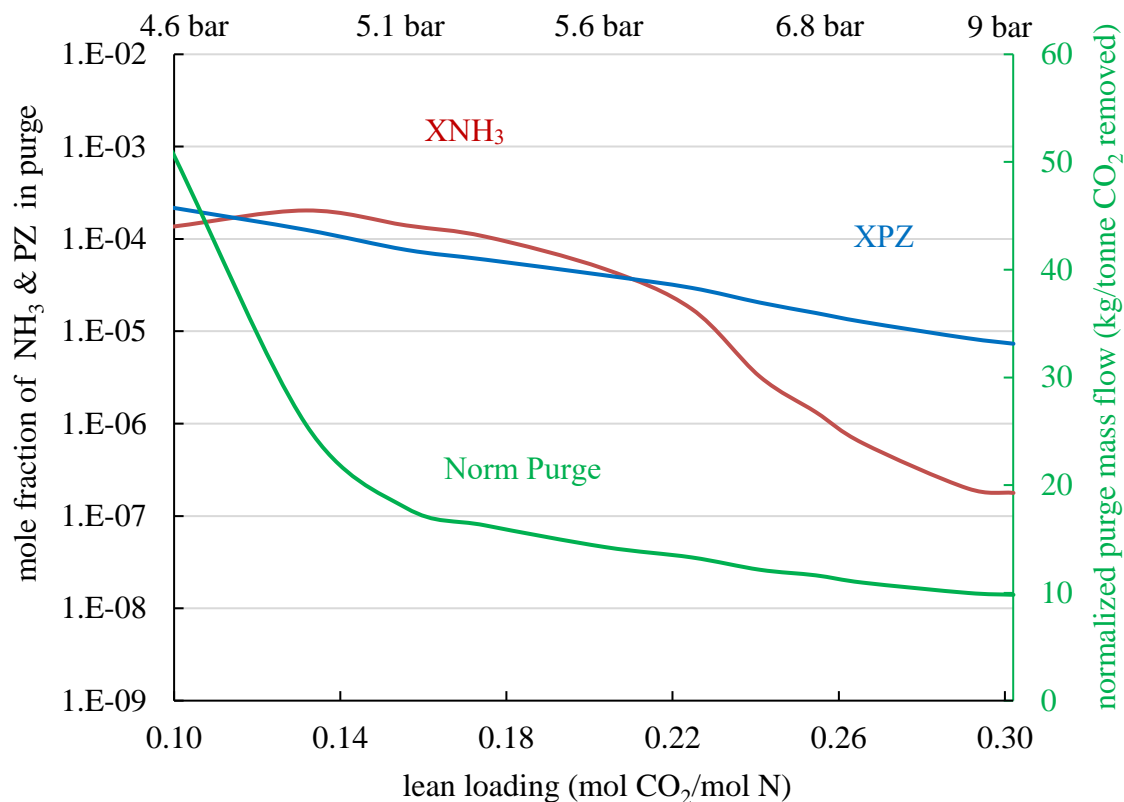


Figure A-8: Total NH<sub>3</sub> and PZ in purge changing with CO<sub>2</sub> lean loading target (5 m PZ, NH<sub>3</sub>/H<sub>2</sub>O=1 ppm; CO<sub>2</sub> rich loading: 0.4 mol/N; cold rich bypass and warm rich bypass are optimized at each lean loading; stripping temperature: 150 °C; reflux ratio: 9).

CO<sub>2</sub> lean loading target is the third factor that affects the effectiveness of ammonia purging. A given CO<sub>2</sub> lean loading corresponds to a specific stripping pressure. Figure A-8 shows the mole fraction of NH<sub>3</sub> and PZ in the purge changing with CO<sub>2</sub> lean loading when the reflux ratio is 9. As lean loading increases, the PZ mole fraction in the purge decreases. NH<sub>3</sub> in the purge first increases and then decreases. This is caused by the changing purge flow rate. As lean loading increases, the mole flow of NH<sub>3</sub> in the purge decreases. At the same time, the total flow rate of the purge first decreases rapidly and

then gently. This makes mol  $\text{NH}_3$ /total purge flow has a maximum point at 0.13 mol/N  $\text{CO}_2$  lean loading, where the stripping pressure is 4.8 bar. The mole fraction of  $\text{NH}_3$  in the purge is higher than that of PZ from 0.13 to 0.2 mol/N  $\text{CO}_2$  lean loading, which indicates that ammonia purging is effective in this range.

#### **4.4 $\text{NH}_3$ Purge Vs AFS**

Figure A-9 compares the mole fraction of  $\text{NH}_3$  and PZ in the purge and the purge flow rate (Figure A-3) to the condensate in initial without ammonia purging configuration (Figure A-1). Compared with initial configuration, ammonia purging with reflux has much lower purge flow rate and mole fraction of PZ. The ammonia purging configuration concentrates  $\text{NH}_3$  to the gas side in the stripper at low  $\text{CO}_2$  lean loading, while to the liquid side at high  $\text{CO}_2$  lean loading. Since the purge is condensed from the gas side, the  $\text{NH}_3$  concentration in the purge of ammonia purging is higher than the condensate of initial regeneration at low lean loadings, and vice versa at high lean loadings.

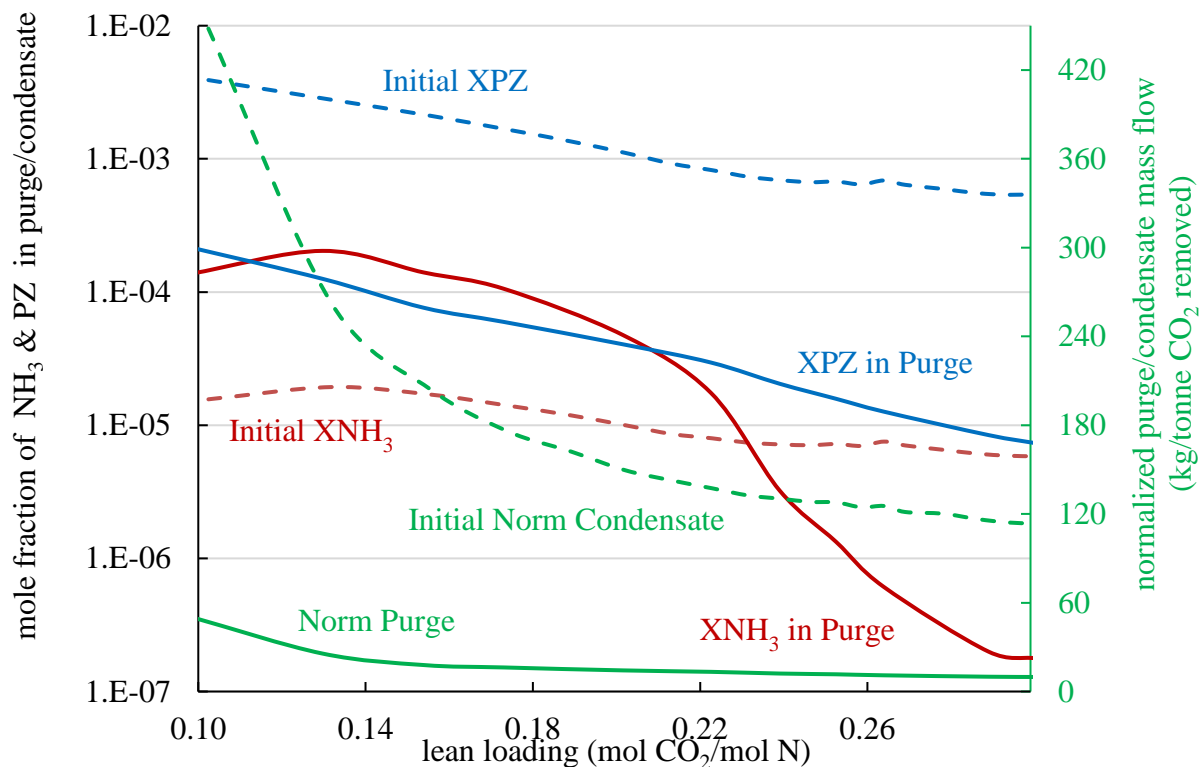


Figure A-9: Total  $\text{NH}_3$  and PZ in purge changing with  $\text{CO}_2$  lean loading compared with initial advanced flash stripper (5 m PZ,  $\text{NH}_3/\text{H}_2\text{O}=1$  ppm;  $\text{CO}_2$  rich loading:  $0.4 \text{ mol/N}$ ; cold rich bypass and warm rich bypass are optimized at each lean loading; stripping temperature:  $150^\circ\text{C}$ ; reflux ratio: 9).

Figure A-10 compares the energy consumption of ammonia purging and initial regeneration, represented by total equivalent work. Using more packing, ammonia purging with requires  $0.2 \text{ kJ/mol CO}_2$  total equivalent work higher than initial configuration.

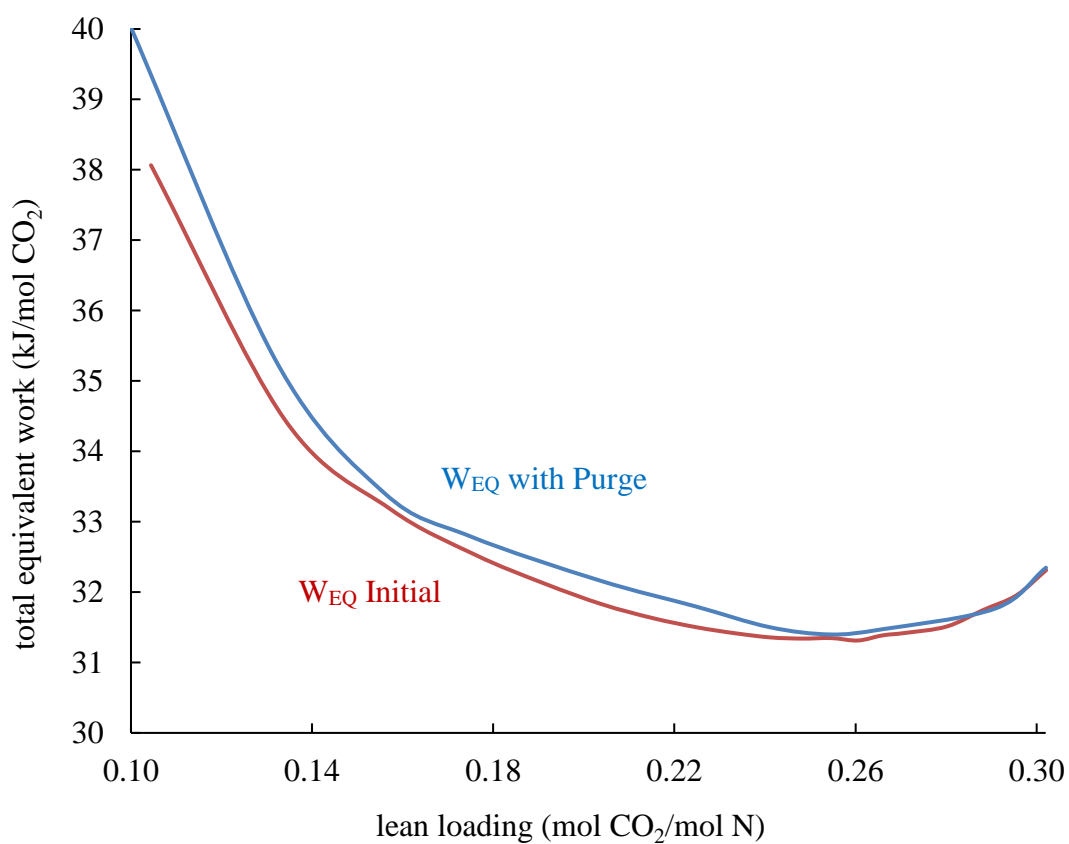


Figure A-10: Total equivalent work changing with CO<sub>2</sub> lean loading (5 m PZ, NH<sub>3</sub>/H<sub>2</sub>O=1 ppm; CO<sub>2</sub> rich loading: 0.4 mol/N; cold rich bypass and warm rich bypass are optimized at each lean loading; stripping temperature: 150 °C; reflux ratio: 9).



## 5 SIDE STREAM $\text{NH}_3$ PURGE AT HIGH $\text{CO}_2$ LEAN LOADING TARGET (FIGURE A-4)

Figure A-8 shows that condensate ammonia purge configuration (Figure A-3) is not effective at  $\text{CO}_2$  lean loading higher than 0.2 mol/mol N. At 0.24 mol/mol N  $\text{CO}_2$  lean loading, where the stripping pressure is 6.4 bar, a side stripper is used to purge ammonia at high  $\text{CO}_2$  lean loadings, as Figure A-4 shows.

In this configuration, instead of purging one part of the condensate from the condenser, all of the condensate is sent back to the top of the stripper. A side stream, which is one part of the liquid flow from one stage of the stripper, is sent to a side stripper to separate the  $\text{CO}_2$ ,  $\text{NH}_3$ , and PZ in it. The bottom stream of the side stripper, which is expected to recover PZ, is sent back to the flash tank.

An ideal side stream should have high  $\text{NH}_3/\text{PZ}$  ratio. Stripping at 6.4 bar, the  $\text{NH}_3/\text{PZ}$  mole ratio in the purge of the condensate purging configuration is 0.155. In the condensate purging, side stream purging, and no condensate or side stream purging, liquid  $\text{NH}_3/\text{PZ}$  mole ratio all have their maximum value at the third stage. In side stream purging, the  $\text{NH}_3/\text{PZ}$  mole ratio at the third stage is 0.169, which is higher than that of the condensate purging configuration. This indicates that stage 3 is a good position to take a liquid flow and send it to the side stripper.

In Figure A-11, the grey line shows the  $\text{NH}_3/\text{PZ}$  mole ratio in the purge of the ammonia purge configuration. It is a reference for the  $\text{NH}_3/\text{PZ}$  mole ratio in the side stream of the side stripper configuration. All other curves show the  $\text{NH}_3/\text{PZ}$  mole ratio in the liquid side of the main stripper. In the side stripper configuration (Figure A-4), the mass flow rate of the side stream (0.85 kg/s) is set the same as that of the purge at a reflux ratio of 9 in the ammonia purging configuration (Figure A-3).

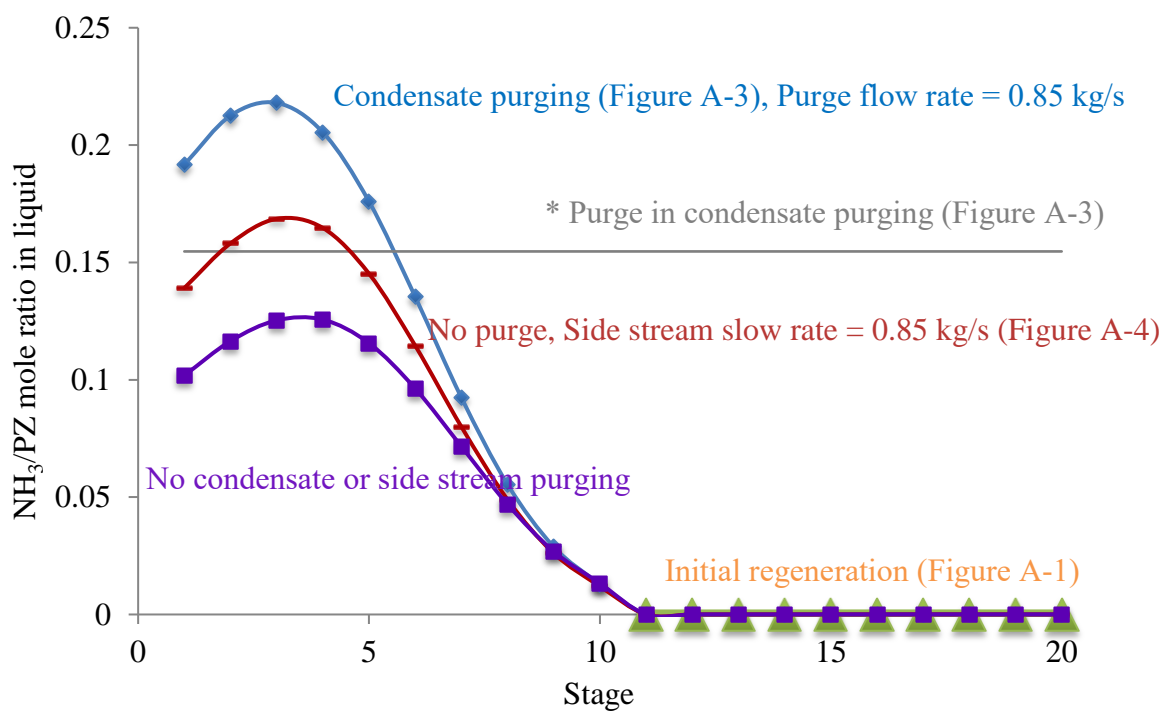


Figure A-11:  $\text{NH}_3/\text{PZ}$  mole ratio in the liquid side at each stage of the stripper (5 m PZ,  $\text{NH}_3/\text{H}_2\text{O}=1$  ppm;  $\text{CO}_2$  rich loading: 0.4 mol/N;  $\text{CO}_2$  lean loading: 0.24 mol/N; cold rich bypass: 6.8%; warm rich bypass: 23%; stripping temperature: 150 °C; stripping pressure: 6.4 bar).

Table A-2: Stream table of ammonia purging by one part of condensate and side stripper (5 m PZ, NH<sub>3</sub>/H<sub>2</sub>O=1 ppm; CO<sub>2</sub> rich loading: 0.4 mol/N; CO<sub>2</sub> lean loading: 0.24 mol/N; cold rich bypass: 6.8%; warm rich bypass: 23%; stripping temperature: 150 °C; stripping pressure: 6.4 bar; the mass flow rate of the side split is the same as that of the purge at reflux ratio of 9; condensing temperature of the side stripper: 155 °C; total distillate rate of the side stripper: 1000 kg/hr; mole reflux ratio of the side stripper: 10).

	Unit	Rich	Lean	Vapor <sup>1</sup>	Reflux	Purge	Side <sup>2</sup>	Bottom <sup>3</sup>	Vapor D <sup>4</sup>	Liquid D <sup>5</sup>
H <sub>2</sub> O	kmol/hr	199327	199747	72	1666	169	171	115	0.79	54
CO <sub>2</sub>	kmol/hr	5	0.07	5759	4	0.444	0.134	1.3E-08	0.137	0.007
HCO <sub>3</sub> <sup>-</sup>	kmol/hr	833	171	0	0.038	0.004	0.011	1.8E-05	0	0.001
PZ	kmol/hr	214	3513	4.7E-11	3.2E-07	3.3E-08	2.8E-05	0.010	1.7E-10	1.3E-07
PZ(COO <sup>-</sup> ) <sub>2</sub>	kmol/hr	2168	1076	0	1.7E-11	2.0E-12	8.6E-11	2.6E-14	0	8.1E-15
PZCOO <sup>-</sup>	kmol/hr	1223	4770	0	3.9E-09	4.3E-10	1.8E-07	9.2E-08	0	1.7E-10
PZH <sup>+</sup>	kmol/hr	6393	7093	0	0.034	0.003	0.010	1.8E-05	0	3.3E-06
H <sup>+</sup> PZCOO <sup>-</sup>	kmol/hr	8002	1548	3.5E-13	2.6E-04	2.8E-05	1.3E-04	8.3E-10	1.0E-19	1.7E-08
NH <sub>3</sub>	kmol/hr	0.03	0.13	1.3E-07	1.3E-07	1.9E-08	3.2E-05	2.4E-07	6.0E-05	4.7E-04
NH <sub>2</sub> COO <sup>-</sup>	kmol/hr	0.02	0.02	0	3.0E-10	4.6E-11	4.0E-08	3.0E-13	0	8.6E-08
NH <sub>4</sub> <sup>+</sup>	kmol/hr	0.17	0.06	0	0.004	5.4E-04	0.002	4.0E-11	0	0.001
Total NH <sub>3</sub>	kmol/hr	0.21	0.21	1.3E-07	0.004	0.0005	0.0016	2.4E-07	6.0E-05	0.0016
Total PZ	kmol/hr	18000	18000	4.7E-11	0.034	0.0035	0.0098	0.0098	1.7E-10	3.5E-06
Total CO <sub>2</sub>	kmol/hr	2659893	5135125	5759	4.404	0.448	0.145	1.8E-05	0.137	0.009
NH <sub>3</sub> /PZ	kmol/hr					0.155	0.169			
Total Mass	kmol/hr	5790120	5532290	254749	30205	3079	3079	2079	20	980

<sup>1</sup>Vapor: CO<sub>2</sub> production after condensed.

<sup>2</sup>Side: Liquid side stream from the third stage of the main stripper.

<sup>3</sup>Bottom: Bottom stream of the side stripper.

<sup>4</sup>Vapor D: Vapor distillate of the side stripper.

<sup>5</sup>Liquid D: Liquid distillate of the side stripper.

Table A-2 shows the stream table of ammonia purging by one part of condensate (Figure A-3) and side stripper (Figure A-4). With the same streams profile of Rich, Lean, Vapor, and Reflux, the mass flow rate of the side stream in the side stripper configuration is set the same as that of the purge at a reflux ratio of 9 in the condensate purging configuration (3079 kg/hr). Compare with the purge in the condensate purging,  $\text{NH}_3$  and PZ in the side stream are more concentrated while  $\text{CO}_2$  in it is much less. The side stream has a higher  $\text{NH}_3/\text{PZ}$  mole ratio.

The side stripper separates  $\text{NH}_3$ , PZ, and  $\text{CO}_2$  in the side stream into the bottom stream, vapor distillate, and liquid distillate. 96% of  $\text{NH}_3$  in the side stream is recovered in the liquid distillate, while 100% of PZ and 94% of  $\text{CO}_2$  are recovered in the bottom stream and vapor distillate separately. Mainly composed of PZ and  $\text{H}_2\text{O}$ , the bottom stream is sent back into the lean solvent.

## 6 CONCLUSIONS

1. Ammonia purging can effectively concentrate ammonia in a small amount of purge, and reduce PZ loss at high reflux ratio, high  $\text{NH}_3$  feed concentration, and lean loading from 0.13 to 0.2 mol  $\text{CO}_2$ /mol N.
2. The side stripper configuration purges more effectively than the condensate purging configuration at high  $\text{CO}_2$  lean loading.

## **Appendix B: Air Stripping and AFS with Compressor Intercooled by parallel cold rich bypasses**

The University of Kentucky has developed a CO<sub>2</sub> capture pilot plant with air stripping using 7 m monoethanolamine (MEA) and brine cooling using CaCl<sub>2</sub>. This work presents the energy performance comparison between the advanced flash stripper (AFS) and air stripper using 5 m piperazine (PZ). One part of the rich solvent was preheated by the compressed CO<sub>2</sub> at each compression stage of the AFS to save the heat duty of the steam heater.

Regeneration and compression design focused on minimizing the energy consumption of the CO<sub>2</sub> capture. The Independence model for PZ in Aspen Plus<sup>®</sup> was used to simulate the stripping and compressing performance. Equation Oriented Modeling in Aspen Plus<sup>®</sup> was used to find the optimum cold rich bypass (CRBP) and warm rich bypass (WRBP), where total equivalent work ( $W_{EQ}$ ) is the minimum.

5 m PZ was used since it is cost effective. Compared to MEA, PZ has greater CO<sub>2</sub> capacity, faster absorbing rate, and lower thermal degradation rate.

### **1 INTRODUCTION**

The equipment specifications for air stripping using 5 m PZ were kept the same as using 7 m MEA. Figure B-1 shows the complete configuration of air stripping and brine cooling in Kentucky.

The yellow block shows the DCC, water wash, and absorber. A pump around was applied to enhance the CO<sub>2</sub> capture rate. As a pilot plant, the CO<sub>2</sub> product from the stripper was recycled to the inlet of the absorber instead of being compressed. The red block shows the regeneration process with air stripper. The CO<sub>2</sub> rich solvent went through two cross exchangers to be preheated by the air and the lean solvent. CO<sub>2</sub> was

stripped out from the reboiling stripper and recycled to the inlet of the absorber. The lean solvent entered the air stripper. The air, whose volume flow rate is one quarter of the flue gas, entered the water evaporator to keep the water balance in the brine by absorbing  $\text{H}_2\text{O}$ . The humidified air entered the air stripper being heated by the lean solvent and was finally sent to the boiler to enrich  $\text{CO}_2$  in the flue gas. Being cooled by the condensates from the  $\text{CO}_2$  product and humidified air, the lean solvent from the bottom of the air stripper had a lower  $\text{CO}_2$  lean loading than the one from the bottom of the reboiled stripper. The blue block shows the brine cooling system. Brine was recirculated to chill the  $\text{CO}_2$  product, lean solvent, and another air flow whose column flow rate was 30 times larger than the flue gas. This large amount of air was chilled and regenerated cooling water at  $28^\circ\text{C}$  from the overall used hot water.

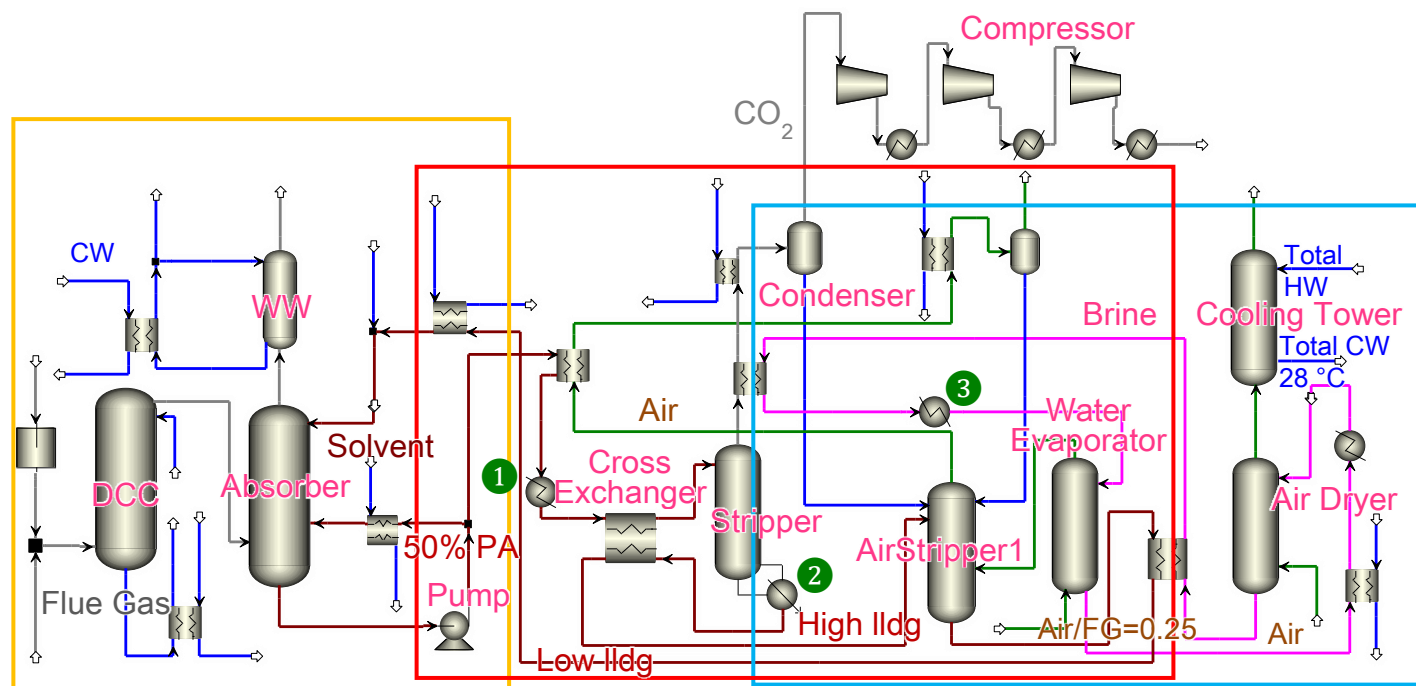


Figure B-1: Complete configuration of air stripping and brine cooling in Kentucky.

When simulating stripping and compressing using 5 m PZ in the Independence model in Aspen Plus<sup>®</sup>, the pump work, compression work, reboiler work, and heat work of the heaters were added up to compare the total equivalent work between air stripper and AFS. The compressed CO<sub>2</sub> at each compression stage of the AFS was intercooled by parallel cold rich bypasses to improve the energy performance.

## 2 METHODS

Both AFS (see Figure B-2) and air stripper were simulated in Aspen Plus<sup>®</sup>. The energy consumption is expressed by  $W_{EQ}$  in units of kJ/mol CO<sub>2</sub>, which is the sum of pump work, compression work, and heat work (see Equation 1). It includes the electricity consumed by rich pump, compression, and equivalent electricity by heaters.

$$W_{EQ}(\text{kJ/mol CO}_2) = W_{PUMP} + W_{COMP} + W_{HEAT} \quad (1)$$

Heat work is calculated from the thermal heat duty by applying Carnot cycle and an efficiency of 90% for a non-ideal expansion in the steam turbines (see Equation 2). For the air stripper, as the red block in Figure B-1 shows,  $W_{HEAT}$  includes the heat work of the preheater (①), the reboiler (②), and the brine heater (③) (see Equation 3).  $T_{STEAM}$  is the temperature of the steam when a heater is considered being heated by steam, which is 5 °C higher than the solvent.  $W_{HEAT}$  of AFS includes only the steam heater.

$$W_{heat}(\text{kJ/mol CO}_2) = 90\% \left( \frac{T_{STEAM} - 313.15}{T_{STEAM}} \right) Q_{heater} \times \frac{1}{N_{CO_2}} \quad (2)$$

$$W_{HEAT} = W_{preheater} + W_{reboiler} + W_{brineheater} \quad (3)$$

Compression work is taken from a polytropic compressor model with a pressure ratio of 2.4 and an efficiency of 0.86 for each stage in Aspen Plus<sup>®</sup>. A three-stage polytropic compressor is used to compress CO<sub>2</sub> from 5~7 bar at 40 °C to a supercritical status of 75 bar at 30 °C (See Figure B-3). When the compressed CO<sub>2</sub> at each compression stage of the AFS was intercooled by cooling water, the CO<sub>2</sub> outlet temperature was 40 °C at the first two intercoolers and 30 °C at the last one. Since the rich inlet temperature is 49 °C, which is 21°C higher than the cooling water, when intercooled by cold rich bypasses, the CO<sub>2</sub> outlet temperature were 55 °C and at last cooled to 30 °C. The rich bypass entered each compression intercooler at the absorber outlet temperature (49 °C) and came out of the intercoolers at its boiling point, which is 113 °C at 6 bar.



Compressor intercooling heat ( $Q_{\text{compintc}}$ ) was used to describe the total heat duty of cooling compressed  $\text{CO}_2$  by cooling water in the intercoolers. Since the heat was transferred from the compressed  $\text{CO}_2$  to the water,  $Q_{\text{compintc}}$  was a negative value. When the compressed  $\text{CO}_2$  was intercooled by cold rich bypasses,  $Q_{\text{compintc}}$  represented the compression heat recovered by cold rich bypasses. Since the bypasses inlet temperature was much higher than cooling water, the compressed  $\text{CO}_2$  temperatures at the second and third compressors inlets were higher than using cooling water. Equation 4 indicated that the compression work increases with the compression inlet temperature  $T_1$ . The compression work using cold rich bypasses cooling would be higher than using cooling water.  $Q_{\text{compintc}}$  using cold rich bypasses cooling would be lower than using cooling water because the 3<sup>rd</sup> stage intercooler could only cool the compressed  $\text{CO}_2$  down to 55 °C. The steam heater heat duty would be reduced by recovering the compressor intercooling heat. The flow rate of cooling cold rich bypasses were varied to match the  $\text{CO}_2$  temperature at compressor intercooler outlets.

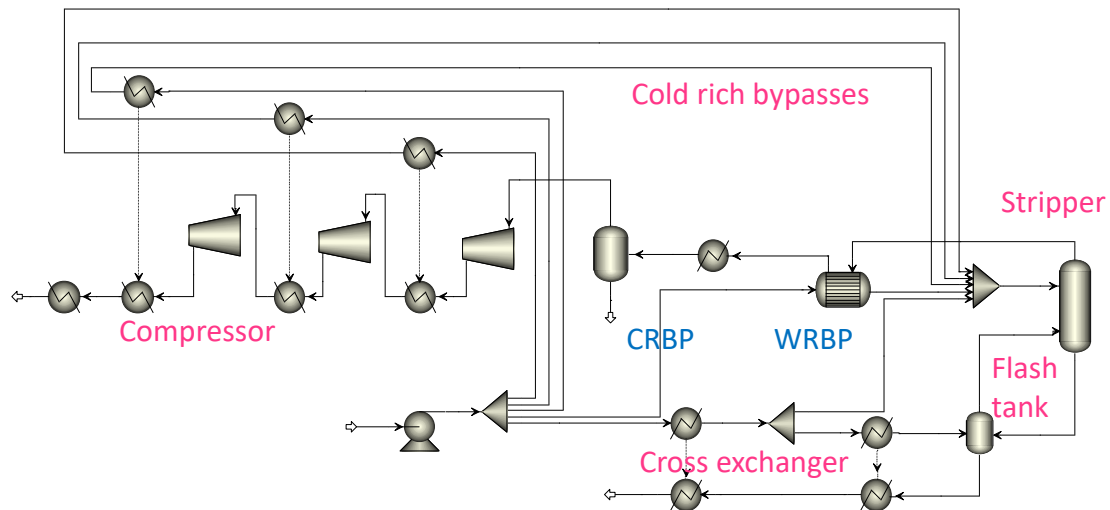


Figure B-2: Advanced Flash Stripper with compressor intercooling heat recovered.

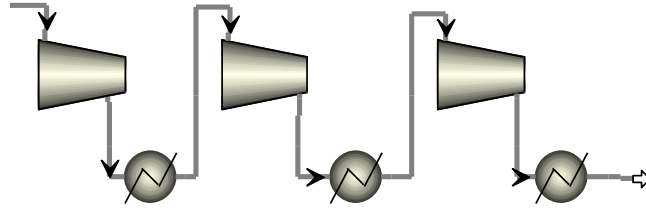


Figure B-3: Advanced Flash Stripper with compressor intercooling heat recovered.

$$W_{comp} = \frac{nR(T_2 - T_1)}{n - 1} \times \frac{1}{\eta} = \frac{nRT_1}{n - 1} \times \left[ \left( \frac{p_2}{p_1} \right)^{\frac{n-1}{n}} - 1 \right] \times \frac{1}{\eta} \quad (4)$$

Some other specifications were applied in the air stripping model. Log mean temperature difference (LMTD) of the cross exchangers in air stripping using 5 m PZ were kept the same as using 7 m MEA. With a stripping temperature at 150 °C, the boilup ratio and stripping pressure were varied to reach the high lean loading. The temperature of the preheater was varied to match the low lean loading. The temperature of the brine heater was varied to keep the water balance of the cooling brine in the air stripper.

### 3 EQUIVALENT WORK OF AIR STRIPPING

Table B-1 shows the energy performance of air stripper changing with delta lean loading. Delta lean loading is the difference between high and low lean loadings. As the preheater heat duty increased, the reboiler heat duty decreased to reach the same stripping temperature, 150 °C. As a result, the solvent temperature at the hot side outlet of the cross exchanger increased. This increasing temperature increased the CO<sub>2</sub> stripped out from the air stripper, which was sent to the boiler. As delta loading increased from 0 to 0.04 mol CO<sub>2</sub>/mol N, the total equivalent work increased from 46.8 to 62.3 kJ/mol CO<sub>2</sub>. In the stripping scope, minimum  $W_{EQ}$  at 0 delta lean loading indicates that air stripping is

not energy efficient.  $Q_{\text{compintc}}$ , which is the maximum heat duty that can be saved from the compressor intercoolers, kept the same at 13.2 kJ/mol  $\text{CO}_2$ .

Table B-1: Energy performance of air stripper changing with delta lean loading (at rich loading of 0.4 mol  $\text{CO}_2$ /mol N and high lean loading of 0.2 mol  $\text{CO}_2$ /mol N).

Low lean loading	Equivalent work (kJ/mol $\text{CO}_2$ )						Heat duty (kJ/mol $\text{CO}_2$ )		
(mol $\text{CO}_2$ /mol N)	$W_{\text{pump}}$	$W_{\text{comp}}$	$W_{\text{reb}}$	$W_{\text{preheater}}$	$W_{\text{brineheater}}$	$W_{\text{total}}$	$Q_{\text{compintc}}$	$Q_{\text{preheater}}$	$Q_{\text{reb}}$
0.20	0.7	8.0	32.9	2.1	3.1	<b>46.8</b>	-13.2	31.7	136.0
0.19	0.7	8.0	32.6	5.0	2.4	<b>48.7</b>	-13.2	49.2	134.9
0.18	1.0	8.0	32.4	7.7	2.0	<b>51.0</b>	-13.2	58.9	134.1
0.16	1.0	8.0	31.8	19.0	2.5	<b>62.3</b>	-13.2	101.9	131.7

Table B-2 shows the energy performance of air stripper changing with high lean loading. We learned that  $W_{\text{EQ}}$  is optimized with zero delta loading for each high lean loading. When studying the air stripping performance over varied high loadings, it was appropriate to fix the delta lean loading at 0.01 mol  $\text{CO}_2$ /mol N. As the high lean loading decreased, the total equivalent work decreased. Although the compression work increased as a result of the decreasing stripping pressure, the compressor intercooler heat duty decreased.

Table B-2: Energy performance of air stripper changing with high lean loading (at rich loading of 0.4 mol CO<sub>2</sub>/mol N and delta lean loading of 0.01 mol CO<sub>2</sub>/mol N).

Lean loading (mol CO <sub>2</sub> /mol N)		Equivalent work (kJ/mol CO <sub>2</sub> )						Heat duty (kJ/mol CO <sub>2</sub> )		
High lldg	Low lldg	W <sub>pump</sub>	W <sub>comp</sub>	W <sub>reb</sub>	W <sub>pre heater</sub>	W <sub>brine heater</sub>	W <sub>total</sub>	Q <sub>compintc</sub>	Q <sub>preheater</sub>	Q <sub>reb</sub>
0.22	0.21	1.2	7.9	33.3	4.6	2.2	<b>49.2</b>	-13.2	49.7	137.9
0.20	0.19	0.7	8.0	32.6	5.0	2.4	<b>48.7</b>	-13.2	49.2	134.9
0.18	0.17	0.6	8.0	32.1	5.3	1.8	<b>47.8</b>	-13.2	48.2	132.6
0.16	0.15	0.6	8.1	31.6	5.8	1.5	<b>47.6</b>	-13.0	47.3	130.6

Comparing the total equivalent work of air stripper and AFS sing 5 m PZ at varied lean loading, air stripping consumed much more energy than AFS (see Figure B-4). The air stripper in Kentucky should be replaced by AFS, the most energy saving regeneration configuration.

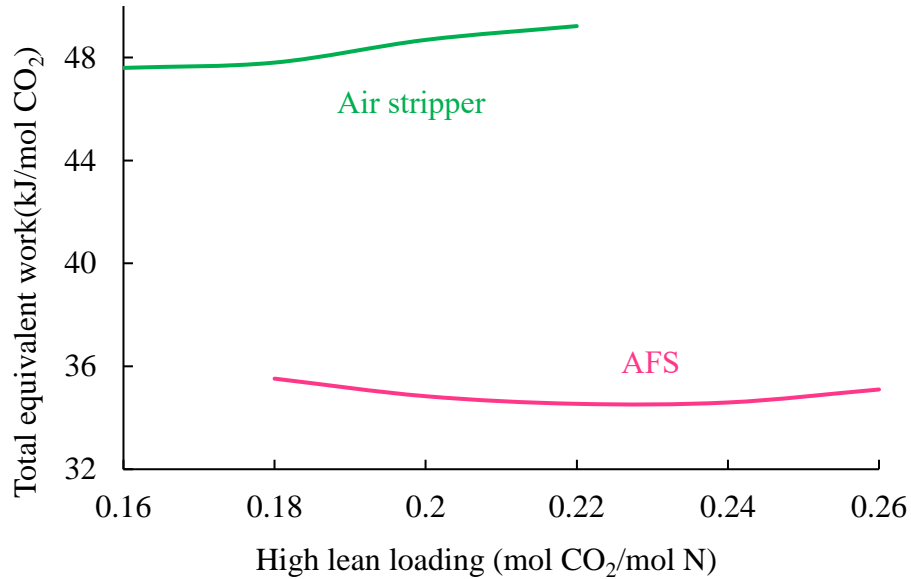


Figure B-4: Total equivalent work of air stripper and AFS at rich loading of 0.4 mol CO<sub>2</sub>/mol N.

#### 4 EQUIVALENT WORK OF AFS

Table B-3 shows the energy performance of the original AFS. As the CO<sub>2</sub> lean loading increased, there was a minimum total equivalent work at 0.22 kJ/mol CO<sub>2</sub> lean loading.  $Q_{\text{compintc}}$ , the maximum heat duty that can be saved from the compressor intercoolers, had not affected the reboiler duty  $Q_{\text{reb}}$ . Compared with  $Q_{\text{crbp}}$ , the heat duty exchanged in the cold rich bypass exchanger,  $Q_{\text{compintc}}$  was considerable to be recovered to reduce  $Q_{\text{reb}}$ .

Table B-3: Energy performance of AFS before recovering the compressor intercooling heat (at rich loading of 0.4 mol CO<sub>2</sub>/mol N).

lean loading	CRBP	WRBP	Equivalent work (kJ/mol CO <sub>2</sub> )				Heat duty (kJ/mol CO <sub>2</sub> )		
(mol CO <sub>2</sub> /mol N)	(%)	(%)	$W_{\text{pump}}$	$W_{\text{comp}}$	$W_{\text{reb}}$	$W_{\text{total}}$	$Q_{\text{compintc}}$	$Q_{\text{crbp}}$	$Q_{\text{reb}}$
0.26	8	25	1.8	7.9	25.4	<b>35.1</b>	-13.3	-21.0	104.9
0.24	9	34	1.4	8.0	25.2	<b>34.6</b>	-13.4	-21.9	104.1
0.22	11	42	1.2	8.0	25.3	<b>34.5</b>	-13.4	-24.3	104.8
0.20	14	49	1.0	8.1	25.8	<b>34.8</b>	-13.4	-28.8	106.7
0.18	19	53	0.8	8.1	26.6	<b>35.5</b>	-13.3	-37.6	110.0

Table B-4 shows the energy performance of the AFS when  $Q_{\text{compintc}}$  was recovered by cold rich bypasses. Compared with Table B-3,  $Q_{\text{compintc}}$ s, the heat used to preheat cold rich bypasses from compression intercoolers, were less, since the compressed CO<sub>2</sub> could only be cooled down to 55 °C by cold rich bypasses instead of 30 °C.  $W_{\text{reb}}$  is reduced by 0.2~0.7 kJ/mol CO<sub>2</sub>. This was reflected the less  $W_{\text{total}}$ . However,  $W_{\text{comp}}$  increased because of the higher compression inlet temperature. This results in a change in  $W_{\text{total}}$ , as Figure B-5 shows.

Table B-4: Energy performance of AFS recovering the compressor intercooling heat (at rich loading of 0.4 mol CO<sub>2</sub>/mol N).

lean loading (mol CO <sub>2</sub> /mol N)	CRBP (%)	WRBP (%)	Equivalent work (kJ/mol CO <sub>2</sub> )				Heat duty (kJ/mol CO <sub>2</sub> )		
			W <sub>pump</sub>	W <sub>comp</sub>	W <sub>reb</sub>	W <sub>total</sub>	Q <sub>compintc</sub>	Q <sub>crbp</sub>	Q <sub>reb</sub>
0.26	8	25	1.8	8.4	24.7	<b>34.9</b>	-12.4	-19.7	102.2
0.24	9	34	1.4	8.4	24.5	<b>34.4</b>	-11.8	-20.9	101.4
0.22	11	42	1.2	8.5	24.9	<b>34.5</b>	-11.5	-23.2	102.8
0.20	14	49	1.0	8.5	25.5	<b>35.0</b>	-11.3	-27.3	105.3
0.18	19	53	0.8	8.5	26.4	<b>35.8</b>	-11.1	-34.8	109.2

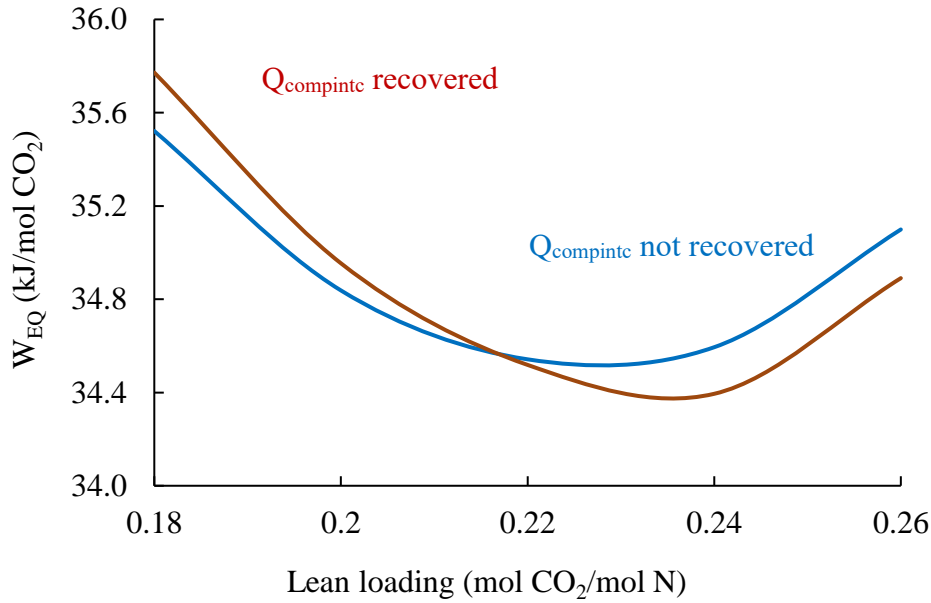


Figure B-5: Total equivalent work of AFS with and without Q<sub>compintc</sub> recovered.

Compared with original AFS, at low CO<sub>2</sub> lean loadings, where low stripping pressure and high compression work were required, the energy performance of Q<sub>compintc</sub> recovered AFS benefited from utilizing Q<sub>compintc</sub>. At high CO<sub>2</sub> lean loadings, where less compression work was required and less Q<sub>compintc</sub> could be used, the energy performance suffered from the increased compression work. On the other hand, when change water cooling to rich bypasses cooling, the heat transfer area of the heat exchangers would be

larger because the lower heat transfer coefficient of solvent. As a result, AFS with  $Q_{\text{compintc}}$  recovered would require a higher heat exchanger capital cost.

Figure B-6 compares the energy performance of AFS with and without  $Q_{\text{compintc}}$  recovered at rich loading of 0.4 mol  $\text{CO}_2$ /mol N and lean loading of 0.22 mol  $\text{CO}_2$ /mol N.

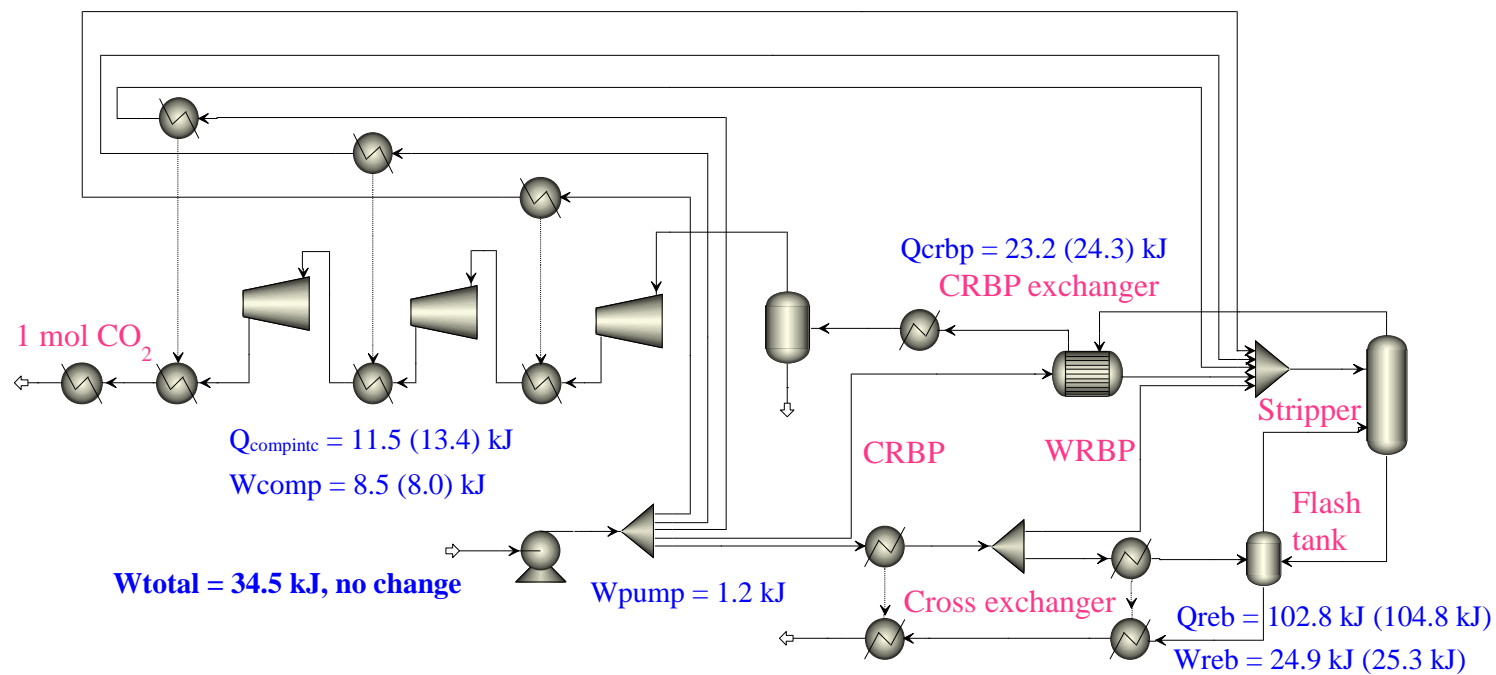


Figure B-6: Energy performance of AFS with and without  $Q_{\text{compintc}}$  recovered.



## 5 CONCLUSIONS

1. Equivalent work does not change much by recovering the compressor intercooling heat due to the trade-offs, while the heat duty decreases.
2. Although air stripper can benefit the boiler and absorber, it requires much more energy consumption.
3. At low CO<sub>2</sub> lean loadings, where low stripping pressure and high compression work were required, the energy performance of  $Q_{\text{compintc}}$  recovered AFS benefited from utilizing  $Q_{\text{compintc}}$ . At high CO<sub>2</sub> lean loadings, where less compression work was required and less  $Q_{\text{compintc}}$  could be used, the energy performance suffered from the increased compression work.
4. Recovering the compressor intercooling heat by a part of rich solvent is not cost-effective.

## References

- Ansari, A. S., Pandis, S. N. 1998. Response of Inorganic PM to Precursor Concentrations. *Environ Sci Technol*, 32, 2706-2714.
- California Energy Commission. 2014. Assessment of Natural Gas Combined Cycle Plants for Carbon Dioxide Capture and Storage in a Gas-Dominated Electricity Market. *CEC-500-2015-002*.
- Ding, J., Lin, Y. J., Rochelle, G. T. 2014. Optimization of stripping piperazine with variable rich loading. *Energy Procedia*, 63, 1842-1853.
- Ding, J., Rochelle, G. T. 2016. Regeneration Design for NGCC CO<sub>2</sub> Capture with Amine-only and Hybrid Amine/Membrane. *Energy Procedia*.
- Frailie, P. T. 2014. *Modeling of Carbon Dioxide Absorption/Stripping by Aqueous methyldiethanolamine/Piperazine*. Ph.D. Dissertation. The University of Texas at Austin.
- Freeman, S. A. 2011. *Thermal Degradation and Oxidation of Aqueous Piperazine for Carbon Dioxide Capture*. Ph.D. Dissertation. The University of Texas at Austin.
- Freeman, B., Hao, P., Baker, R., Kniept, J., Chen, E., Ding, J., Zhang, Y. 2014. Hybrid membrane-absorption CO<sub>2</sub> capture process. *Energy Procedia*, 63, 605-613.
- Heo, J., McCoy, S., Adams P. 2015. Implications of Post-Combustion Carbon Capture for Airborne Particulated Matter. *Environ Sci Technol*, 49(8), 5142-5150.
- Koiwanit, J., Supap, T., Chan, C. W., Gelowitz, D., Idem, R., Tontiwachwuthikul, P. 2014. An expert system for monitoring and diagnosis of ammonia emissions from the post-combustion carbon dioxide capture process system. *Int J Greenh Gas Con*, 26, 158-168.
- Lin, Y. J., Madan, T., Rochelle, G. T. 2014. Regeneration with Rich Bypass of Aqueous Piperazine and Monoethanolamine for CO<sub>2</sub> Capture. *Industrial & Engineering Chemistry Research*, 53 (10), 4067-4074.
- Lin, Y. J. 2016. *Modeling Advanced Flash Stripper for Carbon Dioxide Capture Using Aqueous Amines*. Ph.D. Dissertation. The University of Texas at Austin.
- Madan, T. 2013. *Modeling of Stripper Configurations for CO<sub>2</sub> Capture using Aqueous Piperazine*. M.S. Thesis. The University of Texas at Austin.
- National Energy Technology Laboratory. 2010. Carbon Capture Approaches for Natural Gas Combined Cycle Systems. *DOE/NETL- 2011/1470*.
- National Energy Technology Laboratory. 2010. Cost and Performance Baseline for Fossil Energy Plants. *DOE/NETL-2010/1397*.

- Nguyen, T. 2013. *Amine Volatility in CO<sub>2</sub> Capture*. Ph.D. Dissertation. The University of Texas at Austin.
- Pinder, R. W., Adams, P. J., Pandis, S. N. 2007. Ammonia Emission Controls as a Cost-Effective Strategy for Reducing Atmospheric Particulate Matter in the Eastern United States. *Environ Sci Technol*, 41, 380-386.
- Rochelle, G. T. 2009. Amine Scrubbing for CO<sub>2</sub> Capture. *Science*, 325, 1652–1654.
- Van Wagener, D. H. 2011. *Stripper Modeling for CO<sub>2</sub> Removal Using Monoethanolamine and Piperazine Solvents*. Ph.D. Dissertation. The University of Texas at Austin.
- Voice, A. K. 2013. *Amine Oxidation in Carbon Dioxide Capture by Aqueous Scrubbing*. Ph.D. Dissertation. The University of Texas at Austin.
- Xu, Q. *Thermodynamics of CO<sub>2</sub> Loaded Aqueous Amines*. 2011. Ph.D. Dissertation. The University of Texas at Austin.

## **Vita**

Junyuan Ding was born on Oct 22, 1990 in Anqing, Anhui Province in People's Republic of China. After graduating from Hefei No. 1 High School in June 2008, she enrolled in Tianjin University. She graduated with a Bachelor of Science in pharmaceutical engineering in September 2012. She began her graduate study in Chemical Engineering at the University of Texas at Austin in the fall of 2012.

Permanent email: junyuan.ding1022@gmail.com

This thesis was typed by Junyuan Ding.